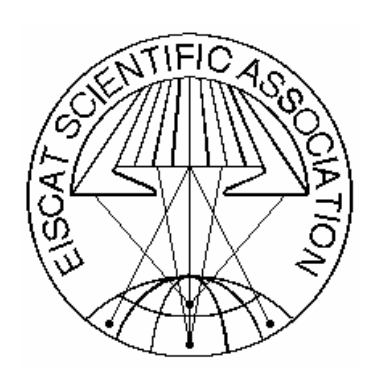
REPORT ON UK EISCAT RESEARCH IN 2000 AND 2001

Prepared on behalf of the UK EISCAT Community by Dr. I.W. McCrea and Ms L. Williams

Rutherford Appleton Laboratory



<u>Cover Illustration</u>: Members of EISCAT's Scientific Advisory Committee admire the steerable dish of the EISCAT Svalbard Radar, during their meeting at Longyearbyen in March 2000. (*Photograph courtesy of Ian W. McCrea*).

INDEX

1.	Introduction		1			
2.	Development of the EISCAT radars during 2000 and 2001					
3.	UK EISCAT	Science: 2000-2001	6			
	3.1.	The Solar Wind	6			
	3.2.	Magnetosphere-Ionosphere Coupling and Reconnection	11			
	3.3.	Storms and Substorms	17			
	3.4.	Large-Scale Convection and Ionospheric Structure	21			
	3.5.	Auroral Physics	22			
	3.6.	ULF Waves	28			
	3.7.	Ionospheric Modification	29			
	3.8.	Ionosphere-Thermosphere Interactions	35			
	3.9.	Tides and Mesosphere	37			
	3.10.	Instrumentation and Techniques	38			
4.	Appendix A:	Papers produced by the UK EISCAT community	40			
5.	Appendix B:	UK EISCAT campaigns in 2000 and 2001	47			
6.	Appendix C:	The UK EISCAT user community	52			

1 INTRODUCTION

This report summarises the highlights of the scientific research undertaken by the UK EISCAT community during 2000 and 2001. The structure follows the familiar pattern used in previous years. In general, the same scientific headings have been used, but the order has been reversed, to start from the solar wind and end at the mesosphere. This has been done in order to give more prominence to some of the most important scientific results to come from the radars during this period. In particular, the section on magnetosphere-ionosphere coupling and reconnection reflects the first use of the EISCAT and ESR data in conjunction with data from the Cluster spacecraft, a relationship that, with the recent extension of the Cluster mission, promises to be extremely productive for many years to come. The section on the use of the EISCAT Heating Facility has been expanded in recognition of the unprecedented volume of new results being produced by the use of that facility. The section on the physics of the solar wind recognises the continuing success of the interplanetary scintillation technique in adding to the understanding of the development and structure of the solar wind on a range of scale sizes.

Section 2, on the recent technical development of the radars, includes a tabular summary of the new experiments which are now available at the mainland radars. These offer a wide range of experimental possibilities and are returning the EISCAT UHF and VHF radars to their rightful place at the forefront of international research in Solar-Terrestrial Physics. As usual, the report includes appendices providing details of published papers using EISCAT data and the EISCAT campaigns carried out during that time. A list of the names and contact addresses of the UK EISCAT community is also included, together with a list of useful phone numbers and email addresses at EISCAT. The report is intended to provide input to EISCAT's own two-yearly international report, which should be published during 2002.

At the time the last of these reports was written, in March 2000, EISCAT's mainland radars were undergoing an extensive renovation, which involved the replacement of most of the hardware and software, as well as the underlying computer systems. It is a tribute to the hard work of all those involved to be able to report that the renovated radar systems became operational before the end of 2000 and that, by the end of 2001, a comprehensive suite of new experiments had been developed and made available to users. The demand for radar time in 2001 was exceptionally high, reflecting the fact that the radars had been unavailable for most of the previous year, making 2001 one of the record years for the number of hours data recorded. The UK remained the largest user of the facilities during this period, and the very healthy number of publications shows that the UK community has continued to be extremely effective in exploiting the EISCAT radars.

The EISCAT Svalbard Radar continued to operate without major problems in 2000 and 2001, at a level significantly above target. A large fraction of the operations during 2001 (both at Svalbard and on the mainland) were geared to new experimental modes supporting the Cluster mission, the science phase of which began in January of that year. Radar observations were also made in support of the FAST and TIMED satellite missions. The EISCAT heating facility has continued to operate reliably and has generated some of the most interesting new science to come from EISCAT in the last two years. The effort to study heater-stimulated airglow (the so-called "artificial aurora") has greatly expanded as a wealth of new observations has demonstrated a complex range of responses to various heating modes and ionospheric conditions. The heater has also been used in attempts to "tag" field lines for subsequent detection by satellites and to explore the potentially very exciting region of the near-Earth magnetosphere in which Alfvén resonance effects may occur. Demand for the heating facility now easily exceeds its target operation of 250 hours per year.

During the next two years, the focus of the system refurbishment will shift to Svalbard, with a planned upgrade of the digital signal processors and user interfaces scheduled for the early summer of 2002. New computers at all sites should facilitate the analysis and operation of the new generation of experiments, some of which make unprecedented demands in terms of real-time data processing speed. The SOUSY Svalbard Radar, scheduled to be taken over by EISCAT in 2002, will provide observations of the mesosphere, stratosphere and troposphere complementary to the ionospheric observations of the ESR. In this way, EISCAT's observing capabilities will be extended downward into an altitude regime which may be of key importance to a complete understanding of solar terrestrial forcing and long-term change. The recent extension of the Cluster mission to the end of 2005 means that EISCAT will continue to be a key ground-based complement to the best-ever in-situ investigation of the magnetosphere throughout this period. The scientific outlook for EISCAT thus continues to be very bright, and the UK community continues to play a leading role in exploiting the possibilities offered by the radar facilities.

Ian McCrea February 2002.

2 DEVELOPMENT OF THE EISCAT RADARS DURING 2000 AND 2001

The renovation and refurbishment of EISCAT's mainland radars was probably the most ambitious maintenance exercise undertaken in the twenty year history of EISCAT. From the end of 1999, the UHF and VHF systems were unavailable for all but passive experiments, while a substantial programme of work was carried out. The old UHF klystron was removed and replaced by a pair of more efficient klystrons manufactured by Thomson CSF of France, each of which is capable of delivering 1.3 MW power at 12.5% duty cycle with pulses of lengths from 1 us to 2ms. One of these klystrons is shown in figure 1. In order to accommodate the new klystrons, the old oil-based cooling system needed to be replaced with a water-based system, requiring substantial modifications in the transmitter hall. The UHF waveguide was also renovated and a number of sections replaced to reduce the amount of reflected power.



Figure 1 One of the new EISCAT UHF klystrons

Much of the receiver chain of both the UHF and VHF radars was removed and replaced at all three sites. The old hardware for the second local oscillators, bandpass and matched filters, radar controllers, analogue to digital converters and digital correlators was scrapped and replaced with state of the art signal processors in which all of these operations were performed in the digital domain. The receiver front end was replaced by a new system offering much lower thermal noise. A structural survey of the UHF antennas revealed worrying cracks in several joints, and this damage was repaired by welding the affected areas. Figure 2 is a picture taken in the Tromsø equipment room after the renovation, showing the new UHF signal processing and control hardware.



<u>Figure 2</u> The new signal processing and control hardware for the Tromsø UHF radar.

The old Norsk Data computer used for controlling the radar and running all background software was replaced by modern unix-based systems and much of the signal processing work was moved onto a new high-performance multi-processor computer acquired specifically for this purpose. The previous EROS control system was replaced by a new monitoring and control system, running in a Windows interface under Unix, which offers most of the same functionality. Examples of the new monitoring and control systems are shown in Figures 3 and 4.

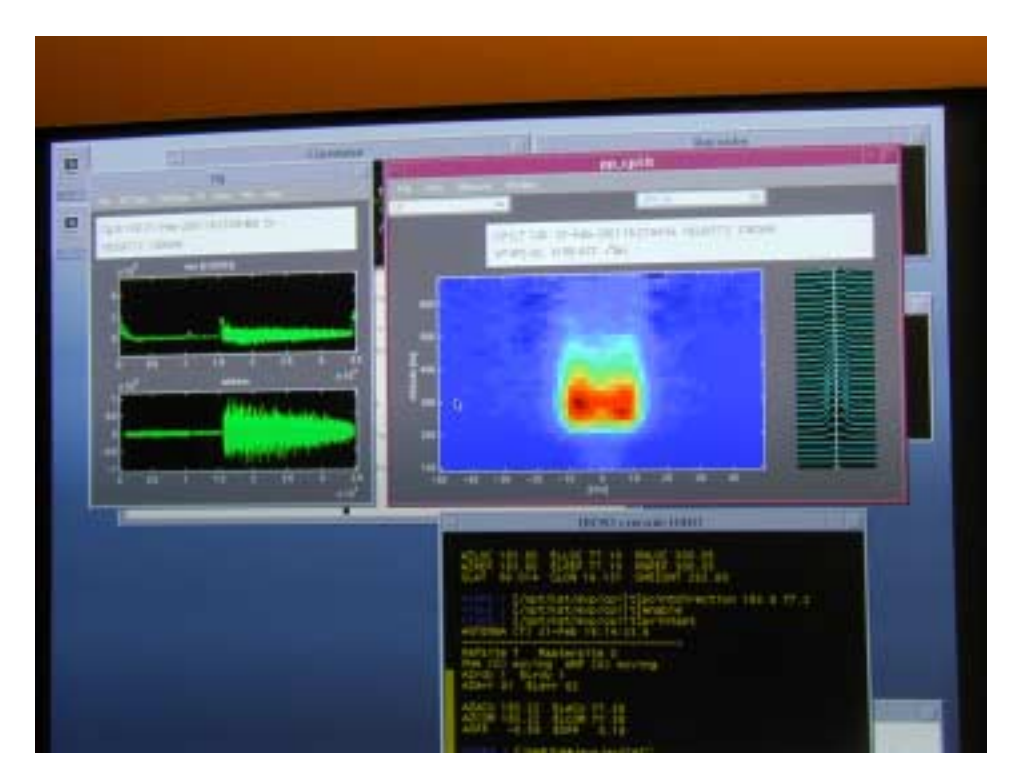


Figure 3 The new data monitoring software from the Tromsø site.

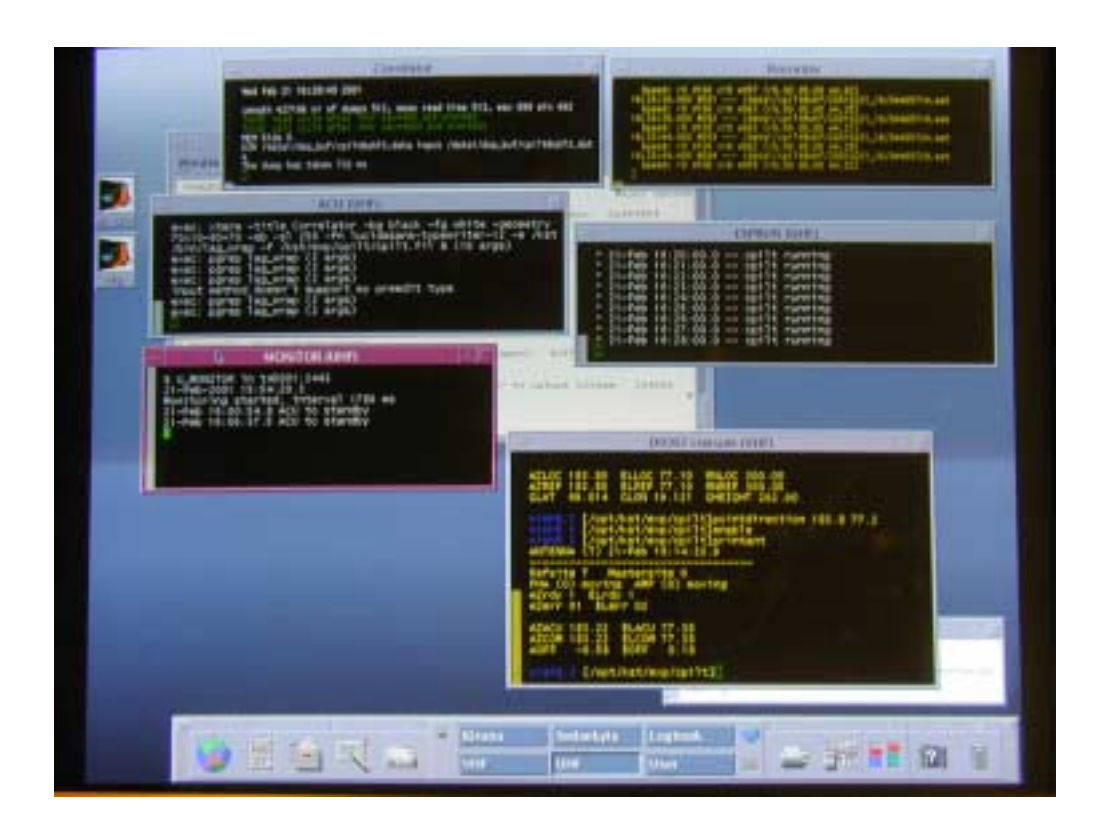


Figure 4 An example of the new windows-based control system for the Tromsø radars.

The first experiment campaign on the renovated EISCAT mainland systems was carried out in November 2000, well in time for the start of the Cluster science phase in January 2001. Initially only a small subset of experiments was available, these being copies of experiments on the old system which had been "retro-fitted" to run on the new hardware. Although these experiments did not exploit the improved possibilities of the new system (e.g. in terms of faster signal processing) they enabled a limited operational capability in the winter season 2000/2001.

During 2001, the number of available experiments on the mainland radars increased rapidly such that, at the time of writing in early March 2002, the range of possibilities available to the experimenter is as large as was the case before the renovation. The added bonus to experimenters is that the system performance and signal processing capabilities are much improved. For example, plasma line measurements are now made routinely as part of most mainland experiments. With further new computing facilities and much increased data storage capacity having been added in recent weeks, it can truly be said that the renovation exercise has restored the EISCAT mainland radars to their rightful place at the forefront of international STP research. Table 1 summarises the modulation schemes currently available, their pre-integration times and range coverage, and the use for which they are intended.

The EISCAT Svalbard Radar continued to operate very reliably during 2000 and 2001, and attracted a high level of usage, particularly during the period where the mainland radars were unavailable. An improved interface with the airport at Longyearbyen has greatly reduced the length of interruptions due to air traffic around the site, as well as offering the possibility to control the transmitters of several instruments (e.g. ESR, SOUSY and in the future, SPEAR) via a common system. The ESR has been the single most important instrument in the Cluster ground-based studies reported later in this document, and in doing so is now fulfilling the role for which it was originally intended. Improved computing and data storage facilities were also added at the ESR site during the past two years.

The tau0 modulation scheme has continued to be used as the basis for all ESR operations, with the default preintegration time being changed from 12.8 to 6.4 seconds, once it had been established that the larger data sets could be handled reliably. A specialised "Cluster mode", in which 6.4 second data dumps are alternated between the field-aligned 42 meter dish and the 32 meter steerable dish pointed at 30° elevation to the magnetic north, has become the basis for much of the ESR operation. A number of results from that mode will be reported here.

<u>Table 1</u> Experiments currently available on the EISCAT radars

Experiment	Radar	Pulse Schemes	Time	Range	Comment
Name		Used	Resolution	Coverage	
tau0	ESR	Alt. Code	3.2, 6.4,	90-1200 km	General purpose ESR
			12.8 s		experiment
tau1	VHF	Alt. Code	5 s	100-1900 km	Replacement for cp4 (single or
		Power Profiles			dual-beam)
tau2	UHF	Alt. Code	5 s	90-750 km	General purpose (replaces cp1)
		Power Profiles			
tau3	UHF	Alt. Code	5 s	90-1400 km	Modified tau2 with more range
		Power Profiles			coverage, used for scanning
tau7	VHF	Alt. Code	5 s	280-2000 km	Under test
					Intended to replace cp7
tau8	VHF	Alt. Code	5 s	90-2000 km	Under test. General purpose
					VHF experiment
arc	UHF/	Alt. Code	0.4 s	90-250 km	High time resolution for auroral
	VHF				studies
D-layer	VHF	Coded pulse-to-	5 s	60-130 km	High spatial resolution for D-
		pulse			layer and PMSE
cp11	UHF	Alt. Code	5 s	90-700 km	Old cp1k converted for new
		Long Pulse			system
		Power Profile			
cp4b	VHF	Long Pulse	10 s	400-1800 km	Old cp4b converted for new
		Power Profile			system
cp7h	VHF	Long Pulse	10 s	280-2000 km	Old cp7g converted for new
		Power Profile			system
gup3	ESR	Alt. Code	10 s	90-875 km	Previous ESR general purpose
		Long Pulse			experiment

The EISCAT Heating facility reached one of its highest-ever peaks of activity in 2001, as new diagnostic tools and more detailed observations showed a wealth of new phenomena. In technical terms, the heating facility has operated reliably with only the usual level of maintenance problems associated with damage to the arrays during the Scandinavian winter.

On the negative side, there have been continued worries about the long-term protection of EISCAT's mainland UHF operating frequencies, chiefly because of competition from mobile telephone networks. At present, the EISCAT frequencies are protected by a series of discretionary agreements with local companies, such that transmitters within a certain distance of the EISCAT facilities do not use frequencies in the EISCAT ion line band. For experiments requiring a broader bandwidth, however, such as interplanetary scintillation studies, it is clear that frequencies around 930 MHz are already unusable. EISCAT has therefore started the development of specialised hardware for undertaking passive experiments around 1420 MHz, a region of the spectrum that is protected for radio astronomy by international agreement. The testing and validation of IPS measurements at the new frequency will be an important milestone in the coming summer.

During the coming months, the Digital Signal Processors at the EISCAT Svalbard Radar will be removed and replaced with more modern systems, allowing greater inter-operability with the mainland. The present java-based operating system at the ESR will also be replaced by a system more similar to the mainland EROS. Once these developments are finished, the programme of renovations will be complete and further technical developments should be more evolutionary in nature. The coming two years should be a very exciting period for EISCAT particularly at Svalbard, with the promise of using the ESR in conjunction with SPEAR. The SOUSY Svalbard Radar will come under EISCAT control, and all of the EISCAT radars will continue to be used in conjunction with the extended Cluster mission as well as with spacecraft like FAST, TIMED and DOUBLESTAR.

3 UK EISCAT SCIENCE: 2000-2001

3.1 THE SOLAR WIND

Studies of the solar wind using EISCAT measurements of interplanetary scintillation (IPS) continued through the period of maximum solar activity in 2000 and 2001 with relatively little interruption in spite of the extensive changes made to the EISCAT system. The solar wind was very complex during this period, showing significant variations with latitude, longitude and time but nonetheless substantial progress has been made towards an improved understanding of the solar maximum solar wind - which differs greatly from the relatively simple bimodal solar wind seen in solar minimum observations.

At solar minimum (from 1992 to mid-1998 during cycles 22 and 23) EISCAT and Toyokawa IPS measurements showed that the solar wind was dominated by fast flow above the polar regions. This extended down to \pm 20-30° latitude and corresponded to large polar coronal holes seen in white-light images of the outer corona. Slow solar wind flow was observed above the narrow, bright streamer belt seen in white light data. During 1998 and 1999 the region of slow wind became broader and more convoluted, reducing the extent of the polar fast streams but introducing narrow regions of fast wind at lower latitudes. During 2000 and 2001, observations showed a solar wind dominated by slow flow, with little or no evidence of fast flow above the poles but with smaller and shorter-lived fast streams observed at middle and low latitudes as equatorial coronal holes opened and closed. Solar activity reached its maximum in 2000 and results from the IPS campaign in September-October 2001 suggested that polar fast streams were beginning to re-emerge as the downward phase of cycle 23 began. These changes are summarised in figure 5.

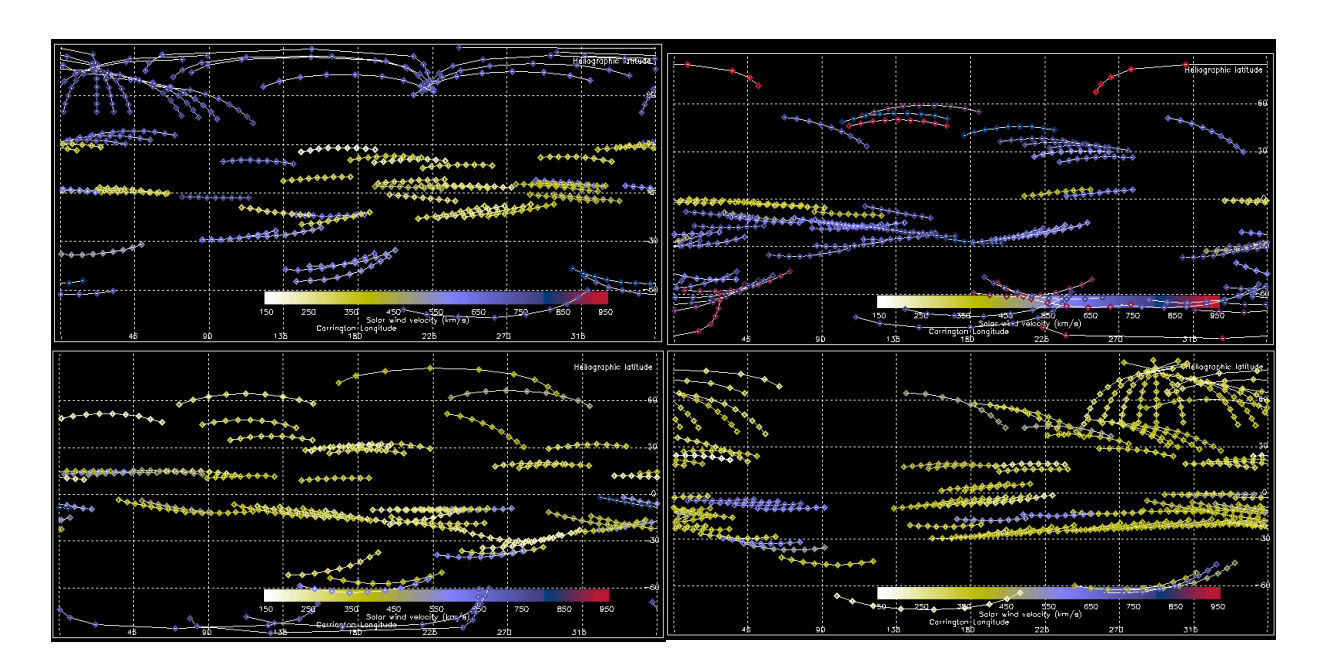


Figure 5 IPS velocities from EISCAT observations made in 1996, 1998, 1999 and 2000 (ordered from 1996 at top left to 2000 at bottom right) projected ballistically to a reference surface at 215 solar radii (1 AU) and plotted against heliographic latitude and Carrington longitude. The evolution of the solar wind from its solar minimum state in 1996 when it was dominated by large polar fast streams, to the slow-wind dominated state in 2000, is most marked. Observations from 1999 indicate that the northern polar fast stream was either undetectably small or absent but a large southern polar fast stream was still present. This southern stream had either contracted or vanished by 2000 (from Canals, A., "Interplanetary scintillation measurements of the solar wind during the rising phase of the solar cycle", to be submitted for Ph.D., University of Wales, April 2002).

The main advances during 2000 and 2001 came from multi-instrument studies of the solar wind in which EISCAT observations made by the group at the University of Wales, Aberystwyth played the leading role. A series of coordinated campaigns involved coronal white-light (and, in 2001, ultra-violet) observations, IPS measurements from MERLIN and EISCAT and in-situ measurements of solar wind velocity from the Wind and Ulysses spacecraft. The combination of these measurements has started to reveal the evolving structure of the three-dimensional solar maximum wind as it flows out from the Sun and the interaction between coronal mass ejections and the background solar wind.

The group at University of Wales, Aberystwyth has continued to make improvements in the analysis and interpretation of IPS data over the past two years, working in conjunction with colleagues at University of California, San Diego and Solar-Terrestrial Environment Laboratory, Nagoya University. The underlying principles remain unchanged, with long-baseline IPS measurements being interpreted as containing contributions from two distinct populations of solar wind with different velocities and densities. Coronal data can then be used to distinguish between regions of the ray-path immersed in fast wind (emanating from dark, low-density coronal holes) and slow wind (found above the bright streamer belt), making it possible to determine the velocities and relative densities of the two components. The improvements made during 2000 and 2001 mainly focus on increasing the accuracy to which "secondary" parameters can be estimated – the intrinsic variation in velocity of a region of solar wind and the random variation in velocity perpendicular to the bulk flow direction being the most important. By using information from in-situ and IPS observations of fast and slow streams it has been possible to place physically realistic constraints on the variation in outflow speed across fast streams and the random perpendicular velocity in slow streams. This reduces the number of free parameters available to fit the data and greatly increases the reliability of the remaining derived parameters.

Comparisons of overlapping velocity measurements from white-light imagers and from IPS observations at MERLIN and EISCAT have made it possible to compare directly the velocities of the large-scale density features seen by white-light instruments and the turbulent structures giving rise to IPS. Since the former are assumed to be pressure-balanced and drifting at the solar wind bulk flow speed, the comparison provides important information on the relationship between scintillation velocity and background flow speed. This information, in turn, is being used to make further improvements to the IPS analysis program suite.

The interpretation of results and the methods used to compare them with coronal and in-situ measurements have also continued to improve. Whenever possible, MHD modelling was used to link IPS and in-situ measurements of solar wind speed with structures observed in the corona by imagers. This offered a significant improvement in the accuracy with which streams of solar wind could be associated with coronal density structures. At the height of solar maximum, however, not even the sophisticated models developed at Science Applications International Corporation (SAIC), La Jolla, were able to describe the rapidly varying corona. Under these circumstances ballistic mapping proved to be more robust.

These improvements to the programme of IPS observations and to the analysis and interpretation methods have led to the following scientific advances during 2000 and 2001:

3.1.1 Solar wind macrostructure

The evolution of the large-scale structure of the solar wind with solar cycle has been studied using a combination of EISCAT IPS and space-based imaging and plasma instruments. At solar minimum, the solar wind was highly bimodal, with distinct fast and slow streams above the large polar coronal holes and the equatorial streamer belt respectively. Co-rotating interaction regions were found above equatorial extensions of coronal holes (Breen et al., 2000b; Bromage et al., 2000) and were clearly detectable in observations as close to the Sun as 40 solar radii (Breen et al., 2000b). As solar activity increased over 1998 the streamer belt became wider and more convoluted (Moran et al., 2000; Breen et al., 2000d), and by 1999 the northern polar fast stream was no longer detectable (Breen et al., 2000d; Breen et al., 2002c). The southern polar fast stream remained detectable into 2000, suggesting that there may be an asymmetry between the northern and southern hemispheres of the Sun. This would be consistent with results from the Toyokawa IPS system and with magnetic field measurements from Ulysses, as recently reported by Kojima and Forsyth respectively. The change in solar wind velocity distribution seen at high latitudes in 1998-99 was very rapid, with a sharp change to a slow-wind dominated heliosphere (Fallows et al., 2002a). The change from a solar minimum to a solar maximum wind was much more abrupt than the change from maximum to minimum-type wind in the declining phase of cycle 22 (Fallows et al., 2002a).

Co-ordinated observations from coronal imagers, interplanetary scintillation measurements from EISCAT and insitu data have been used to study the evolution of the solar wind with increasing distance from the Sun (Breen et al., 2000b; Bromage et al., 2000; Breen et al., 2000d; Breen et al., 2002a). Intensive programmes of measurements were carried out using the LASCO instruments on SoHO, EISCAT, Wind and Ulysses during the second Ulysses orbit. These have revealed significant changes in the longitudinal structure of the solar wind between 25-60 solar radii (IPS measurements) and the orbits of the spacecraft (at 1 AU and 1.25-4.5 AU respectively). An example is shown in figure 6. Velocities measured by IPS were generally consistent with those seen in-situ, except in cases when large longitudinal gradients in solar wind speed were seen in the in-situ data. In these cases the IPS results suggested that solar wind velocities varied much more near the Sun than they did at the spacecraft (Breen et al., 2002c). The degree of "self-smoothing" in solar wind velocity increased with distance from the Sun. Velocities seen at 4.5 AU (960 solar radii) by Ulysses were much more uniform than those seen by Wind at 1 AU (215 solar radii). These were in turn less variable than those seen at 25-65 solar radii by EISCAT. The underlying mechanism is proposed to be stream-stream interaction between narrow regions of solar wind with different velocities. It is suggested that this is an important process in converting the highly non-uniform slow wind observed in the corona into the less variable flow seen at 1 AU and beyond.

Solar wind speed km/s

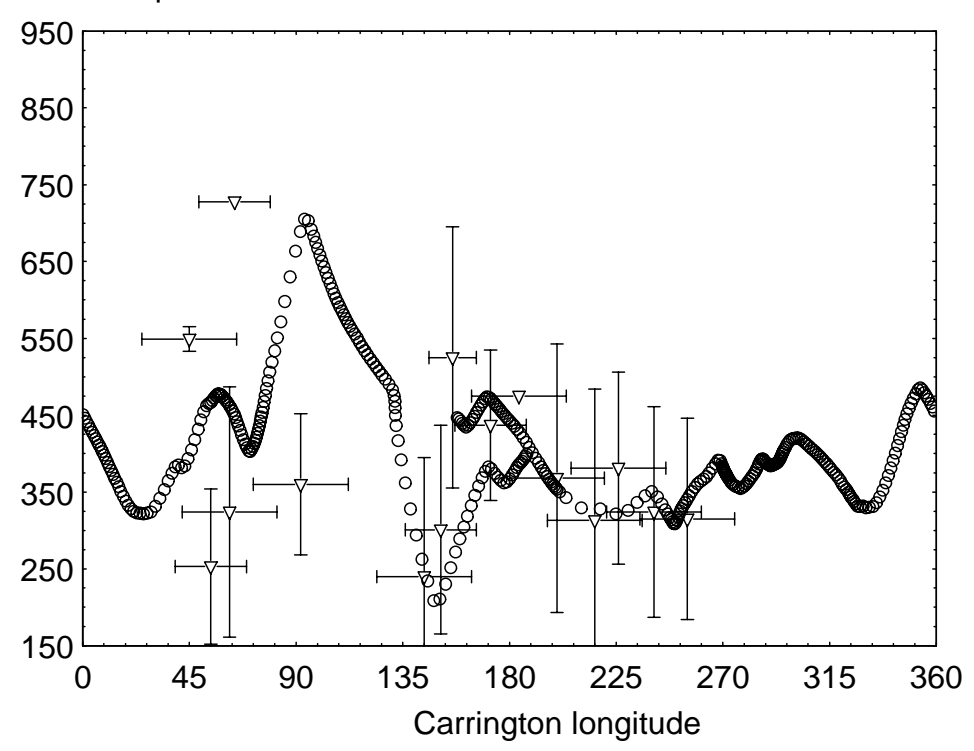


Figure 6 Ulysses in-situ speed measurements (circles) and EISCAT IPS speeds (triangles) from within ±10° of the latitude of Ulysses during its fast equatorial scan in Carrington rotation 1976 (May 2001), mapped to a uniform heliocentric distance of 30 R using either a ballistic projection for EISCAT results and a MHD mapping for Ulysses and plotted as speed vs. Carrington longitude. The large vertical bars in the EISCAT data points represent an upper bound on the variation in solar wind speed across the width of the stream observed and are not estimates of statistical error (from Breen et al., 2002c)

The evolution and propagation of coronal mass ejections (CMEs) has been studied using a combination of ultraviolet and white-light measurements from the EIT and LASCO instruments on the SoHO spacecraft and EISCAT IPS measurements. The results of this study (which will be submitted for publication shortly) demonstrate that it is possible to identify common features in LASCO white-light data and IPS observations and trace the evolution of the velocity of the event out into interplanetary space. The case studies carried out to date suggest that most CMEs tend towards the background solar wind velocity within 30-50 solar radii of the Sun and that interaction between different regions of CMEs may be an important mechanism in their evolution.

3.1.2 Solar wind microstructure

Direct comparisons of the drift velocities of density features observed by white light instruments and turbulent-scale structures measured by EISCAT and MERLIN IPS have established that structures on spatial scales of ~10,000 km and ~100 km drift at similar speeds in the slow solar wind, even close to the Sun. This suggests that the features are drifting with the background solar wind "like leaves in a stream" and that the variation of velocity with heliocentric distance measured by white-light and IPS observations traces out the acceleration profile of the slow wind (Breen et al., 2000c). Observations of fast streams suggest that close to the Sun the small-scale turbulent structure giving rise to IPS may be moving faster than the background flow (Breen et al., 2002b). The fast solar wind starts accelerating closer to the Sun than the slow wind and accelerates much more rapidly (Breen, 2001; Breen et al., 2002b).

Careful analysis of EISCAT observations of fast streams of solar wind over solar minimum and during the rising phase of cycle 23 have shown that the random variation in plasma velocity perpendicular to the bulk flow direction falls away as distance from the Sun increases, as shown in figure 7. If the random variations in transverse velocity are interpreted as the signature of large-amplitude, low frequency Alfvén waves propagating in the fast solar wind then the results suggest that these waves may carry more energy than previously thought (Canals et al., 2002).

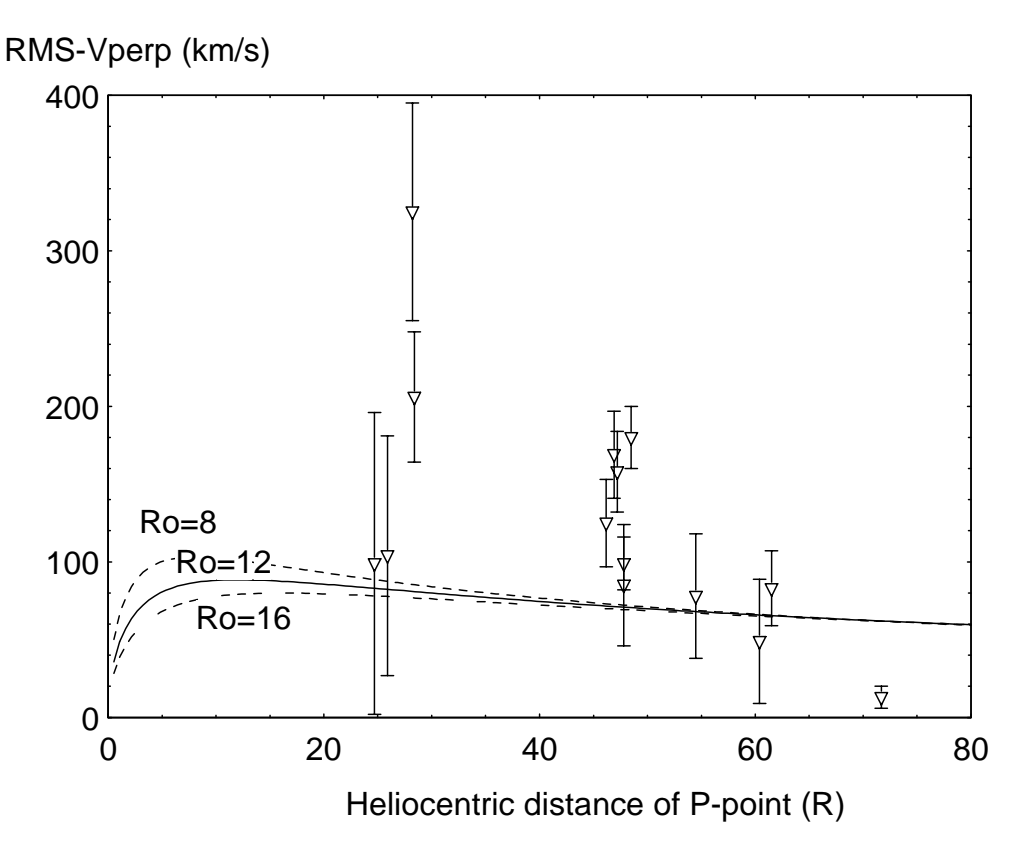


Figure 7 Values for the random velocity perpendicular to the bulk flow direction in the fast solar wind derived from EISCAT IPS measurements (triangles) plotted against heliocentric distance. The three curves plotted are the predicted variation of random perpendicular velocity with distance if the transverse perturbations are introduced purely by Alfvén waves propagating in a spherically-expanding solar wind adequately described by the WKB approximation. R_o, the Alfvén critical distance, is taken to be 8, 12 and 16 solar radii for the three curves. The results suggest that random transverse velocities are larger closer to the Sun than expected for a WKB wind and that large-amplitude, low-frequency Alfvén waves may be of more importance in solar wind acceleration than previously thought (Canals et al., 2002).

In each set of EISCAT observations of interplanetary scintillation the maximum frequency of significant scintillation is determined. This corresponds to the maximum frequency present as the diffraction pattern of the scattering sweeps past the antenna. The results are then separated into those cases where a fast- or a slow-stream dominates the scattering. When the reciprocal of cut-off frequency is plotted against solar distance the values all lie on a straight line passing through the origin, as shown in Figure 8, suggesting that the smallest scale present in the diffraction pattern is proportional to the solar distance of the line-of-sight. The relationship between the reciprocal of the cut-off frequency and heliocentric distance is remarkably linear.

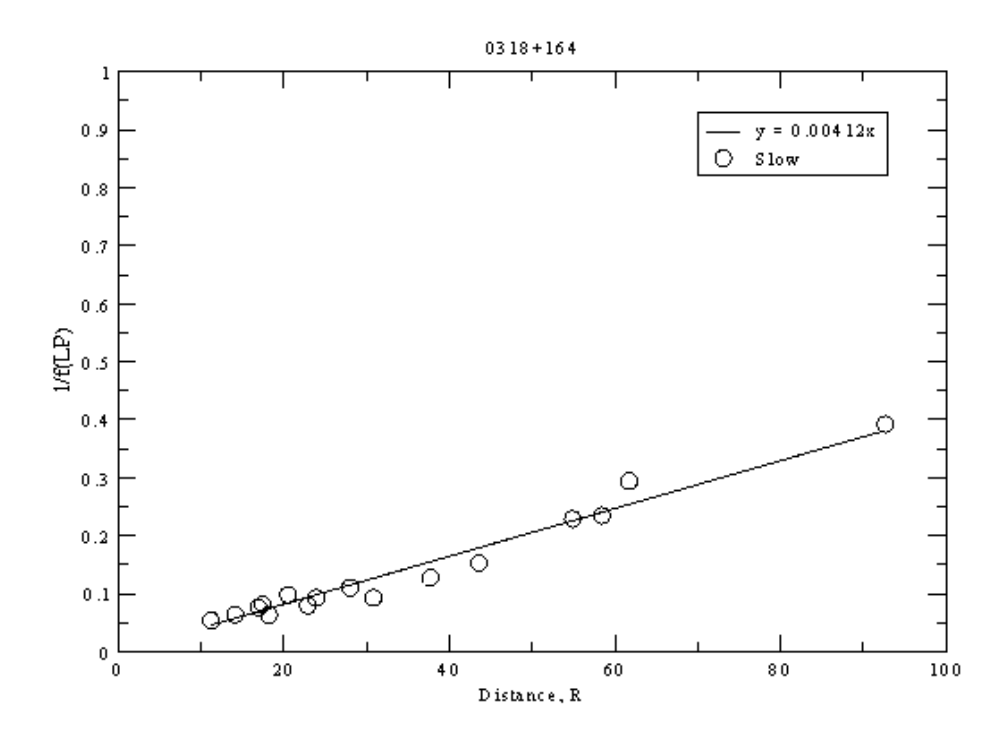


Figure 8 Maximum frequency at which significant scintillation was detected vs. heliocentric distance for slow-wind dominated observations of the strong compact source 0318+164 (CTA-21). The smallest scale present in the diffraction pattern is proportional to heliocentric distance.

Studies of the intensity of observed scintillation in observations dominated by fast and slow streams show that the scintillation index ($\sigma(I)/\langle I \rangle$, where I is the signal power) decreases with increasing distance from the Sun according to a power-law within the weak scattering regime. Within the slow stream, the scintillation index is approximately twice that found in the fast stream (Fallows et al., 2002b).

Taken together, these results represent a significant improvement in our understanding of the evolving solar wind. The data taken by EISCAT during 2000 and 2001 represent the finest solar maximum data set covering the inner regions of the solar wind yet obtained. As we move into 2002, the improving stability of the new EISCAT control system should make it possible to obtain even better observations during the declining phase of solar cycle 23. A particularly exciting prospect is the forthcoming upgrade to the EISCAT remote sites, allowing 2-channel wide-bandwidth observations centred on 1420 MHz. Not only will this make it possible to receive over a wide bandwidth free of GSM interference, but it will enable observations to be made closer to the Sun, increasing the overlap between EISCAT and LASCO data. A further advantage is that the effects of source structure can be taken into account much more easily, as astronomical radio sources are routinely mapped at frequencies close to 1420 MHz. With these improvements, EISCAT IPS should be entering a new and even more productive era.

3.2 MAGNETOSPHERE-IONOSPHERE COUPLING AND RECONNECTION

3.2.1 Co-Ordinated EISCAT and Cluster Studies.

The start of the science phase of the Cluster mission marked a very important point in the development of EISCAT since, as well as being the spur for the mainland renovation, this mission was one of the original drivers for the development of the EISCAT Svalbard Radar. Data from the ESR have played a key role in the first tranche of Cluster Ground-Based papers, which have recently appeared in a special issue of Annales Geophysicae.

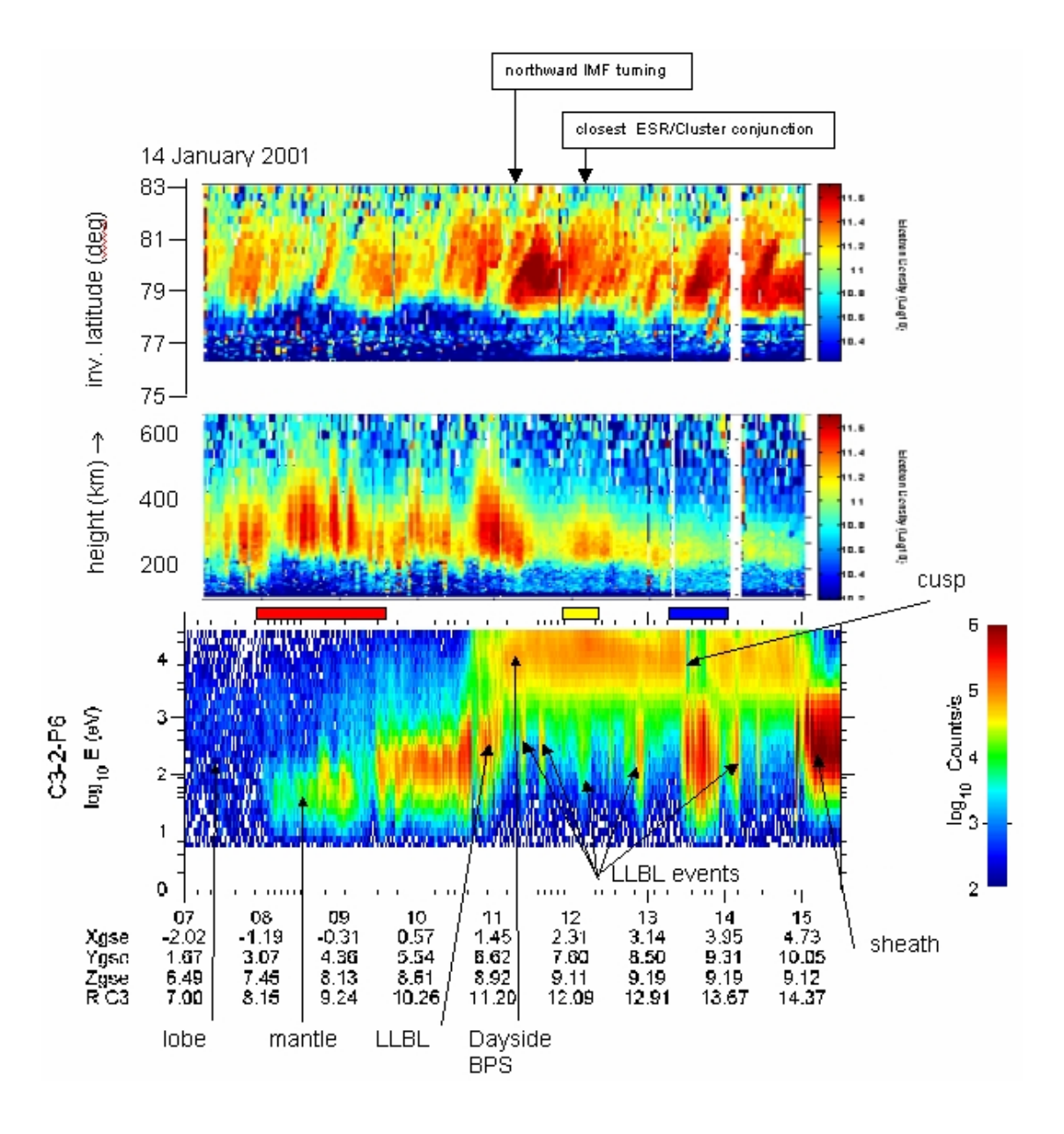


Figure 9 Plot showing simultaneous observations of electron density by the EISCAT Svalbard Radar steerable antenna (top) and fixed antenna (middle panel) during the experiment of 14 January 2001. The lower panel shows ion measurements made by one of the Cluster spacecraft, at the same time, as it moved from the lobe into the magnetosheath.

Lockwood et al. (2001a) discuss measurements made during the interval between 0800 and 0930 UT on 14 January 2001. At this time, the four Cluster spacecraft were moving from the central magnetospheric lobe, through the dusk sector mantle, on their way towards intersecting the magnetopause near 1500 MLT and 1500 UT. Throughout the interval, the EISCAT Svalbard Radar (ESR) at Longyearbyen observed a series of polewardmoving transient events of enhanced F-region plasma concentration ("polar cap patches"), with a repetition period of the order of 10 minutes (shown in figure 9). Allowing for the estimated solar wind propagation delay of 75 (±5) minutes, the interplanetary magnetic field (IMF) had a southward component during most of the interval. The magnetic footprint of the Cluster spacecraft, mapped to the ionosphere using the Tsyganenko T96 model (with input conditions prevailing during this event), was located to the east of the ESR beams. Around 0905 UT, the DMSP-F12 satellite flew over the ESR and showed a sawtooth cusp ion dispersion signature that also extended into the electrons on the equatorward edge of the cusp, revealing a pulsed magnetopause reconnection. The SuperDARN HF backscatter radars imaged the consequent enhanced ionospheric flow events. The average convection patterns (derived using the AMIE technique using data from the magnetometers, the EISCAT and SuperDARN radars, and the DMSP satellites) show that the associated poleward-moving events also convected over the predicted footprint of the Cluster spacecraft. Cluster observed enhancements in the fluxes of both electrons and ions. These events were found to be essentially identical at all four spacecraft, indicating that they had a much larger spatial scale than the satellite separation of the order of 600 km. Some of the events show a correspondence between the lowest energy magnetosheath electrons detected by the PEACE instrument on Cluster (10-20 eV) and the topside ionospheric enhancements seen by the ESR (at 400-700 km). Lockwood et al. suggested that a potential barrier exists at the magnetopause, preventing the lowest energy electrons from entering the magnetosphere. This barrier is reduced when and where the boundary-normal magnetic field is enhanced. Polar cap patches are then produced by the consequent enhanced precipitation of the lowest energy electrons, making them, and the low energy electron precipitation, fossil remnants of the magnetopause reconnection rate pulses.

On the same day, the four Cluster spacecraft passed through the northern magnetospheric mantle in close conjunction to the EISCAT Svalbard Radar (ESR) and approached the post-noon dayside magnetopause over Greenland between 1300 and 1400 UT. During that interval, a sudden reorganisation of the high-latitude dayside convection pattern occurred after 1320 UT, as reported by Opgenoorth et al. (2001), most likely caused by a direction change of the solar wind magnetic field. The result was an eastward and poleward directed flow channel, as monitored by the SuperDARN radar network and also by arrays of ground-based magnetometers in Canada, Greenland and Scandinavia. The flow channel initially expanded eastward and later poleward between 1320 and 1340 UT. The four Cluster spacecraft, and the field line footprints covered by the eastward looking scan cycle of the Sondrestrømfjørd incoherent scatter radar were then engulfed by cusp-like precipitation with transient magnetic and electric field signatures. In addition, the EISCAT Svalbard Radar detected strong transient effects of the convection reorganisation, a poleward moving precipitation and a fast ion flow channel in association with the auroral structures that suddenly formed to the west and north of the radar. From a detailed analysis of the coordinated Cluster and ground-based data, it was found that this extraordinary transient convection pattern had moved the cusp precipitation from its former pre-noon position into the late post-noon sector. This allowed for the first and quite unexpected encounter of the cusp by the Cluster spacecraft. These findings illustrated the large amplitude of cusp dynamics, even in response to moderate solar wind forcing. The global ground-based data proved to be an invaluable tool to monitor the dynamics and width of the affected magnetospheric regions.

Transient reconnection at the dayside magnetopause is perhaps the principal mechanism whereby energy from the solar wind is deposited into the near-Earth environment. Such bursts of reconnection are termed flux transfer events (FTEs). Still using data from January 14, 2001, Lockwood et al. (2001b) studied a series of transient entries into the low-latitude boundary layer (LLBL) of all four Cluster spacecraft during their outbound pass through the mid-afternoon magnetopause. The events took place during an interval of northward IMF, as seen in the data from the ACE satellite. The solar wind propagation delay of 75 minutes on this day was well defined by the two studies described above. With an additional lag of 16.5 minutes, the transient LLBL events correlated well with swings in the IMF clock angle (in GSM) to near 90°. Most of this additional lag was explained by the ground-based observations, which revealed signatures of transient reconnection in the pre-noon sector that then took 10-15 minutes to propagate eastward to 15 MLT, where they were observed by Cluster. The eastward phase speed of these signatures agreed very well with the motion deduced by the cross-correlation of the signatures seen on the four Cluster spacecraft. The evidence that these events were reconnection pulses included transient erosion of the noon 630 nm (cusp/cleft) aurora to lower latitudes and transient and travelling enhancements of the flow into the polar cap, imaged by the AMIE technique. Poleward-moving events propagating into the polar cap were also seen by the EISCAT Svalbard Radar (ESR). A pass of the DMSP-F15 satellite revealed that the open field lines near noon had been opened for some time. More recently opened field lines were found closer to dusk, where the flow transient and the poleward-moving event intersected the satellite pass. The events seen by Cluster had ion and electron characteristics predicted and observed by Lockwood and Hapgood (1998) for a Flux Transfer Event (FTE), with allowance for magnetospheric ion reflection at Alfvénic disturbances in the magnetopause reconnection layer. Like FTEs, the events had scale sizes of about 1 R_E in their direction of motion and showed a rise in the magnetic field strength. Unlike most FTEs, however, they showed no pressure excess in their core and hence, no characteristic bipolar signature in the boundary-normal component. However, most of the events were observed when the terrestrial magnetic field was southward, i.e. on the edge of the interior magnetic cusp, or when the field was parallel to the magnetic equatorial plane. Only when the satellites began to emerge from the exterior boundary (when the field was northward), did the events start to show a pressure excess in their core and the consequent bipolar signature. Lockwood et al. identified these events as the first observations of FTEs at middle altitudes.

In a study that employed magnetic field observations from the first month of Cluster science operations, Wild et al. (2001) compared the in-situ and ionospheric signatures of pulsed reconnection at the dayside magnetopause. Several clear FTEs were observed during an outbound pass through the high-latitude post-noon magnetospheric boundary adjacent to the cusp on 14 February 2001. During this time, the magnetic footprint of the spacecraft passed centrally through the fields-of-view of both the CUTLASS Finland and Iceland HF radars of the SuperDARN system, across the location of the field-aligned beam of the ESR, and just equatorward of the northward-pointing low-elevation beam of the latter system. The occurrence of FTEs corresponded to a southward turn of the interplanetary magnetic field (IMF). Examination of the CUTLASS radar data from the conjugate ionosphere revealed antisunward-moving regions of HF scatter, which have been termed poleward-moving radar auroral forms (PMRAFs), as well as pulsing in the flow. The ESR observations showed a complex varying and structured polar ionosphere related to the occurrence of FTEs. The authors concluded that the observations left no doubt that the Cluster and radar signatures were directly related, and provided a direct demonstration of the input of momentum and energy into the magnetosphere-ionosphere system resulting from pulsed reconnection at the magnetopause, as originally envisaged in outline by Dungey.

3.2.2 EISCAT studies of Flux Transfer Events

Observations from the EISCAT VHF radar, taken on 23 November 1999, have offered a new insight into the signatures of FTE activity observed by the HF coherent scatter radars. Davies et al. (2002) present CP-4 observations of series of poleward-propagating F-region plasma density enhancements, which, the authors concluded, were fossil signatures of transient reconnection, having been formed by structuring of the ionosphere in the cusp region in response to processes associated with FTEs. Simultaneously, PMRAFs were observed by the CUTLASS HF coherent scatter radar at Hankasalmi in Finland. Figure 10 demonstrates pictorially the simultaneous occurrence of transients in electron density and HF backscatter power, using data from azimuthally aligned beams from the two radar systems. Although it is accepted that PMRAFs, which are commonly observed near noon by HF radars, are related to FTEs, the specific mechanism for the generation of the field-aligned irregularities within such features is not well understood. Interpreting the HF observations with reference to the plasma parameters diagnosed by the incoherent scatter radar led the authors to suggest that the field-aligned irregularities within the PMRAFs are generated by the gradient-drift mechanism due to the presence of structure in the electron density.

CUTLASS Finland and EISCAT VHF Observations

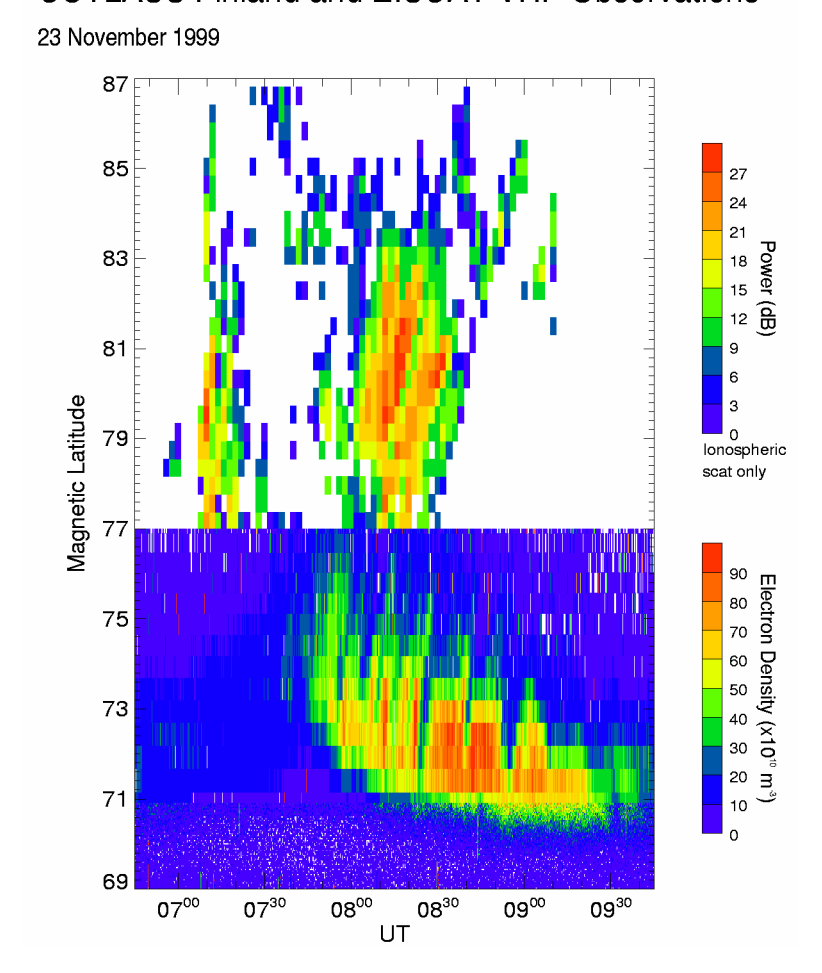


Figure 10 Composite plot of backscattered power from beam 7 of the CUTLASS radar at Hankasalmi and electron density from beam 1 of the EISCAT VHF radar, as a function of magnetic latitude between 0645 and 0945 UT on 23 November 1999. Observations below 77° are from the VHF radar and those above, from the Finland radar.

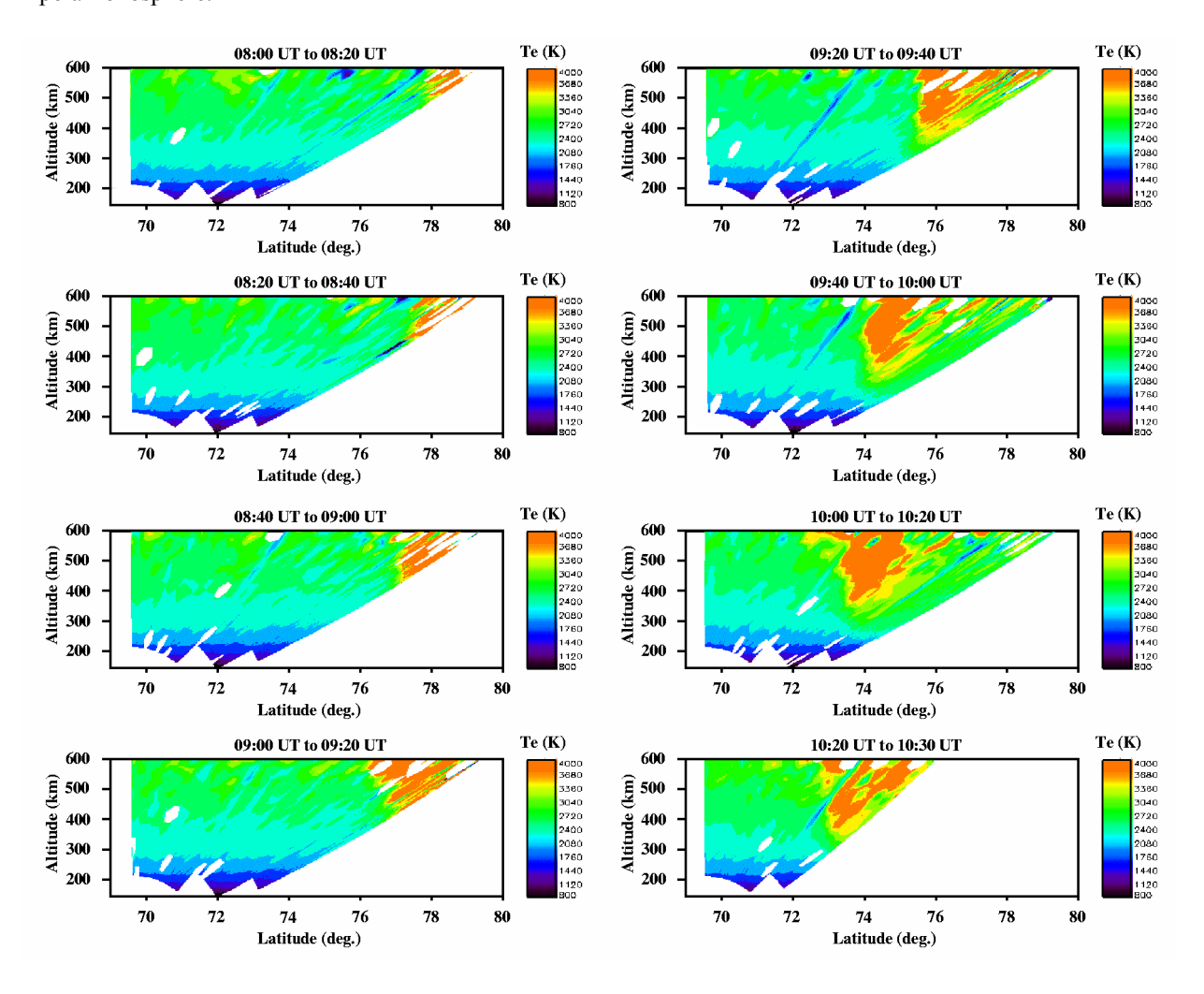
A related study of the formation of polar patches in the cusp was undertaken using the EISCAT Svalbard radar (ESR) in conjunction with observations from the CUTLASS Finland HF radar (Ogawa et al., 2001). The authors showed that two suppressions in electron density were associated with enhancements in the ionospheric flow greater than 1.5 km s⁻¹. In one event the cause of the reduction in electron density was enhanced chemical reactions as a result of enhanced ion temperatures, which in turn resulted from the ion frictional heating. In the second event, no enhanced ion temperatures were observed, but the suggestion is that the suppressed plasma density was transported by the enhanced ion velocities from earlier local times.

Khan et al. (2002) present multi-instrument observations using the meridian scanning photometer (MSP) at Ny Ålesund, the ESR and the CUTLASS HF system, to investigate the dynamics of the cusp region during pulsed reconnection events. The optical data obtained from the MSP indicated the presence of several poleward-moving auroral forms (PMAFs), which have been previously identified as the auroral signature of pulsed reconnection. These PMAFs were also coincident with PMRAFs and pulsing in the flow observed the HF radar. Furthermore, the optical green line (557.7 nm) luminosity indicated a dark auroral band bounded poleward and equatorward by intense luminosity. Through comparison of this region in the optical emission with the HF radar backscatter, the authors inferred that the equatorward edge of the optical dark region in the 557.7 nm emissions provided an accurate representation of the location of the open/closed field line boundary. The ESR observations showed increases in electron density and electron temperature occurring in conjunction with the optical PMAFs similar to the theoretical predictions of Davis and Lockwood (1996), who used an auroral precipitation model to predict ESR observations in the vicinity of the cusp. Although the modelling analysis appeared to explain some of the observations made by the ESR, the model was limited by not being able to account for plasma flow or IMF variations, both of which modify the ionospheric structure considerably.

3.2.3 Footprints in the dayside ionosphere of solar wind/magnetosphere coupling processes

A series of case studies by the Radio and Space Physics group of the University of Wales, Aberystwyth, has enabled identification of signatures in the dayside ionosphere of magnetopause reconnection processes, including steady-state lobe reconnection, equatorial reconnection in summer and a gradual trend in IMF clock angle.

A multi-instrument investigation provided a comprehensive picture of signatures of lobe reconnection under steady positive Bz with small clock angle. The measurements were made by six complementary experimental techniques – radio tomography, all-sky and meridian scanning photometer auroral optics, incoherent and coherent scatter radars and satellite particle detection (Pryse et al., 2000a). The optical green-line footprint of the reconnection site was found to lie in the sunward convection of the lobe cells. Downstream, in the region of red-line emission and increased electron temperatures observed by the ESR radar, indicative of softer precipitation, the reverse energy dispersion of the incoming ions was identified by DMSP satellite measurements. A steep latitudinal density gradient at the equatorward edge of the precipitation marked the adiaroic boundary separating the open field lines of the polar lobe cells and the closed field of viscous-driven cells. An enhancement in plasma density to the south of the gradient revealed that ionisation was being reconfigured as it was thrust against the boundary by the anti-sunward flow of the viscous cells near magnetic local noon. While each instrument individually provided valuable information on particular aspects, the study demonstrated that together the different experiments complemented each other to give a consistent and comprehensive picture of the dayside polar ionosphere.



<u>Figure 11</u> Data from a sequence of poleward scans by the Tromsø UHF radar, showing a sharp transition in electron temperature, inferred to correspond to the open-closed field line boundary.

Another multi-instrument study identified signatures of equatorial reconnection with Bz negative in the summer ionosphere where optical measurements under daylight conditions were unavailable (Pryse et al., 2000b). Ion energy dispersion signatures from three DMSP passes were used as indicators of the reconnection. The footprint, seen first to the north in a tomographic reconstruction, moved in response to increasing Bz magnitude through the field-of-view of the ESR radar, where it was identified by enhanced electron temperatures and densities. Ion dispersion effects were seen as the signature moved, with density contours in the bottom-side F layer rising in response to a softening of the particle spectrum. The most striking signature was found in the spatial structure of F-region electron temperatures measured by the EISCAT mainland radar in the form of a region of enhancement with a steep equatorward boundary (figure 11) at the leading edge of the DMSP ion energy dispersion. This transition in electron temperature marked the location of the boundary, mapping from the reconnection site between closed field lines and those open to magnetosheath precipitation.

Observations using the ESR showed the response of the spatial structure of the cusp ionosphere to a rotational trend in IMF clock angle that moved the reconnection from the lobe to equator (Pryse et al., 2002). Enhanced topside electron temperatures again marked the footprint of the reconnection with temporal changes in the spatial distribution reflecting the change from lobe (figure 12) to equatorial reconnection (figure 13). Discrete spatial enhancements in ion temperature were linked to ion-neutral frictional heating where the field lines were being convected rapidly from the reconnection location. The corresponding electron densities showed structures consistent with discrete particle precipitation, field-aligned currents and convection flows driven by the IMF.

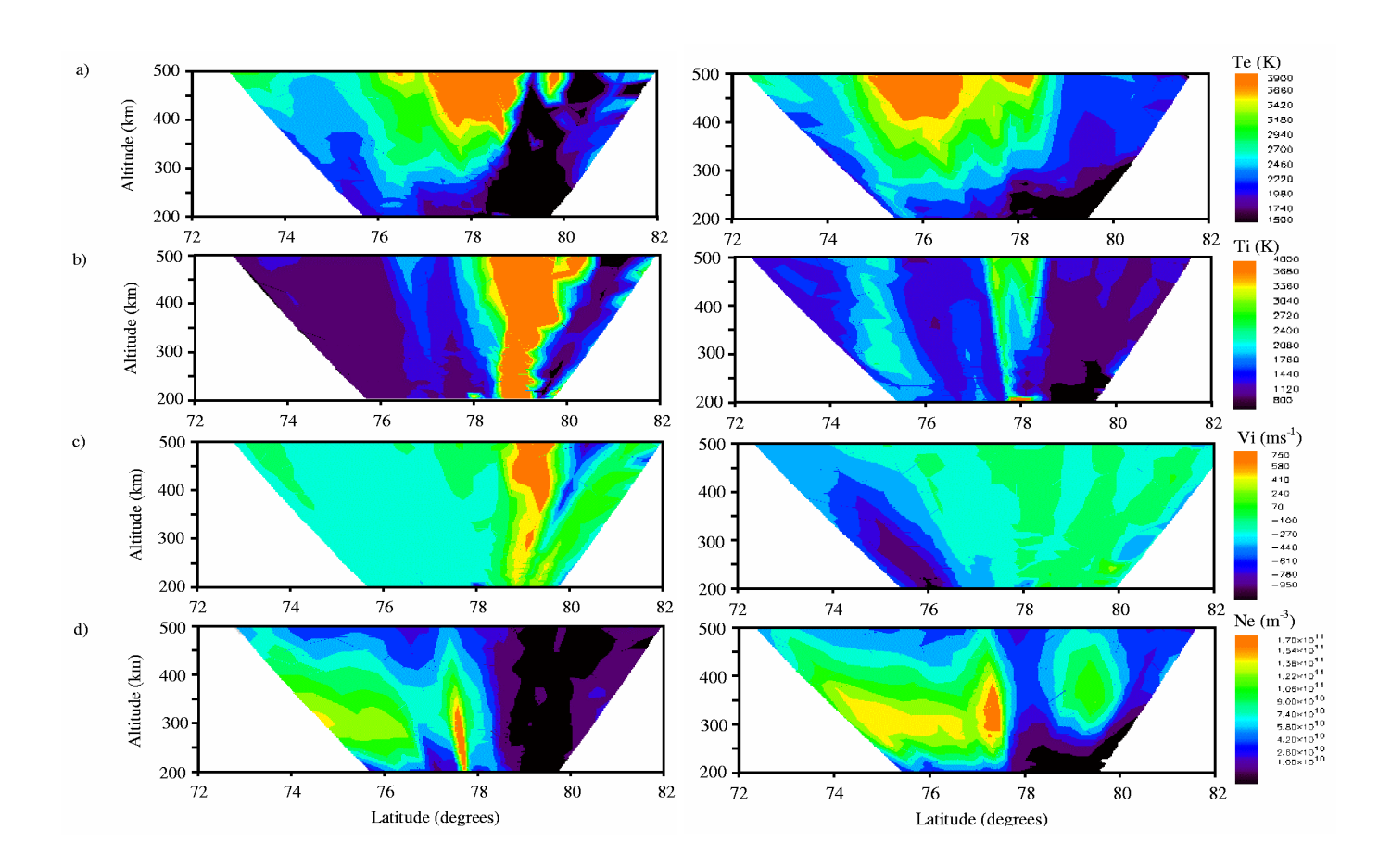


Figure 12 Data from a scanning EISCAT Svalbard Radar experiment showing the location of the reconnection footprint during a period of lobe reconnection.

<u>Figure 13</u> As for figure 12, but showing data from a period of dayside reconnection.

3.3 STORMS AND SUBSTORMS

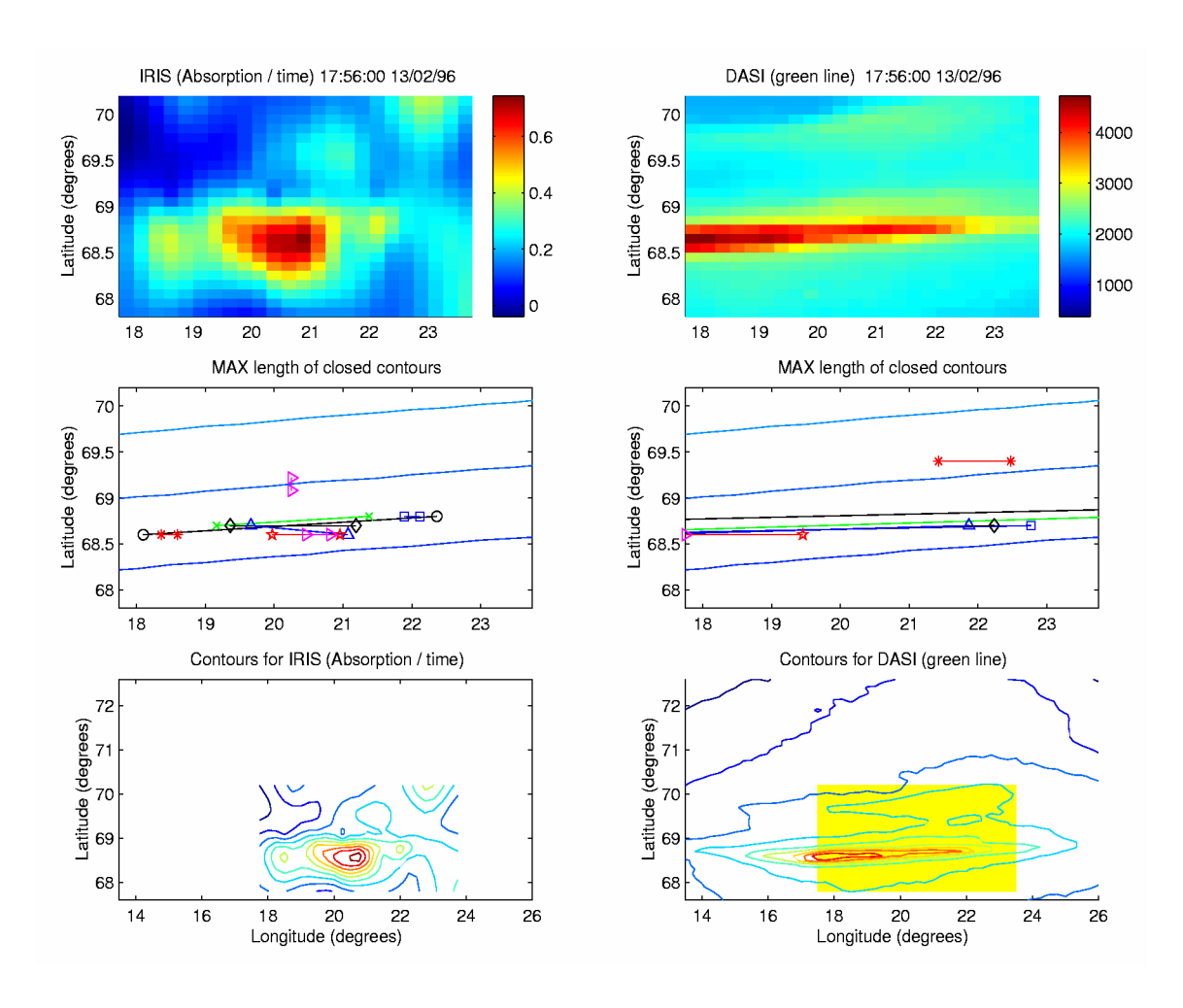
3.3.1 Expansion Phase Studies

CP-4 data taken by the EISCAT VHF system in December 1992 were used in the study of plasma conditions in the vicinity of the poleward-expanding substorm auroral bulge (Davies et al., 2000; Fox et al., 2001). The bulge was characterised by a region of enhanced F-region electron temperature resulting from precipitation, the leading edge of which was straddled by a narrow band of elevated ion temperature. The latter indicates a region of high plasma flow resulting in frictional heating of the ion population. The split beam nature of the VHF radar during this experiment provided the opportunity of beam swinging to derive the vector velocities in the plane of the two radar beams. However, conventional beam swinging, in which line-of-sight velocities from the same range gate along each of the two VHF beams are combined, was considered inappropriate in the bulge region. This is because plasma flow is likely to be ordered by the feature itself, which was found to change markedly in orientation during its poleward progression. Instead, a novel method of velocity determination combined line-of-sight velocity estimates, which were equidistant from the electron temperature boundary. Careful analysis revealed a region of high-speed plasma flow along the leading edge of the bulge consistent with the ion temperature observations. The flows were taken to be produced by the strong change in conductivity at the boundary, and the requirements of current continuity. Lester (2000) reviewed the ionospheric flows associated with the different phases of the substorm, including their effect on EISCAT observations.

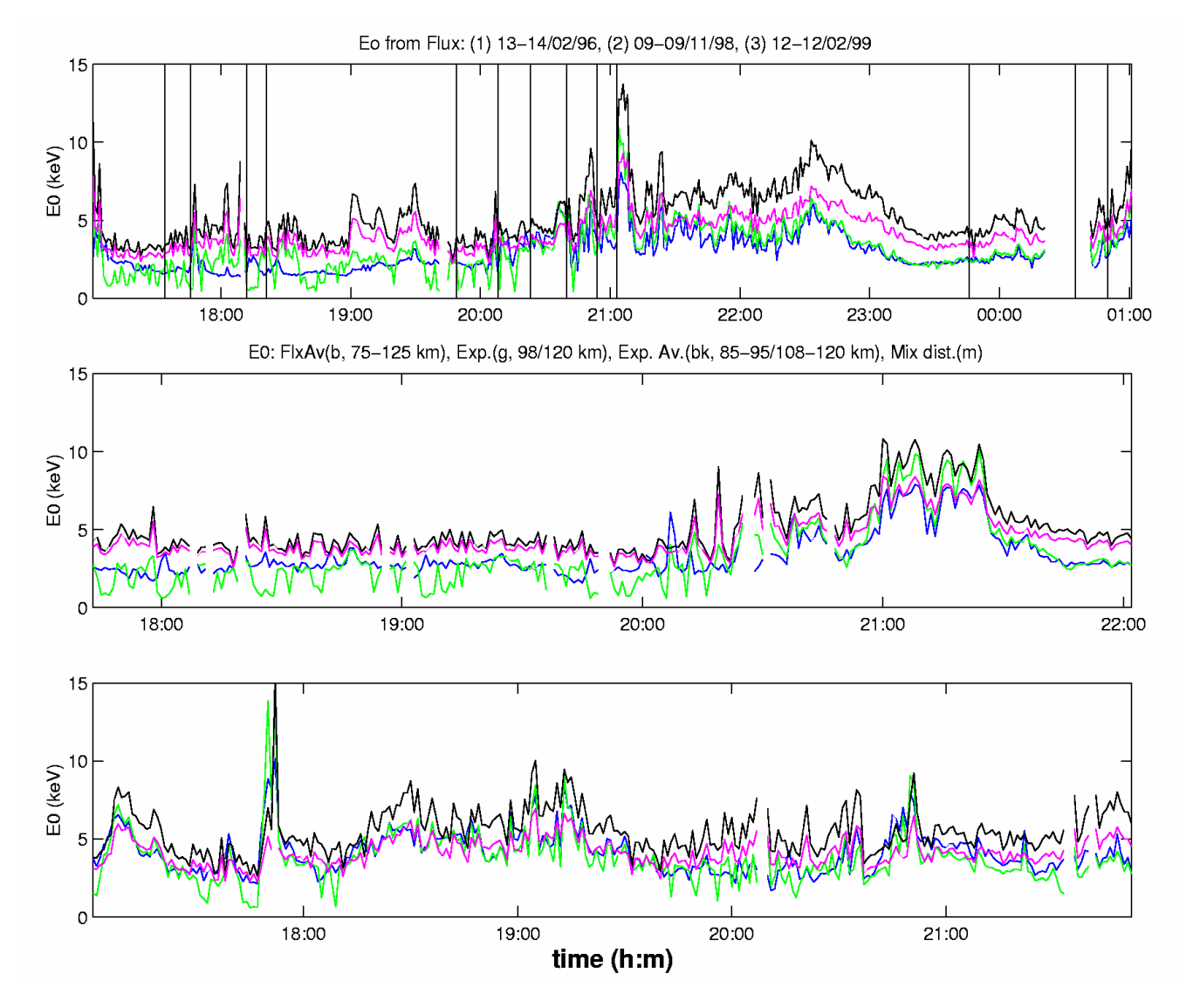
On 21 August 1998, a sharp southward turning of the IMF resulted in an isolated substorm over Northern Scandinavia and Svalbard. At this time, EISCAT was running the UK special programme SP-UK-CSUB, which combined operation of both the mainland VHF and Svalbard UHF incoherent scatter radars. The former, in split beam mode, was directed northward at low elevation while the latter was pointed southward, also at low elevation. The incoherent scatter observations were used in conjunction with measurements from the CUTLASS HF coherent scatter radars, ground magnetometers and the Polar UVI imager. These allowed the electrodynamics of the impulsive substorm electrojet to be studied in great detail during its first few minutes of evolution at the expansion phase onset (Yeoman et al., 2000). The expansion phase onset was characterised by a strong enhancement of the Fregion electron temperature, again signifying the precipitation of particles, and UV aurora. The regions of enhanced electron temperature and UV aurora both subsequently expanded poleward, although it is notable that the enhanced electron temperatures associated with the substorm-disturbed region extended some 2° further poleward than the UV auroral signature. The initial flow response to the substorm expansion phase onset was the suppression of flow within the substorm-disturbed electrojet, which extended up to some 300 km poleward of the initial region of auroral luminosity, imposed over a timescale of less than 10 seconds. The authors suggested that the high conductivity region of the electrojet acted as an obstacle to the flow, resulting in low electric field in a region where the conductivity had not actually been enhanced. Rapid flows were observed at the edge of this high conductivity region. Subsequently the flow enhanced, flowing around the expanding auroral feature in a direction determined by the flow pattern prevailing before the substorm intensification. Following this interval, after a northward turning of the IMF, evidence of a transpolar arc was observed (Wild, 2000; Wild et al., 2000).

The response of the ionosphere to the enhanced precipitation during the expansion phase of this substorm (Yeoman et al., 2000) has also been investigated by Gauld (2000) and Gauld et al. (2002). More specifically the authors studied the impact of such ionospheric changes on both the absorption and propagation of the HF radio waves of the CUTLASS system. EISCAT data from the SP-UK-CSUB experiment, and IRIS riometer measurements were used as input to a modelling study which has indicated that moderate to severe HF absorption can occur during substorm events. The absorption may lead to a complete loss of HF radar backscatter. Significant propagation changes may also result, which lead to the enhanced viability of very low elevation angle propagation during the substorm expansion phase, with a reorganisation of the HF backscatter location which is highly characteristic of SuperDARN substorm observations.

Simultaneous observations with the IRIS, DASI and EISCAT systems (on 13 Feb. 1996, 9 Nov. 1998, and 12 Feb. 1999) have been employed in a study of the spatial distribution and temporal evolution of auroral forms and precipitation regions during substorm activity (del Pozo et al., 2002b). The simultaneous operation of EISCAT allowed an estimation of the particle precipitation spectrum to be made. The analysis of the 2D distributions of absorption and the 557.7 nm emissions allowed the identification of absorption patches corresponding with optical auroral forms, and the associated ionisation regions defined by close contours of either constant absorption or green-light intensity. Figure 14 shows a well-defined arc feature from simultaneous observations by the IRIS and DASI systems in the common field of view of IRIS at 1758 UT in 13 February 1996. The various symbols, and corresponding line segments show the length and elongation axis of the closed contours in both absorption and 557.7 nm emission. The spatial distribution of the harder precipitation responsible for the enhanced absorption appeared more structured than the narrower arc feature seen by DASI. Overall there is a close correspondence between the two observations. The middle panels of figure 14 show the length and orientation of the features defined by the closed contours. Moreover, the features showed a clear alignment with the magnetic L-shells (set of transverse lines across the panels). The bottom panels display the contour plots for the two 2D images, in their respective fields of view. The yellow patch on the right shows the IRIS field of view. The 1996 IRGF model gave the L-shell locations. In addition, an estimate was made of the characteristic energy of the electron precipitation over the common field of view of IRIS and DASI (del Pozo et al., 2002c). The authors suggested that acceleration associated with diffusion processes in the magnetosphere long before precipitation may be controlling the shape of the energy spectrum.



<u>Figure 14</u> Simultaneous riometer (left) and optical (right) observations of a well-defined arc feature on 13 February 1996. The middle panels show the length of the features and their orientation with respect to the L-shells. The bottom panels show the observations in the context of the IRIS field-of-view.

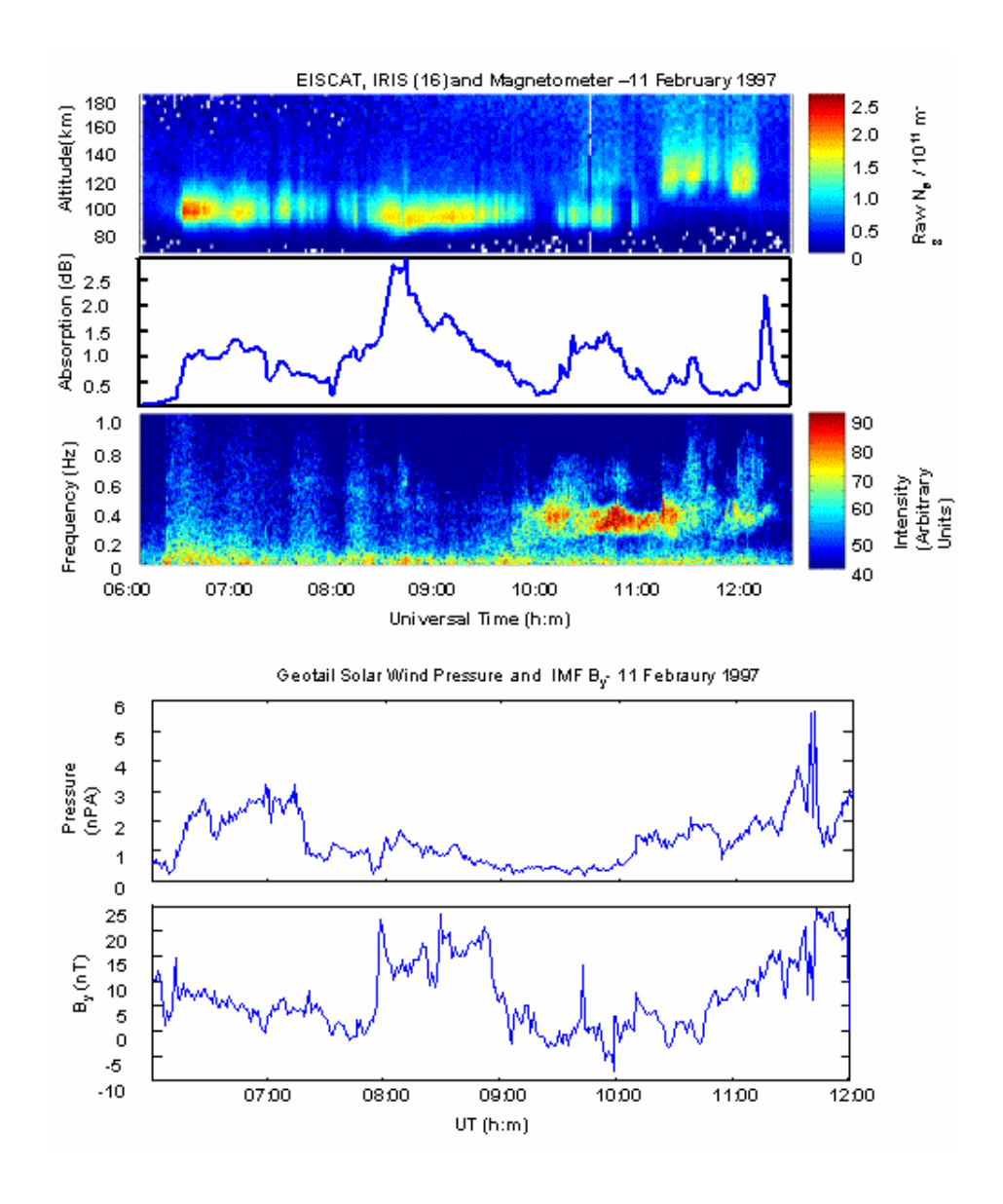


<u>Figure 15</u> Variation of flux-averaged electron energy in the 1-200 keV range, and characteristic energies in various energy ranges (see text for key) in three intervals of EISCAT data. Vertical bars in the top panel show times of substorm onset, as indicated by pi2 activity.

Figure 15 illustrates the flux-averaged energy <E> (blue) over the electron spectrum in the 1-200 keV range, together with the estimated characteristic energies assuming an exponential distribution, (1) in the 98-120 km height range (green) and (2) in the 89-117 km range (black). The magenta line gives the estimate considering a mixed distribution, which is exponential from 120 to 98 km (2-20 keV) and Maxwellian at higher energies. For the 13-14 Feb. 1996 period (top frame), the vertical lines indicate the times of substorm onsets as indicated by bursts in pi2 activity. There is a good correlation between these pi2 bursts and increases in characteristic energy (hardening of precipitation).

The generally close correspondence between the blue and green curves, particularly in top and bottom panels, shows that the flux-averaged energy, which gives a good representation of the characteristic energy Eo, is well estimated by an exponential spectrum in the 98-120 km range. This means that most of the electron flux is concentrated at the lower energy side of the spectrum. On the other hand, the estimate of Eo from an exponential distribution over the full energy range (black curve) is systematically greater than <E>, which means that the flux at higher energies is stronger than in the exponential approximation. This is evidence of the presence of acceleration processes and the fact that a Maxwellian - or even a modified power law - spectrum may give a better representation of higher energy fluxes. The cyan curve shows the estimate of Eo considering the mixed exponential/Maxwellian distribution.

A case study of varying precipitation in the morning sector, and across noon, during an active period on the 11 February 1997 was made using the EISCAT UHF radar and the imaging riometer (IRIS) at Kilpisjärvi. Data from a chain of wide beam riometers and two pulsation magnetometers were also used, in conjunction with satellite and HF radar measurements (see figure 16). Nightside observations were provided by the CANOPUS array of instruments (including a meridian scanning photometer, magnetometers and riometers). The authors suggested that the precipitating electrons at EISCAT were linked to substorm injection and subsequent gradient-curvature drift. A controlling influence from the solar wind has been identified in the form of small-scale pressure changes at the magnetopause, leading to increases in pitch angle scattering in an already unstable energetic population of electrons. The time separation of absorption increases across the IRIS field of view has provided an estimate of the characteristic energy of precipitation. This is due to a lag in the drift time of particles on lower L-shells. Observations of electron density from EISCAT verified that the estimate is reasonable in supporting the gradient-curvature drift theory.



<u>Figure 16</u> EISCAT, IRIS and pulsation magnetometer data from 11 February 1997 compared to lagged solar wind pressure and IMF B_y observations by GEOTAIL. The precipitation appears to be controlled by changes in scattering and diffusion caused by variations in solar wind pressure and direction.

A small increase in particle penetration into the ionosphere has been discussed in relation to increased radial diffusion producing higher energy electrons at lower L shells (Kavanagh et al. 2001). This assumption is based on a dramatic change in the geomagnetic field orientation, transmitted from the IMF, and a near simultaneous increase in precipitation. This precipitation led to enhanced absorption in the nearby riometers, coupled with more energetic particles being injected at the nightside. The electron precipitation then decreased, at the same time as an increase in ion fluxes, the latter being identified in data from an overflight of DMSP F10. This was accompanied by structured pulsations in the Pc1 band. The possibility that these ions arose from the LLBL or BPS has been dismissed. This is not only because of the relatively large distance to the cusp, but also because Pc1 waves were observed to increase in intensity at lower L-shells. Instead it was suggested that the ion precipitation was due to a growth in EMIC waves resulting in pitch angle scattering of ions into the loss cone. This was attributed to an interaction between an enlarged plasmasphere and energetic ring current during the recovery phase of a small to moderate geomagnetic storm. At this later time (>13 MLT), IRIS was located under a region of strong poleward convection. The flows observed by CUTLASS were found to be comparable with the movement of strong absorption patches as derived from the IRIS keogram. This suggested that ExB drift was governing the precipitating particles at this time rather than L-shell separation of the drifting electrons as at event onset (0615 UT to 0637 UT).

3.3.4 Auroral absorption and electric field during substorm and E-region instability conditions

Simultaneous 2-D images from imaging riometer (IRIS) and STARE radar observations have been employed in the study of the spatial extent and structure of 'instability' patches (regions of enhanced coherent backscatter). The temporal evolution of the absorption regions and their correspondence with scattered power and velocity distributions were also investigated. EISCAT provided the electric field and other parameters in the D and E region for the identification of plasma turbulence regimes perpendicular to the magnetic field. In a related study, the correspondence between auroral absorption, electric field and E-region conductivity during the various phases of a substorm was investigated. An overall, inverse dependence between the electric field and the auroral absorption was found that may be explained by the conservation of the perpendicular ionospheric current across the region of enhanced conductivity. The conductivity gradient would generate an opposite ionospheric electric field that reduced the total field. Absorption is basically determined by the high energy side of the precipitation spectrum, thus only if both the 'soft' and 'hard' components were part of the same particle distribution would there be a one to one correlation between increased conductances and absorption. If separate populations of 'soft' and 'hard' energetic particles existed, absorption could increase independently of the electric field strength. Another study of E-region instability, using the EISCAT and STARE systems was carried out by Nielsen et al. (2001). A large high-resolution data set, consisting of joint observations of plasma waves (STARE) and of electron drift velocities (EISCAT) was used to thoroughly investigate the relationship between the wave phase velocities, the electron drift speeds, and the ion acoustic velocity in the unstable E-region.

3.4 LARGE-SCALE CONVECTION AND IONOSPHERIC STRUCTURE

3.4.1 IMF Dependence of Convection

The IMF B_y-dependence of flow in the high-latitude ionosphere has been investigated statistically by Khan and Cowley (2001), based on an extensive database of EISCAT UHF Common Programme 1 (CP1) observations. This was the first study to show that such a response is indeed present, with eastward perturbation flows being present for IMF B_y positive, and westward flows for B_y negative. These flows were found to be of substantial amplitude on the nightside, but to diminish to undetectability by day. Theoretical analysis then showed that the effect is due to a distortion of the magnetospheric field lines, which map an essentially unchanging equatorial magnetospheric flow into the ionosphere. The field distortion is produced by the appearance of a Y-directed perturbation field inside the magnetospheric cavity which has the same sense as the IMF B_y field, such as has been observed by spacecraft, and which is expected theoretically in a magnetically open magnetosphere. The theory shows that the flow effect is much larger on the nightside compared with the dayside because of the extension of the nightside field lines into the tail, compared with the compression of the undisturbed field by the solar wind on the dayside. The theory is able to account for the EISCAT observations both in form and magnitude, and represents an important demonstration of the origin of the IMF By-related asymmetry effects in the terrestrial magnetosphere-ionosphere system.

3.4.2 Coherent Scatter Spectra and High-Latitude Boundaries

Woodfield et al. (2000; 2002a; 2002b) used EISCAT mainland and ESR radar observations with the aim of identifying the mechanisms responsible for the generation of high and variable spectral widths observed by the CUTLASS HF radars on the nightside. The boundary between low and high spectral width in HF radar observations has previously been linked, in this nightside sector, to the polar cap boundary. Woodfield et al. (2000; 2002a; 2002b) presented observations from a total of three intervals, each corresponding to very different geomagnetic conditions. One interval had no associated electrojet activity, the second was during a transition from quiet to active conditions with a clear ion frictional heating event indicating the location of the flow reversal boundary, and the third during an isolated substorm. The work of Woodfield et al. (2000; 2002a; 2002b) indicated that a relationship exists, at least on closed field-lines in the 0300 to 0800 MLT sector, between elevated electron temperature, indicating particle precipitation, and high HF radar spectral width. The power spectra which exhibited high spectral width values were found to be both single-peaked and multiple-peaked, however the authors found that regions of ion frictional heating appeared to correspond to HF scatter in which the spectra were mainly multiple-peaked. The authors concluded that the interpretation of the boundary between low and high HF spectral width as an ionospheric proxy for the open/closed field line boundary might be an over-simplification.

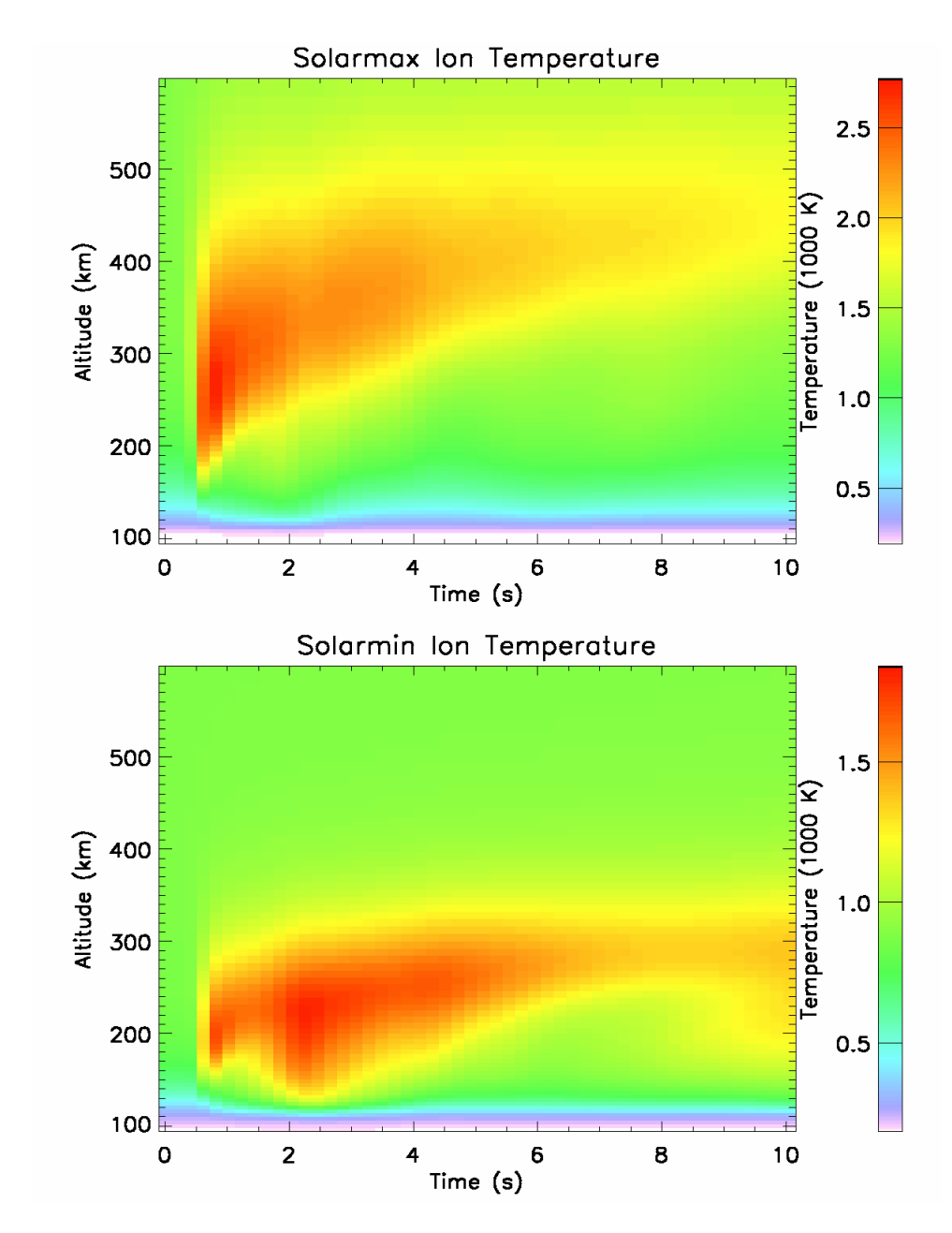
3.4.3 Structure in the polar-cap plasma

Sources of plasma in the polar cap and the mechanisms that give rise to patchy structure are open questions, where the balance between the roles of precipitation and convection are not yet well understood. Observations by the ESR have revealed electron density enhancements in the magnetic noon sector with Bz southward that were identified as possible candidates for polar-cap patches (Smith et al., 2000). Supporting measurements by the EISCAT mainland and CUTLASS radars indicated that the origin of the structures lay upstream at lower latitudes, with the modulation in density being attributed to variability in soft-particle precipitation in the cusp region. The structure in the precipitation appeared to be linked to changes in the location of the reconnection site, following a changing Bx component, resulting in different energy distribution of the precipitating particles. In other studies, enhanced densities observed in tomographic images equatorward of the reconnection footprint appeared to be signatures of the tongue-of-ionisation (TOI). Development of the mapping investigations of the polar cap ionosphere have revealed the TOI penetrating to the nightside and being seen in the midnight sector by the ESR as enhanced cold plasma (Berry, 2000).

3.5 AURORAL PHYSICS

3.5.1 Combination of Auroral Measurements and Models

The combination of modelling with measurements from radar and optical instruments continues to be the most important part of the EISCAT research being carried out at Southampton. The new direction involves optical measurements from Svalbard, using an imaging spectrograph, which provides high spectral resolution measurements of the signatures of both proton and electron aurora. The existing one-dimensional auroral model that simulates the signatures of electron precipitation has now to be combined with code to account for the effects of proton precipitation. Protons can be the source of a considerable flux of secondary electrons, which cause emissions indistinguishable from those caused by primary electrons. Modelling is the only way of separating these. Although it is also impossible to separate the two effects in the radar measurements, they provide important input parameters to the model, and are especially valuable in providing temperatures during proton events, several of which have been measured in the two winters so far with the spectrograph in Svalbard.



<u>Figure 17</u> 2-D model results showing the effect of ion heating in a region between two field-aligned currents.

Collaborative work between the University of Southampton and the University of Alaska has continued, with EISCAT measurements providing the evidence that the three-fluid simulation of the ionosphere-magnetosphere system is a realistic approach. First results of a highly improved two-dimensional simulation have been published, using as motivation a specific auroral event observed both optically and with the mainland radar, using the high temporal resolution of the PULSE experiment. The model is unique in that it resolves the dynamic and nonlinear electromagnetic interaction between the ionosphere and the magnetosphere. It aims to model the fast temporal and small spatial scales associated with filamentary aurora. The research concentrated on the ion and electron heating by different sources, i.e. ion heating from plasma-neutral friction and electron heating resulting from energetic particle precipitation and ohmic dissipation in strong field-aligned currents. A consistent explanation of several observed events confirmed the result published by Lanchester et al. (2001) that rapid heating beside auroral arc elements can be caused by large field-aligned current densities.

Figure 17 shows ion heating results from the model for a region between two field-aligned current layers where the ions are driven by Alfvén waves. The ion temperature increases by frictional heating as a function of time for both solar minimum and solar maximum conditions. The differences are mainly the result of ionospheric conditions responsible for the reflection of Alfvén waves. The EISCAT observations with which this result is compared were obtained during solar minimum (January 1995) and are shown in figure 18. The change in height of the maximum in ion temperature with time was observed in a region outside but close to an optical arc. The maximum ion heating appeared below 200 km (compare with figure 17).

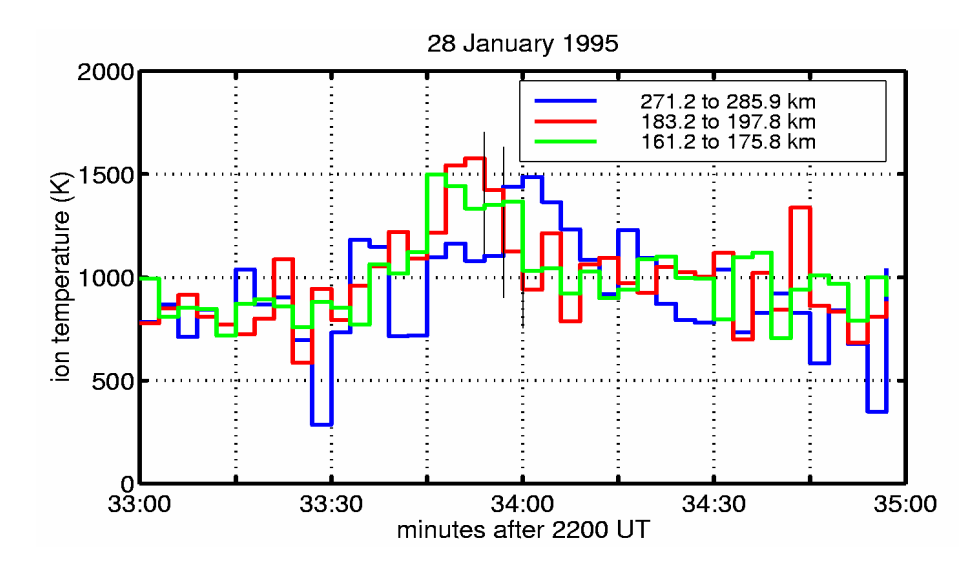
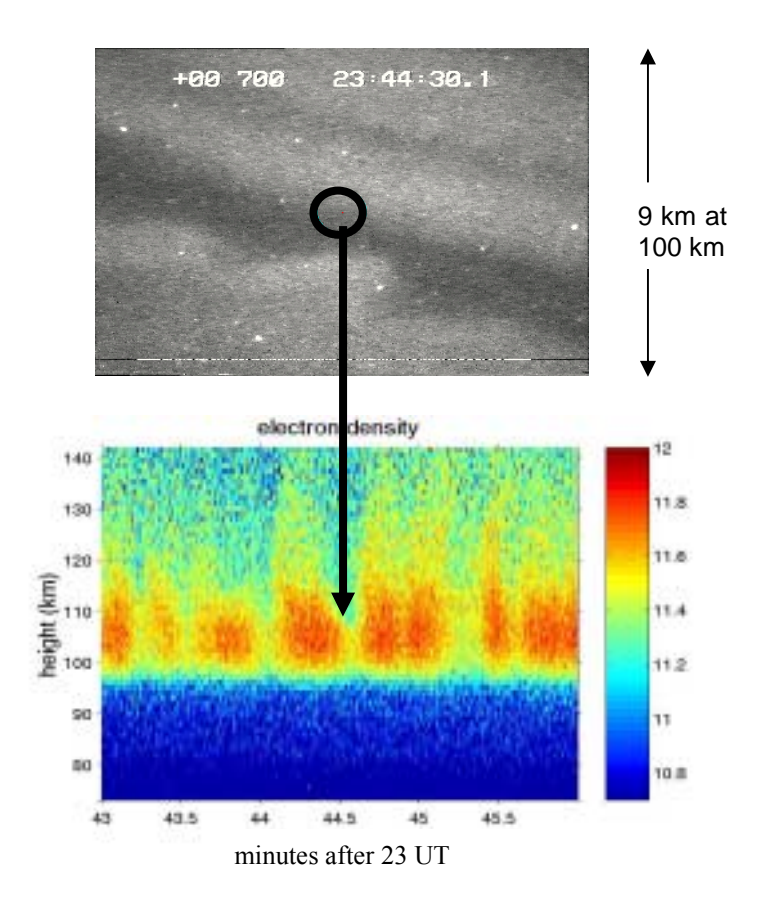


Figure 18 EISCAT ion temperature variations obtained during an ion heating event on 28 January 1995.

During an optical/radar campaign in December 1994, there were several nights when the dominant auroral signatures were the result of both pulsating arcs and the passage of dark patches and lanes within diffuse aurora, often known as 'black aurora'. An example of this is presented in figure 19 showing data obtained with a very narrow angle camera (Max Planck Institute) which images 9 km x 13 km at auroral heights in the field-aligned direction. The changes in electron density during the passage of these dark lanes are also shown in figure 19. Without the benefit of optical data, the signatures could be interpreted as pulsating aurora; the camera showed, however, that spatial features moving through the radar beam caused the variations. The arrow links the time of the image to the radar measurement. The relationship between electron density and optical signature is dependent on the recombination rate and is not instantaneous. Modelling of the density profiles has shown that the energy flux varied between 5-15 mWm⁻² with a sinusoidal variation with time. The energy spectra of the particles causing these features were a combination of Maxwellians throughout, with a distinct monoenergetic component superimposed. The peak energy of this component varied between 5-10 keV, slightly out of phase with the flux variations. The profiles at heights around 120-130 km appeared to be affected by horizontal electric fields during the times of low energy flux. The ongoing work is to identify if field-aligned currents can be detected in the dark regions through changes in the temperatures. This is made extremely difficult by the low signal-to-noise in these regions.

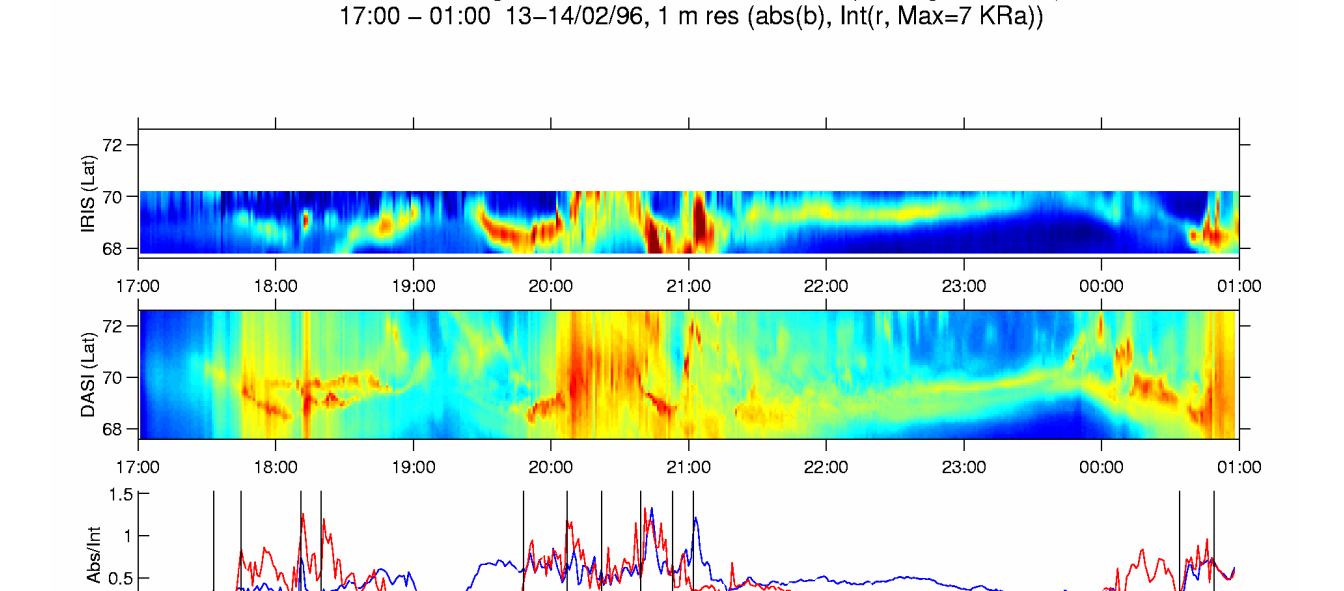


<u>Figure 19</u> Optical and radar data from an interval in December 1994 showing that the apparent temperal variations in the electron precipitation in fact arise from a series of spatial features moving through the observing volume.

3.5.2 Multi-instrument studies of arc dynamics and electrodynamics

Data from the EISCAT incoherent-scatter radar, the IRIS Riometer, the IMAGE magnetometer network as well as the Sussex, DASI and FMI all-sky cameras have been employed in a case study during three multiple substorm onsets (del Pozo et al., 2002a). Observations from the various instruments were compared to establish the concurrency of the radar, optical and absorption signatures of arcs, and to make a detailed study of their dynamics.

Figure 20 shows composite plots for the observation period 13 to 14 February 1996 from 1700 to 0100 UT. Keograms are shown of IRIS absorption at 19.25° longitude (top panel) and DASI 557.7 nm optical emissions (second from top) for the respective fields of view of the instruments. The maximum values, and the corresponding latitudes, for the absorption and the luminosity (normalised to the absorption), in the common field of view, are shown in the third and fourth panels, respectively. The colour scales for the absorption (in dB) and light emission in log Rayleighs are shown on the foot of the figure. The maximum light intensity at the longitude of Tromsø was 7 kR. The vertical lines on the third panel from the top on period (a) mark the times of the multiple expansion phases taken from pi2 pulsations. These times were 1734, 1746, 1812, and 1821 UT, for substorm 1; 1949, 2008, 2023, 2038, 2054, and 2103 UT, for substorm 2; and 0035, 0054 and 0118 UT for substorm 3. Maxima in luminosity and absorption 'spikes' generally corresponded with the pi2 bursts when the substorm westward current disturbance was seen within the common field of view.



21:00

21:00

time (h:m)

IRIS/DASI Keograms, Max Int and Lat of Max (at Long. 19.25° E)

Figure 20 A composite plot of observations from 13 to 14 February 1996 showing keograms of IRIS absorption and optical emission, together with their maximum values and corresponding latitudes. Vertical lines in the third panel mark substorm expansions as shown by pi2 pulsations.

23:00

23:00

2

00:00

00:00

3

log10(DASI, R)

3.5

2.5

01:00

01:00

22:00

22:00

0

Sarfargaleev et al. (2000) analyzed the response of the azimuthal component of the ionospheric electric field to auroral arc activity. They chose three intervals of coordinated EISCAT and TV observations on 18 February, 1993. These intervals included three kinds of arc activity: the appearance of a new auroral arc, the gradual brightening of the existing arc and variations of the arc luminosity. The arcs were mostly east-west aligned. In all cases, the enhancement of arc luminosity was accompanied by a decrease in the westward component of the ionospheric electric field. In contrast, an increase of that component appeared to be connected with arc fading. This observed response was assumed to have the same nature as the "short circuit" of an external electric field by the conductor.

Bogdanova et al. (2001) used a model to predict the motion of nightside auroral arcs during the expansion phase of a magnetospheric substorm. The model was based on the hypothesis that reconnection in the magnetotail plays a central role in substorm development. Auroral arcs were interpreted as the ionospheric manifestation of upward field-aligned currents, induced by shock waves generated during one or more reconnection pulses in the vicinity of an X-line in the magnetotail current sheet. The non-uniform plasma medium in the magnetotail led to dispersion of the shock waves, resulting in poleward and/or equatorward moving auroral arcs. They showed that the morphology and location of the arcs depended on the reconnection electric field in the diffusion region, the plasma density distribution in the magnetotail, and the location of the magnetotail X-line. Comparison of the results with actual observations showed that the proposed model could explain the small-scale structure and several other features associated with observed auroral intensifications.

٥

71

(670 cm) (70 c

19:00

19:00

0.8

20:00

20:00

18:00

18:00

0.4

Absorption(dB)

0.6

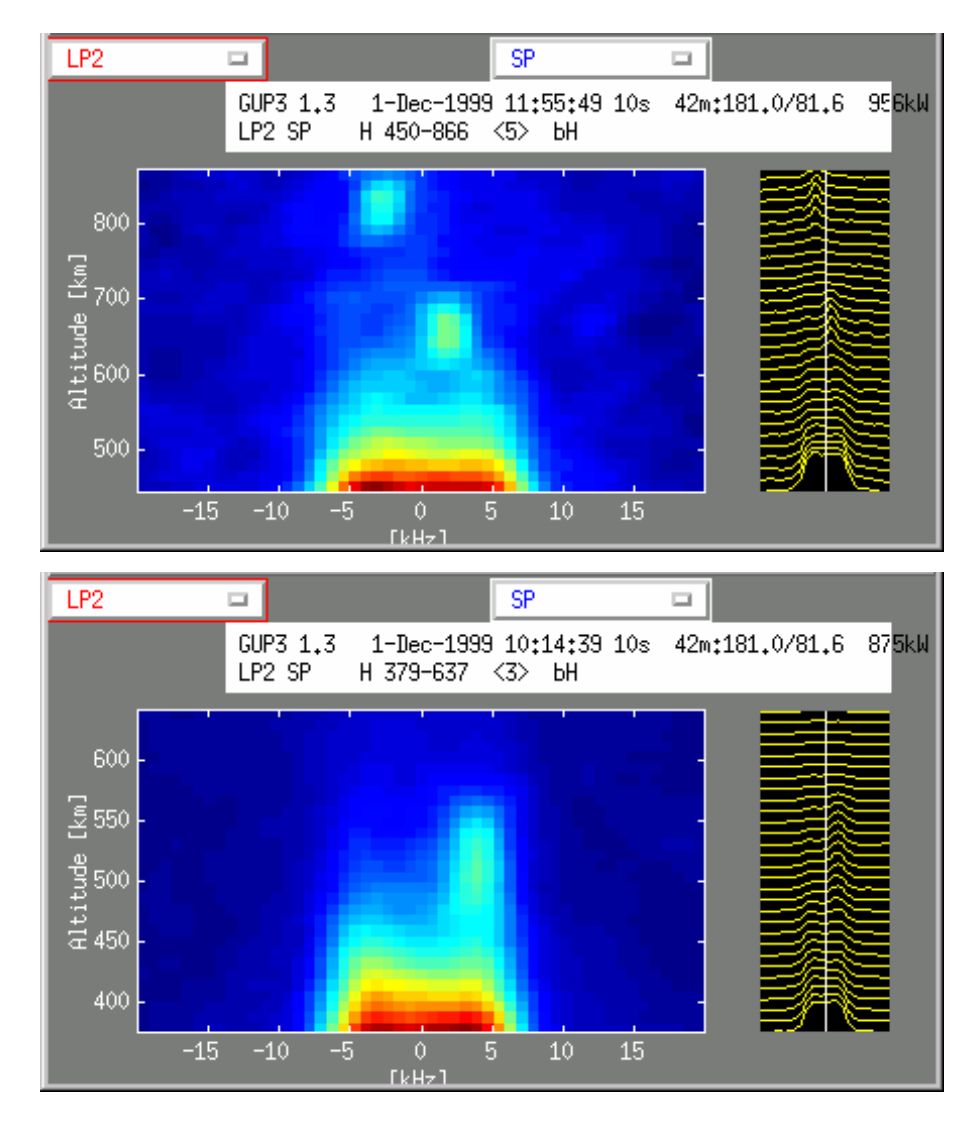
0.2

3.5.3 Cosmic radio noise absorption in the vicinity of auroral arcs

It is well known that Cosmic Noise Absorption (CNA) may occur in the same region as auroral particle precipitation. This is called auroral absorption and it is caused by electron density enhancement in the D- and lower E-region due to energetic particle precipitation. However, in some cases CNA can occur outside of arcs, but in the vicinity of them. The data shows that the hard precipitation into the D-region cannot fully explain the observed CNA. A part of the apparent absorption is produced by high electric fields and plasma instabilities in the E-region. To study under which conditions such events occur, simultaneous optical, CNA and plasma parameter measurements were made by researchers from the University of Lancaster. An all-sky camera made optical measurements at Kilpisjarvi, Finland, (69.02°N, 20.87°E), CNA measurements were taken by the IRIS imaging riometer at Kilpisjarvi and plasma parameters were measured by the EISCAT radar at Tromsø. Details of the mechanism producing the absorption are still under investigation.

3.5.4 Anomalous spectra and auroral instabilities

Work has been undertaken at Sheffield Hallam University using ESR observations made with the gup3 experiment during 1999. Using an automated search programme, times at which enhanced ion line spectra are present in the long pulse data have been identified. Some typical examples, from the data taken on December 1st 1999 are shown in figure 21.



<u>Figure 21</u> Asymmetric ion line spectra measured using the EISCAT Svalbard Radar 42 meter dish on 1 December 1999.

Further examples of such phenomena were reported by Porteous et al. at the 10th EISCAT Workshop in Japan. A small modification to the program, which makes use of the power profile, has enabled occurrences of probable satellites to be distinguished from naturally enhanced spectra in the F region. This method is now being used to obtain statistics of the frequency with which these enhanced spectra occur at different times of the day and in the different seasons of the year. These studies will be expanded in future, using the much larger alternating code data sets available from the gup3 and tau0 experiments.

3.6 ULF WAVES

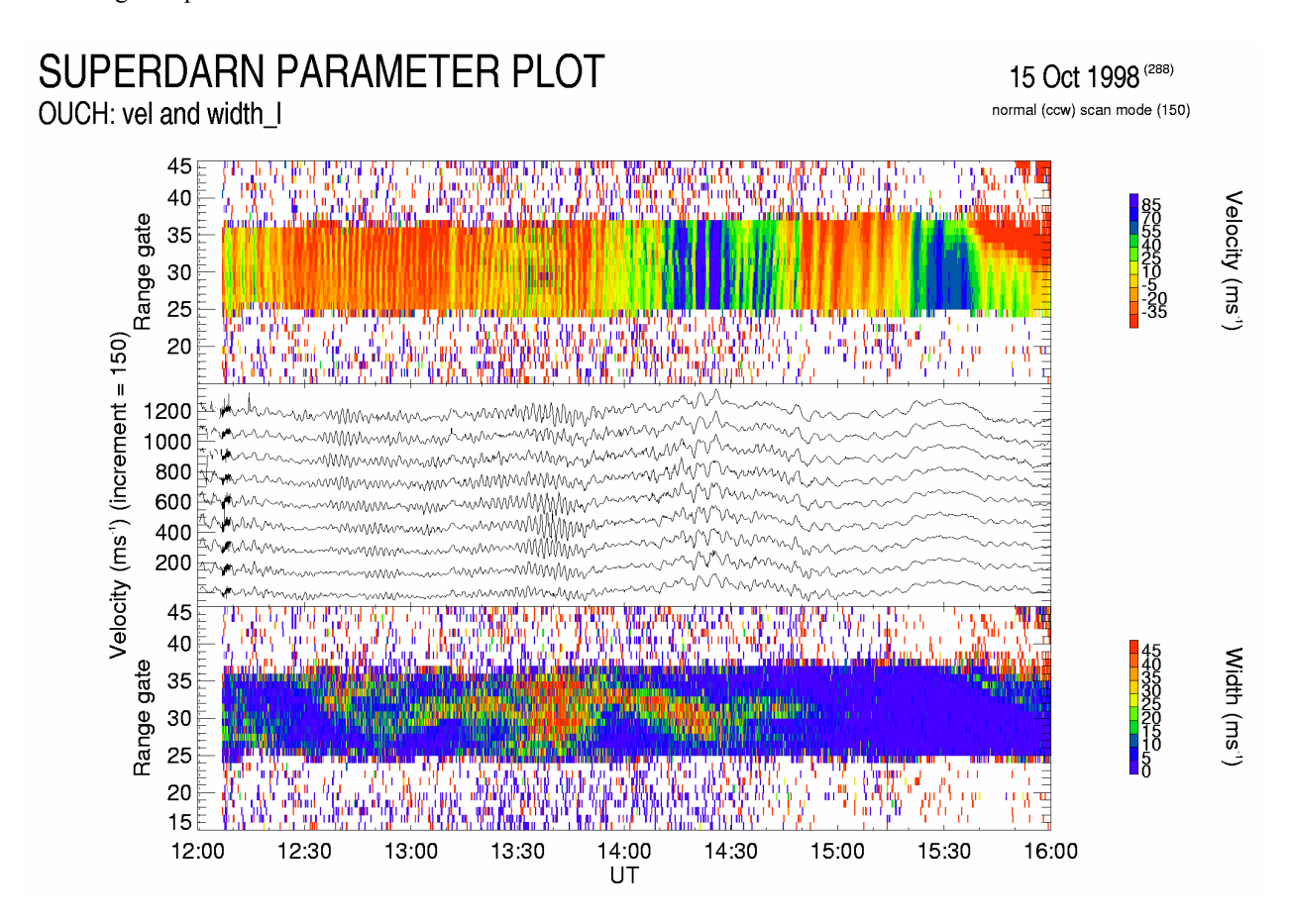
3.6.1 Naturally Occurring ULF waves

Lester et al. (2000) presented observations of a Pc5 wave made using CP1 observations from the EISCAT UHF radar. Although the incoherent scatter technique is ideal for such work, such observations of ULF waves by EISCAT are rare. The authors found that, at least for their interval of wave activity, the relative contribution of the ionospheric conductance and the wave electric field in generating the magnetic perturbation of the wave observed by ground magnetometers varied markedly. This gives important insight into the dominant processes in ULF wave generation.

Moreover, much research has been done into naturally occurring ULF waves in heater-generated artificial CUTLASS HF radar backscatter. The UK special programme SP-UK-OUCH employed the EISCAT high power HF heating facility at Tromsø to generate artificial field-aligned irregularities, which produce high power backscatter observed by both the Iceland and Finland radars of the CUTLASS HF coherent scatter system. The coherent scatter radars were operated in a high spatial and temporal resolution mode, while the heater generated irregularities continuously over a period of several hours. The CUTLASS observations were supplemented by operation of the EISCAT mainland UHF radar, when the latter was available. This technique has proven to be one of the most exciting developments in the use of the Tromsø heater in the last decade; in fact, work involving SP-UK-OUCH has proved pivotal in Dr Darren Wright attaining a PPARC Advanced Fellowship. The artificial scatter can be turned on when natural irregularities are not present, enabling the observation of background geophysical processes at will. Both large-scale field line resonances and small scale particle-driven ULF waves can be observed in this way. Such small scale sized waves, which are generally undetectable by conventional methods, were detected in the line-of-sight velocity data set from the CUTLASS Finland radar and conjugately by the EISCAT mainland UHF radar. Within the volume of intersection of the three UHF receiver beams, the three measured components of line-of-sight ion velocity can be combined to provide the 3-dimensional ion velocity vector. The investigation of these small-scale waves has been the focus of recent research by the Leicester group in this area. Yeoman and Wright (2000; 2001) reported an interval where both drift mode and drift-bounce mode waves were detected in the afternoon sector on 18 October 1999. Conjugate observations from the Polar CAMMICE instrument indicated that the drifting magnetospheric ring current plasma exhibited a non-Maxwellian ion distribution function (IDF). The study identified the 35-45 keV energy range of the plasma as that which fed energy into the drift mode initially and then stimulated the drift-bounce resonance. These two modes represent different harmonic structures of the ULF wave electric field in the magnetosphere. This is the first time a common plasma population has been identified as the energy source for both wave types. Using a similar method, Baddeley et al. (2002) have also identified the plasma population responsible for driving a drift-bounce resonant wave on the morning of 26 October 1999. These waves occur predominantly in the pre-noon sector and, in this case, protons with energies around 10 keV were responsible for its generation.

Furthermore, observations made during SP-UK-OUCH experiments have also demonstrated that the spectral widths, measured by the CUTLASS radars, associated with such particle driven waves are higher than the usually low widths related to artificial irregularities (Wright et al., 2001). Figure 22 demonstrates that the regions of these spectral width features are also spatially localized in the same way as the observed wave activity. Wright et al. (2001) have postulated that the observations may be explained by the existence of ion-cyclotron waves being generated during the wave-particle interactions which generate the small scale waves. This indicates that such experiments provide a good proxy for cusp related HF radar backscatter since the high spectral widths observed in this region are thought to be the result of spectral broadening by similar high frequency wave activity.

A great deal of the heater-related research described in this report is relevant to the future operations of the SPEAR radar (Wright et al., 2000). The system, which is under construction by the Leicester group, is due to be deployed later this year and first operations will occur in Spring 2003. Not least, this system will provide a unique means of exploring the ULF waves modes and their generation mechanisms, which occur in the polar cap and cusp regions of the magnetosphere.



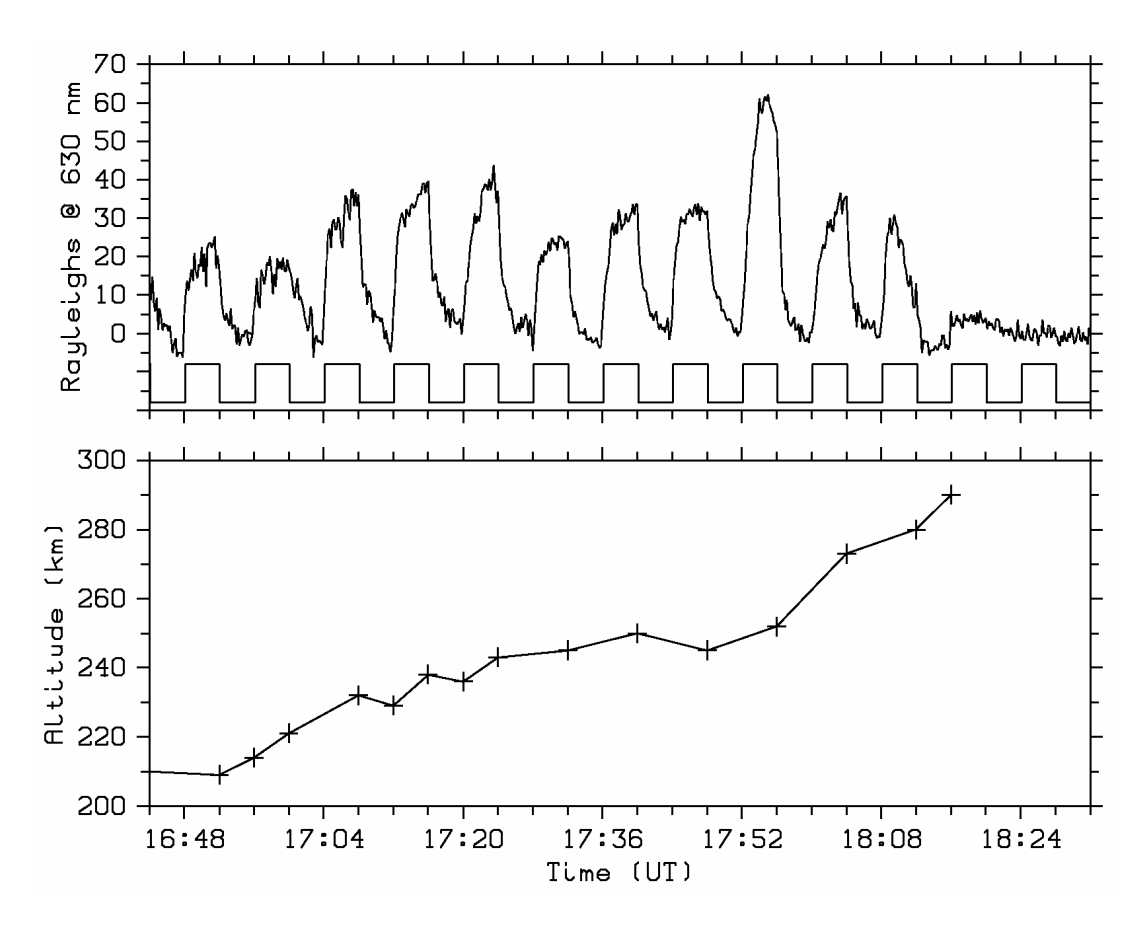
<u>Figure 22</u> CUTLASS measurements during the run of SP-UK-OUCH on 15 October 1998 showing range-time-velocity data (upper panel) from beam 5 of the CUTLASS Finland radar. The band of scatter represents measurements of heater-generated irregularities and the line-of-sight flows are modulated by the ULF wave activity. Stacked time series at various range gates through this region (middle panel) indicate the presence of particle driven (drift-bounce mode) waves in the interval 1230 to 1400 UT. The longer period waves later in the interval are the signatures of a large-scale field line resonance. The radar spectral widths (lower panel) indicate enhanced widths associated with the particle driven wave activity (after Wright et al., 2001).

3.7 IONOSPHERIC MODIFICATION

3.7.1 Heater-Stimulated Airglow

In a collaborative project between Lancaster University, MPAE (Germany) and IRF (Sweden), artificial aurora have been generated in the F-layer using the EISCAT HF-facility. There have been several campaigns investigating various aspects of the phenomenon since the initial successful observation of a 630 nm artificial aurora in February 1999 (see previous EISCAT report). For example, in October 1999, EISCAT beam swinging experiments found that the electron temperature enhancements due to HF pumping sharply maximise along the magnetic field line. In November 2000, frequency stepping experiments found that the artificial aurora disappears when pumping on the third electron gyro-harmonic frequency and the first 557.7 nm artificial aurora was observed. In February 2001 HF beam swinging experiments showed that the optical emission always appears on the magnetic field line regardless of the HF beam pointing direction; and in November 2001 the first 427.8 nm artificial aurora was observed.

On 21 February 1999 an HF-induced artificial aurora at 630 nm was observed by the Digital All-sky Imager (Kosch et al., 2000a). DASI is located near Skibotn (69.35° N, 20.36° E) in Norway, about 50 km from EISCAT. The transmitter was operated in a 4-min on, 4-min off sequence at 4.04 MHz O-mode with the beam pointing vertically. The effective radiated power was estimated to be 73 MW. The optical emission reached a peak intensity of about 100 R above background and appeared equatorward of the HF beam's projection on the reflection altitude, which was obtained from ionograms. The top panel of figure 23 shows the average intensity of the airglow above background for 630 nm. The square wave shows the HF on/off cycle. The bottom panel shows the variation of the 4.04 MHz O-mode reflection height as determined from real-height inversion of ionograms during the experiment.



<u>Figure 23</u> Intensity of 630 nm airglow on 21 February 1999 compared to the heater cycle (upper panel). The lower panel shows the time variation of the 4.04 MHz O-mode reflection height.

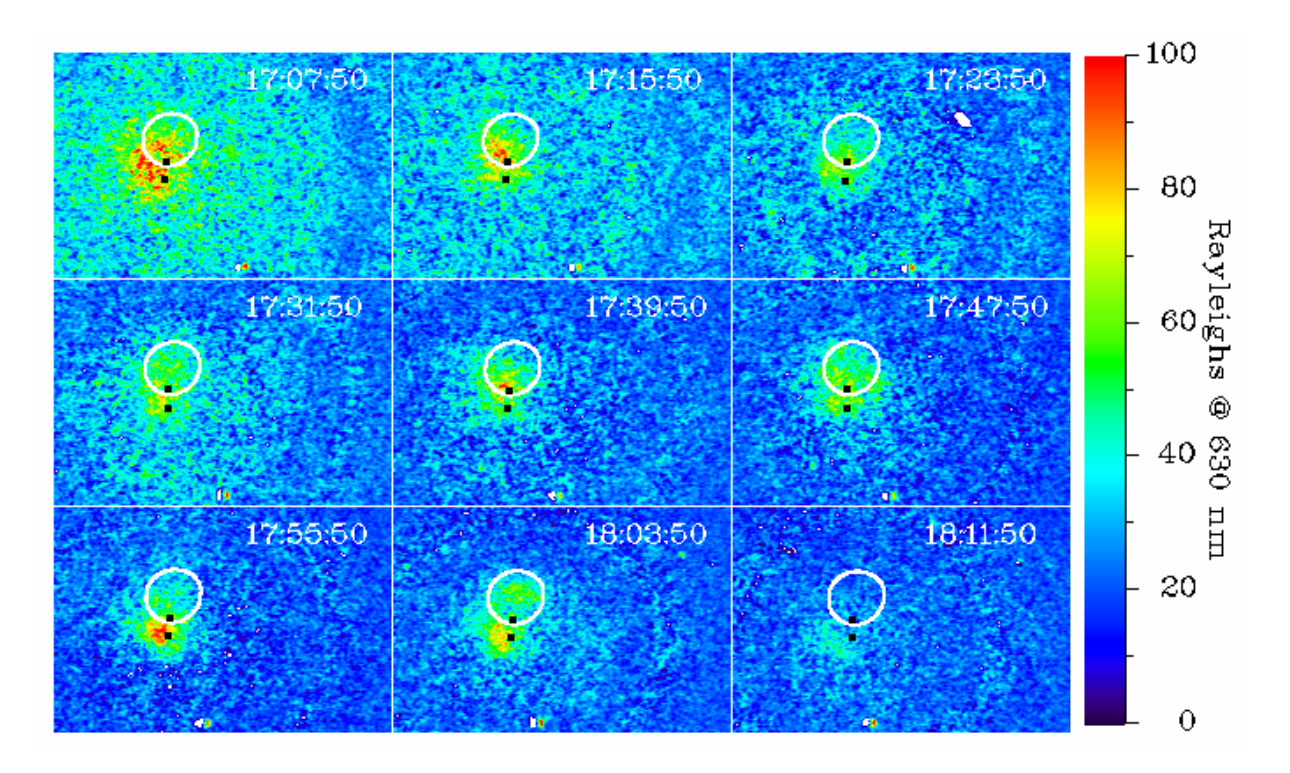


Figure 24 Imager data from Skibotn on 21 February 1999 showing heater stimulated airglow in the last 10 seconds of each "heater on" period. The white circle represents the mapping of the heater beam at the 3 dB level, while the black squares represent the Spitze angle (inside the circle) and the location of the Tromsø field line (outside the circle).

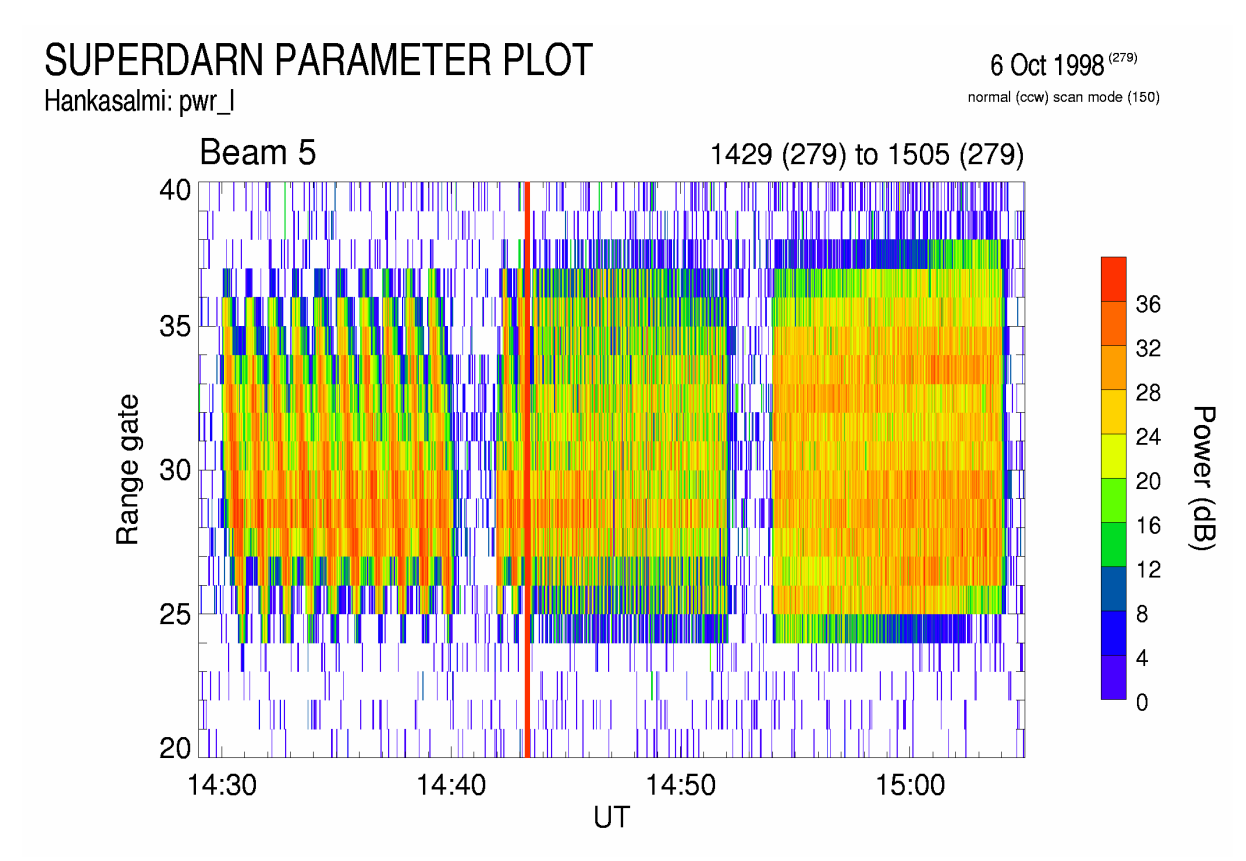
Each panel of figure 24 shows the last 10 second integration image of an HF "heater on" cycle in false colour. The field of view is in the zenith above Skibotn with north and east to the top and right, respectively. The images are background subtracted and calibrated into absolute Rayleighs at 630 nm. The start time of each integration is overlaid in the images. The white circle is the real-height mapping of the modelled HF beam at the –3 dB level. The black square inside and outside the circle corresponds to the Spitze angle (6°) and the magnetic field line through the HF facility (12.8°), respectively. Generally, the region of maximum aurora was always displaced towards the magnetic field line (zenith angle = 12.8° S) passing through the HF-facility. This was a unique feature of these observations. Artificial aurora is thought to be excited either by electrons energised to several eV by plasma turbulence, or by thermal electron temperature enhancement. Such localisation towards the magnetic field is unexpected for both mechanisms and suggests this feature may be important at high latitudes. There is also a small but growing body of evidence that various HF pumping effects maximise in the vicinity of the Spitze (6° S) and magnetic dip angles. Ion and plasma line enhancements are most strongly observed between the Spitze and magnetic dip angles both on the topside and bottomside of the ionosphere. O-mode HF pumping clearly results in significant electron temperature enhancements, which maximise sharply along the magnetic field aligned direction.

3.7.2 Artificial Irregularities

During the UK EISCAT campaign in October 1998, the heater was operated such that it included spatial sweeping experiments that utilised the capability of the heater to change its pointing direction instantaneously. The pointing direction of the heater beam was steadily altered from 30° north to 30° south in periods of 1 minute, 10 seconds and 1 second. Dhillon (2001) found that the maximum backscatter power from the artificially generated F-region field-aligned irregularities, observed by the CUTLASS Finland radar, was greater for the 1-minute scans than that for the 10-second and 1-second scans. This was due to the heater beam exciting a particular area for a comparatively longer time (see figure 25). For the case of 10-second and 1-second sweeps, the backscatter power level was lower because a particular area of the ionosphere was being excited less strongly. Simultaneous EISCAT UHF data revealed that the electron temperature was generally higher for 1-minute spatial sweeps than that for the 10-second and 1 second spatial sweeps. However it was actually found that the strongest heating effect occurred for the periods where the pointing direction of the heater beam was not varied during the period of "heater on". While the CUTLASS backscatter from the northernmost and southernmost extents of the heated patch decayed away between consecutive sweeps, the backscatter power in the central region of the heated patch did not fall as much. The central

part of the heated patch was illuminated almost continuously due to the sizable width of the heater beam. It was found that the highest backscatter powers occurred to the south of the centre of the heated patch, corresponding to the heater beam pointing in the field-aligned direction. This indicates that heating generates irregularities most effectively in this direction. Moreover, preliminary results reported by Dhillon (2001) and Dhillon et al. (2002) have indicated that the coherence time of field-aligned irregularities generated artificially by the EISCAT heater is typically at least an order of magnitude longer than that for naturally occurring irregularities.

Kolesnikova et al. (2002a) investigated the temporal characteristics of the growth of artificial F-region irregularities produced by the EISCAT heater in the F-region. They found that their observations were consistent with the weak nonlinear theory of the thermal oscillating-two-stream instability, which is thought to be responsible for the heater-generated irregularities at Tromsø. Robinson (2002) has also developed a new theory of the interaction between HF radio waves and heater generated irregularities which for the first time includes multiple scattering effects; this theory is in good agreement with a range of experimental observations carried at Tromsø.



<u>Figure 25</u> Backscatter power observations from beam 5 of the CUTLASS Finland radar. Three 10-minute intervals when the heater beam was being swept spatially from 30° north to 30° south are shown. From 1430 to 1440 UT, this scanning period was 1 minute. From 1442 to 1452 UT, the scanning periods were 40 seconds and 10 seconds, with the change from 40 seconds to 10 seconds indicated by the vertical line just before 1444 UT. From 1454 to 1504 UT, the scanning period was 1 second.

Robinson et al. (2000) reported the first ever example of an artificial ULF wave being excited by the HF heater and subsequently detected by the FAST spacecraft. During UK special programme (SP-UK-HEAT) operation on 8 October 1998, the heating facility at Tromsø was employed to impose a 3 Hz modulation on the pre-existing current system, which constituted the auroral electrojet, resulting in the injection of field-guided ULF waves into the magnetosphere. The electric and magnetic field signatures of the waves were detected directly by the FAST spacecraft, at 2500 km altitude, mapping convincingly in spatial extent to that region of the ionosphere illuminated by the heater. More unexpectedly, the satellite observed a signature in the field-aligned downward electron flux. This was postulated by the authors to have resulted from the interaction of the ULF waves with the upper boundary of the ionospheric Alfvén resonator, due to the presence of a highly localised parallel electric field. Moreover, the electron fluxes observed by FAST were velocity dispersed, which enabled their acceleration region to be located at several hundred kilometers above the spacecraft.

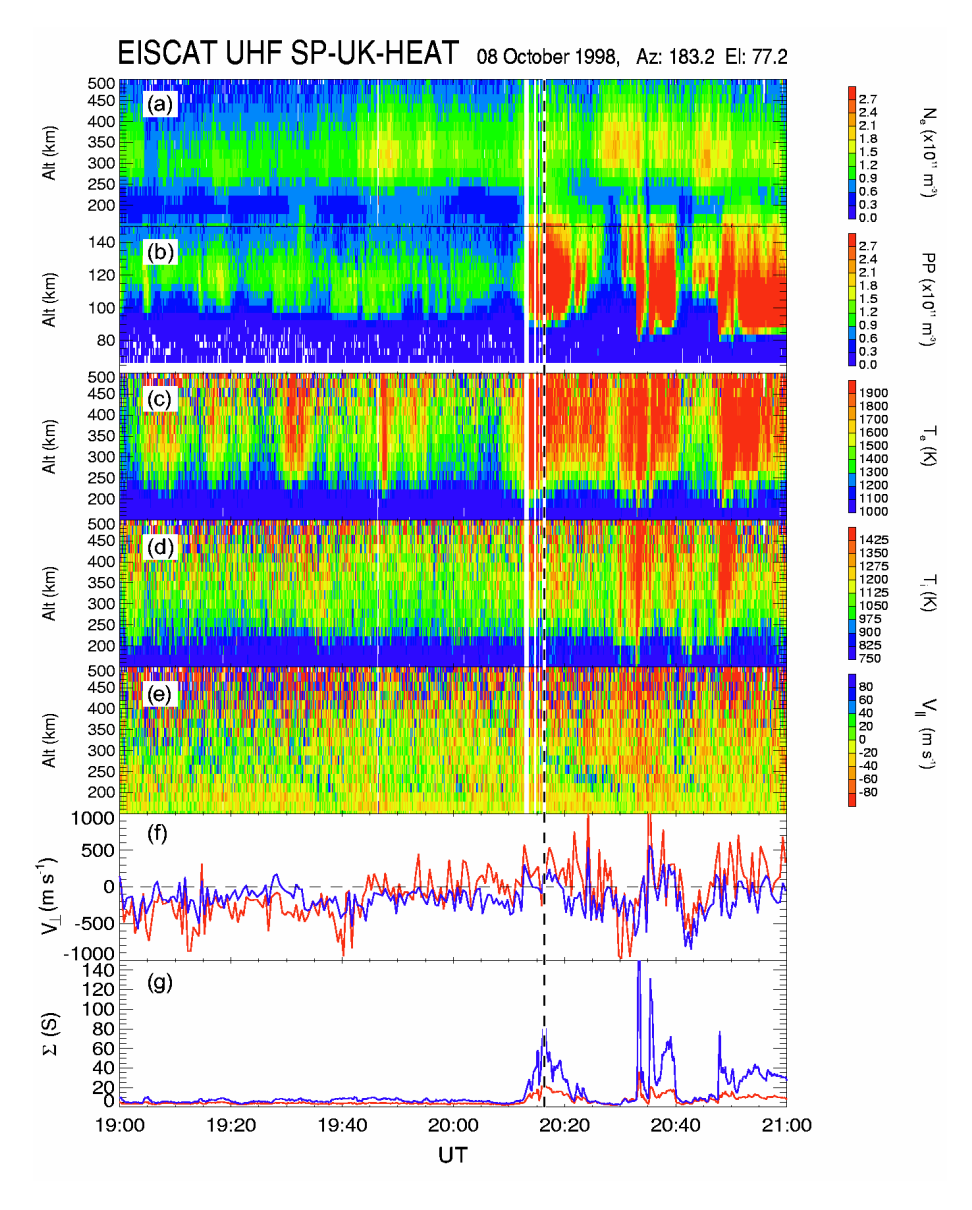


Figure 26 Data taken during the EISCAT Special Programme of 8 October 1998 in which a ULF wave was artificially stimulated using the heater, and subsequently detected by the FAST satellite. The panels show the electron densities measured by the long pulse (a) and power profile (b), long pulse measurements of the electron and ion temperatures and field-parallel ion velocities ((c), (d) and (e), measurements of the field-perpendicular ion velocity (f) and the derived values of the height integrated Hall and Pedersenconductivities (g). The power profile measurements (b) and (g) show the occurrence of substorm activity after 2015 UT.

Wright et al. (2001b) has evaluated these results in the context of the prevailing ionospheric conditions during the experiment and discussed the significance of the substorm activity, which occurred during this interval. The occurrence of the substorm is revealed by evidence of precipitation in simultaneous EISCAT UHF observations, which are reproduced in figure 26. This technique, which can be used to 'tag' narrow flux tubes, could play an important part in overcoming mapping issues between ground- and space-based observations of phenomena which couple the ionosphere and magnetosphere. Field-line tagging is, in fact, one of the key capabilities of the SPEAR facility, currently under construction on Svalbard (Wright et al., 2000).

A theoretical model was subsequently developed in an attempt to explain these observations, which provided general quantitative agreement with the observed field and particle flux strengths associated with the artificial ULF wave (Kolesnikova et al., 2002b). This involved detailed modelling of the modification of the electrical conductivity of the lower ionosphere and the subsequent generation of Alfvén waves within a highly localised source region. The EISCAT UHF data provided information about the electrojet current and the plasma densities in the ionosphere. Knowledge of the electron density profile was, in fact, crucial in determining both the excitation efficiency of the ULF wave, and its subsequent propagation characteristics in the magnetosphere. Cash et al. (2002) investigated in more detail the time history and spectral content of the observed downward electron fluxes by considering the effects of a localised parallel electric field on the electron energy distribution. Furthermore, the authors demonstrated that a power law electron energy distribution described the time variations in the observed fluxes better than the Maxwellian distribution assumed in the modelling work of Kolesnikova et al. (2002b).

3.7.4 Validation of CUTLASS system performance

Both the EISCAT mainland and Svalbard sites lie under the combined field-of-view of the CUTLASS HF coherent scatter radars of the SuperDARN network enabling both systems to be used in concert. The incoherent and coherent scatter techniques are highly complementary in nature, with incoherent scatter supplying the in depth information necessary for the accurate interpretation of coherent returns and HF scatter, in return, providing the potential for a large-scale convection pattern in which context to place the incoherent scatter observations. The common observing volume of the coherent and incoherent scatter radar systems has also offered the opportunity of an inter-comparison of the velocity field deduced from the two techniques. Results presented by Davies et al. (2000), based on the EISCAT special programme SP-UK-CSUB, revealed the irregularity drift speed from the HF radar at Hankasalmi to be in good agreement with ion velocities from the VHF radar and indeed the EISCAT Svalbard radar (ESR). This study supports the view that the motion of F-region irregularities is governed by the ambient plasma flow, but is also highly useful for system validation purposes.

Currently the ground location of HF returns for the SuperDARN radars are routinely determined by a simple range finding algorithm, which takes no account of the prevailing HF propagation conditions. This is in spite of the fact that both direct E- and F-region backscatter and 1½-hop E- and F-region backscatter are commonly used in geophysical interpretation of the data. The accuracy with which the location of backscatter can be determined is becoming a critical issue, not least due to the increasing importance of the multi-instrument approach to solar-terrestrial physics research. HF radar backscatter which has been artificially-induced by the EISCAT heater has been used to provide a range calibration for the SuperDARN radars, employing the entire dataset collected so far during runs of SP-UK-OUCH (Yeoman et al., 2001). The known ground range, the measured radar slant range, and the group path calculated by a ray-tracing simulation have been compared. The modelled group path and measured slant range agree remarkably well. The standard algorithm for backscatter ground range location is found to be accurate to within 16 km and 60 km for direct and 1½-hop backscatter, respectively. Any 2½-hop backscatter would result in very significant range errors. Jones et al. (2001) have reviewed general propagation aspects of the CUTLASS radars, including propagation during artificial modification experiments.

3.8 IONOSPHERE – THERMOSPHERE INTERACTION

3.8.1 Variability of Joule Heating

A considerable fraction of the solar wind energy that crosses the magnetopause ends up in the high-latitude thermosphere-ionosphere system as a result of Joule heating, the consequences of which are very significant and global in nature. Often Joule heating calculations use hourly averages of the electric field, rather than a time-varying electric field. This leads to under-estimates of the heating. A study by Rodger et al. (2001) has determined the magnitude of this under-estimate of Joule heating by analysing electric field data from the EISCAT Incoherent Scatter Radar. It was found that the under-estimate by using hourly-averaged electric field values is of order 20%, with an upper value of about 65%. Using their analysis procedure, the authors showed that these values are remarkably insensitive to changes of solar flux, magnetic activity and magnetic local time, implying that the electric field fluctuations are linear related to the amplitude of the electric field. They then used a coupled ionosphere-thermosphere model to calculate the local changes these under-estimates in heating rate caused to the neutral temperature, mean molecular mass and meridional wind. These changes were each in the order of a few percent. These variations cause a reduction in the peak F-region concentration of around 20% in the summer hemisphere at high latitudes, and about half this level in the winter hemisphere. Rodger et al. suggested that these calculations could be used to add corrections to modelled values of Joule heating.

3.8.2 EISCAT and Fabry-Perot Interferomenters

F-region thermospheric winds follow, but generally lag behind, the ion drift pattern of magnetospheric convection. Analysis of the ion-neutral momentum exchange equation shows that ion-drag and thermal pressure are the major contributors to neutral momentum forcing at F-region heights with relatively minor effects from coriolis, advection and viscous forces. An ion-neutral coupling time constant (e-folding time τ_{in}) has been defined, which describes the time taken for the neutral gas velocity to approach the ion velocity after a step change in convection.

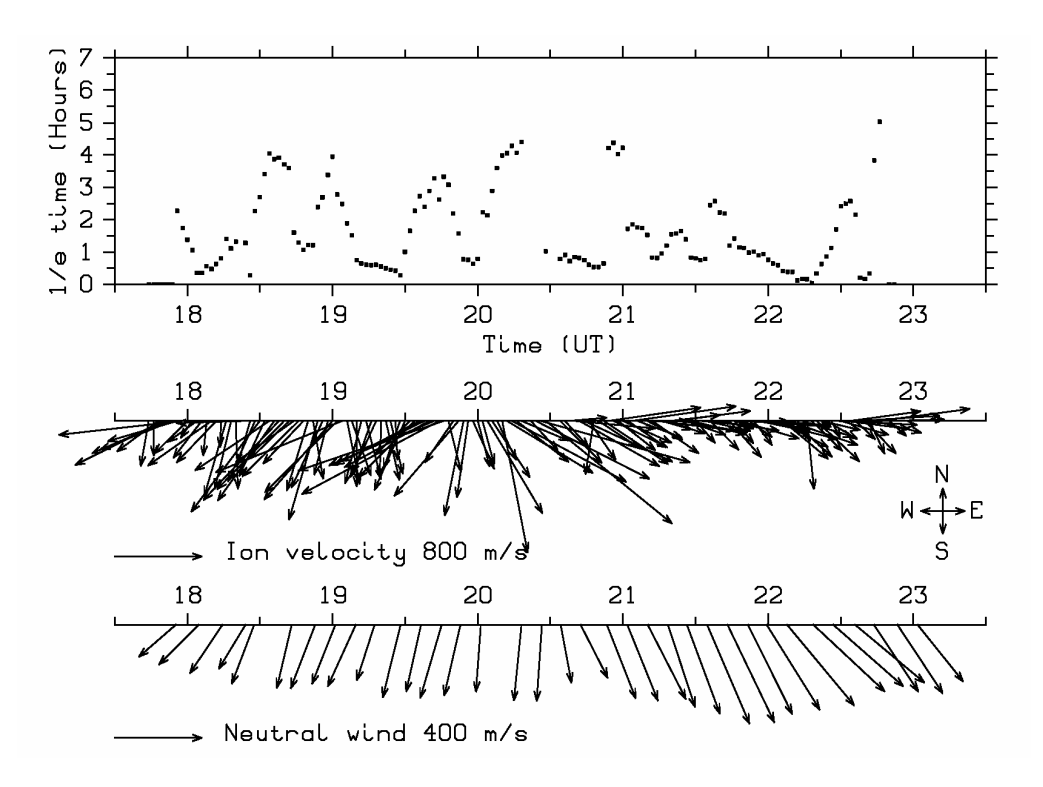


Figure 27 Measurements of the ion-neutral coupling time constant τ_{in} (top panel) together with ion velocities measured by EISCAT and neutral winds measured by FPI at Skibotn on 9 November 1998.

$$\tau_{in} = \frac{(V_i - U_n)}{\partial U_n / \partial t}$$
 sec

where V_i is the ion drift velocity and U_n the neutral wind vector. EISCAT and the Skibotn (69.35° N, 20.36° E) Fabry-Perot interferometer have observed F-region ion drift and neutral winds, respectively. For 9 November 1998, figure 27 shows τ_{in} (top panel), V_i at 250 km altitude (middle panel), and U_n in the upper thermosphere (bottom panel) from observations of the 630 nm airglow emission (Kosch et al., 2001a). As expected, V_i and U_n displayed the same general pattern with the ion flow being more variable than the neutral wind. Clearly, ion-drag was the major forcing term with the zonal wind component being westward prior to 2030 UT and eastward thereafter. τ_{in} varied between 0.5 and 5 hours and had an average of 1.8 hours, which is consistent with previous satellite measurements of 0.5 to 3.5 hours. This result is the first high-latitude measurement of τ_{in} using ground-based observations.

Work at University College London has focussed on studies of the coupling between the magnetosphere and thermosphere. A key aspect of this work is the investigation of how thermospheric inertia delays the deposition of energy and momentum into the upper atmosphere, or conversely, when the driver is turned off acts, as a flywheel and returns energy to the ionosphere/magnetosphere due to the neutral wind dynamo.

EISCAT observing time has been allocated to the study of these effects but conditions have not yet been ideal in terms of a sudden change of driving electric fields, so the data have so far been used mainly as tests of the necessary analysis routines. The experiment was done in conjunction with the UCL Fabry-Perot Interferometers at Svalbard and Kiruna. Over the past two years the analysis of the FPI data to give temperatures has improved immensely and so both neutral wind and temperature are now available for ion-neutral coupling studies. The instruments are now calibrated regularly and reliable absolute temperatures have been available for two seasons. The database (back to 1981) has also been reanalysed, and although it is difficult to give absolute temperatures when no calibrations are available, the relative temperatures are available for much of the last 2 solar cycles! This work has been helped by the availability of EISCAT data near the Kiruna instrument. The comparison is useful, since the minimum Ti values from the radar can be considered as a passable calibration level for the Tn from the FPIs when conditions are quiet.

In collaboration with RAL (C.J.Davis visiting fellowship) the UCL group are examining why the simple meridional wind derivation from radar data only works in the average sense. Their study has investigated whether alternative insights can be derived from the comparison of detailed radar and FPI data (for example, in sudden increases or cessations of the electric fields). Their work also considers the discrepancies in modelled winds and energy inputs found when the highly averaged satellite or radar data is used as the high-latitude plasma flow and particle precipitation input to models such as CTIP (the Coupled Thermosphere Ionosphere and Plasmasphere model). Codrescu (2000) has attempted to quantify the way that ignoring the small- and meso-scale structure in the electric fields causes global numerical models to underestimate Joule heating. The study at UCL seeks to improve on Codrescu's results noting that, while Joule heating is underestimated, ion drag is overestimated. Estimates could be much improved by the use of ion velocities calculated from tristatic data, as opposed to averaged velocities derived from Millstone Hill "Foster fields", and a better accounting for the role of meso-scale ion-neutral interactions in determining the Joule heating. These are two areas where data from the EISCAT radars and an upgraded FPI could offer a substantial improvement. Further recent work at UCL has included a study of gravity wave activity in the FPI data. These have been related to wave signatures in the Cutlass radar data and it is planned to use EISCAT and ESR measurements to characterise them in more detail. A paper is also in preparation on the possibility of eddy motion in the thermosphere, which expresses severe reservations about the "turbillon" theory put forward by Lilensten and Amblard (2000).

3.9 TIDES AND THE MESOSPHERE

3.9.1 Tidal Measurements by the EISCAT Svalbard Radar

One of the most unexpected results to arise from the EISCAT Svalbard Radar has been the surprising discovery that strong tidal or quasi-tidal modes are present in the ionosphere above Svalbard with periods of 24, 12 and 8 hours. Classical theory, based on Hough modes, suggests that tides so close to the North Pole should be extremely weak, so that the results reported by van Eyken et al. (2000) appear extremely puzzling. These authors showed that semi-diurnal oscillations with amplitudes as large as 50 ms⁻¹ could be observed. Weaker diurnal and ter-diurnal modes were also seen. Both the semi-diurnal and ter-diurnal modes displayed the consistent phase progression with height expected from tidal modes. At the lowest heights, around 93 km, there was evidence of a 2.5 day planetary wave, together with other oscillations which could have arisen from non-linear interactions between tides and planetary waves. In order to confirm these conclusions, a number of long ESR experiments have been undertaken in the last two years – the longest being a 15-day continuous Common Programme in February 2001, the results of which are presently under investigation.

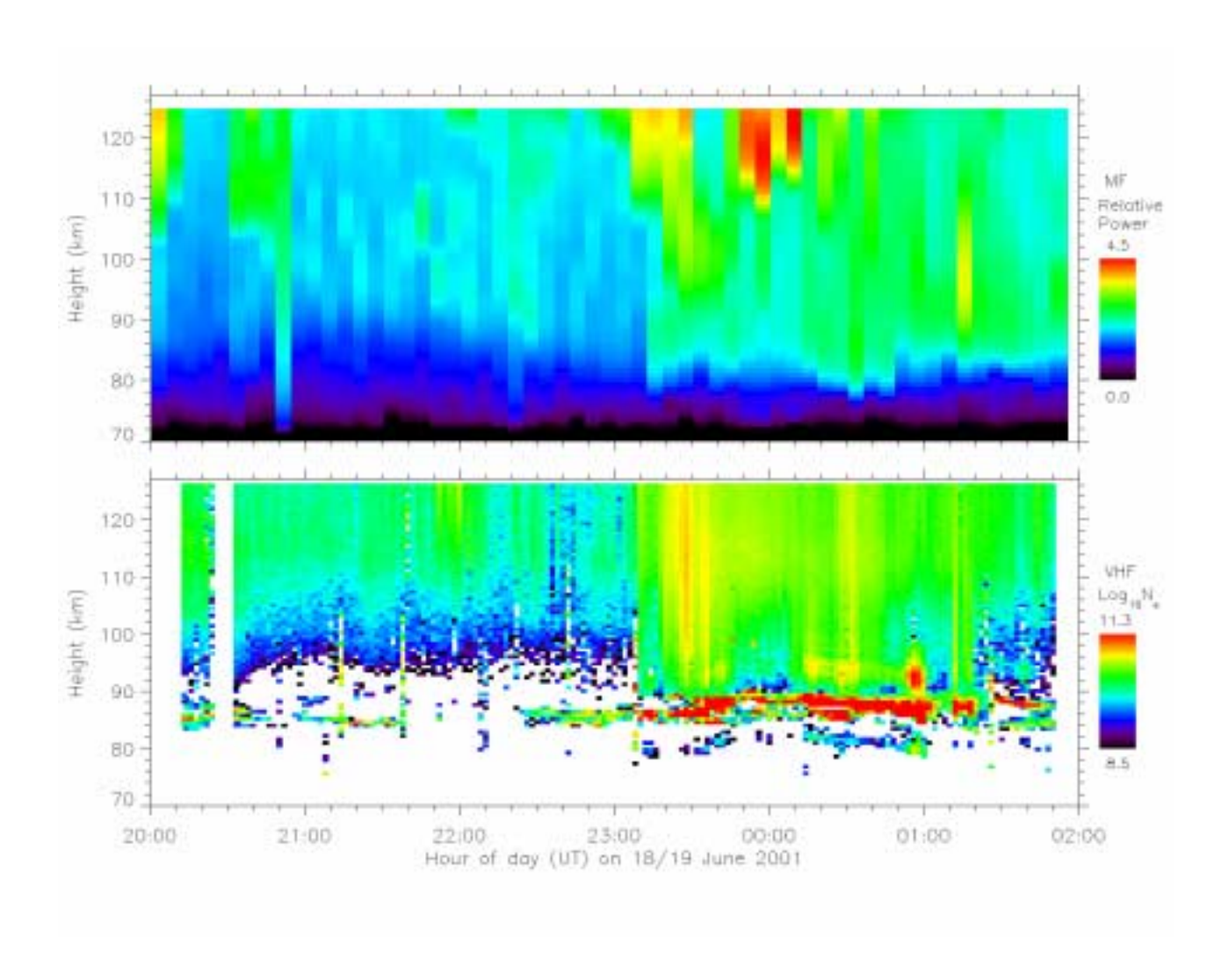
3.9.2 Polar Mesosphere Summer Echoes

During June 2001, an UK campaign took place to co-ordinate EISCAT observations with the MIDAS (Middle Atmosphere Dynamics and Structure) rocket campaign at Andøya, Norway. A joint UK/Norwegian experiment, SP-UK-MFPS, was run on the EISCAT VHF radar using time allocated to Owen Jones (BAS), Alan Aylward (UCL) and Ulf-Peter Hoppe (FFI, Norway). The overall aim was to carry out a "Multi-Frequency PMSE Study" which formed part of an on-going inter-hemispherical comparison of the high-latitude mesosphere using measurements from northern Norway and the Antarctic.

The new EISCAT "D-layer" experiment, a successor to cp6 based on coded pulse-to-pulse correlation, was run for several hours on consecutive nights around midnight, successfully covering the launch of both MIDAS-instrumented rockets from Andøya. The new experiment was able to monitor both the background D-region ionisation and the occurrence of Polar Mesosphere Summer Echoes (PMSE), recording spectral information at several different frequency resolutions simultaneously. In addition, the Dynasonde (digital ionosonde) at Tromsø was operated in a mesospheric mode in order to record partial-reflection scatter from the ionised D-region and to measure neutral wind velocities.

Analysis of the data sets is currently underway with the aim of understanding the contribution of the background D-region to the formation and variation of PMSE. An example of simultaneous data at both 224MHz (EISCAT VHF) and 3.15MHz (dynasonde MF) is illustrated in figure 28. Both coloured panels cover the same time and height ranges, with the upper panel showing the strength of partial-reflection scatter seen by the Dynasonde, and the lower panel the electron concentration seen by EISCAT-VHF radar. These parameters are related, though not directly comparable, and serve to highlight several features. In particular, the strong PMSE evident at VHF near 85-90 km were absent at MF, as expected, given the large difference in radar wavelength and corresponding scale sizes probed. However, the background ionisation in the D-region was seen by both radars, particularly in features such as the sharp precipitation-enhanced increase in electron concentration at 2310 UT. This increase corresponded to a noticeable strengthening of the PMSE layer – one of a number of phenomena under study using the MFPS dataset.

Work on PMSE at University College London has been revisited by Yakov Istumin, a Leverhulme Visiting Professor at APL for 6 months from October 2001. Prof. Istumin has recently completed some previously unfinished theoretical work explaining PMSE in terms of ice formation at the mesopause and the effect this has on the electron diffusion coefficients. A paper reporting these results is in preparation.



<u>Figure 28</u> A comparison of simultaneous data taken by the EISCAT Dynasonde at MF frequencies (upper panel) and the Tromsø VHF radar (lower panel) on 18 to 19 June 2007. The same features of the background D-region are visible with both instruments, but the PMSE layers are seen by the VHF radar (particularly after 2300 UT) are not visible at MF.

3.10 INSTRUMENTATION AND TECHNIQUES

3.10.1 Imaging Spectrograph Platform

As reported in the previous UK EISCAT report, the UCL-Southampton spectrograph platform was deployed on Svalbard in December 1999, and has since been used in a number of ESR campaigns. In these experiments, spectrograph measurements of emissions arising from electron and proton precipitation have been supported by field-aligned ESR data (see also section 3.5.1). The main scientific goal of these studies has been to measure the location and time history of the precipitation above the ESR. Detailed analysis of the emission spectrum can be used to investigate the energy spectra of the precipitating electrons and protons, which can then be related back to their magnetospheric source regions.

Analysis of a strong proton aurora on Nov 26th 2000 has shown that the blue-shifted wing of the H-beta line is not fully measured by the spectrograph with the present filter and suggests further experiments are needed with wider filters. Measurements of both H-alpha and H-beta line filters are required in order to account for any contaminating features in the respective profiles. Potential contamination in the H-beta profile originates from the Vegard-Kaplan bands of N2 and atomic oxygen, while H-alpha lies in the spectral region of the N2 1st Positive bands. Any contamination from these nitrogen and oxygen lines has to be carefully allowed for in the interpretation of proton aurora spectra. The current "nitrogen" filters have already made excellent measurements of the electron-precipitation induced aurora with far greater detail than has been obtained previously.

Much work has been done in collaboration with H Frey (University of California). The need for a full energy analysis has become very clear. In the data taken so far, there are several excellent events when the IMAGE satellite measured from above emissions that were seen in different wavelengths by the spectrograph below. Comparisons between the two are the only way that the Ly-alpha emissions can be truly quantified, since there is no information in the satellite measurements about the energy of the precipitating particles. Photometer measurements provide the background high time resolution emissions in the field of view, and also provide the essential means of calibrating the intensity of the spectrograph. The narrow-angle imager on the platform also helps to put the images into context. A clearer understanding has now been gained of the spectral limitations than when the platform was first designed. This area of spectroscopy, looking at little studied emissions, has revealed much new science already. More photometer barrels are needed, combining new wavelength measurements and associated background measurements to clear up some of the remaining questions.

Problems with the detector that was originally supplied with the HITIES spectrograph have meant that several interim detectors had to be tried while the original was being repaired. This has, however, had some benefits, as it has allowed different detectors to be compared. One of the detectors tried out was a new type that has been developed at UCL for astronomical work. First examination of the data shows that this detector – the MIC detector – appears to have been a great success. The improvement over a bare CCD, which results from the complete absence of detector-induced noise, was immediately apparent and features were observed in the real-time image for the first time. During a proton event of moderate intensity, structure along the slit image was clearly observed. In addition the Hydrogen beta line was seen to consist of two components – one Doppler broadened, as recorded during earlier observations with the bare CCD, and a previously unobserved narrow line at the same wavelength. The spectrograph has recently been refitted with the repaired Pixelvision camera and further measurements are being made in order to obtain a quantitative comparison.

4 APPENDIX A: PAPERS BY MEMBERS OF THE UK EISCAT COMMUNITY

2000

- Breen, A.R., C.F. de Forest, B.J. Thompson, J.F. McKenzie, A. Modigliani, P.J. Moran, C.A. Varley and P.J.S. Williams, "Comparisons of interplanetary scintillation and optical measurements of solar wind acceleration with model results", *Advances in Space Research*, **26(5)**, pp.781-784, 2000a.
- Breen, A.R., P.J. Moran, C.A. Varley, P.J.S. Williams, A. Lecinski, B.J. Thompson and L. Harra-Murnion, "Interplanetary scintillation measurements of the solar wind above low-latitude coronal holes", *Advances in Space Research*, **26(5)**, pp.789-792, 2000b.
- Breen, A.R., S.J. Tappin, C.A. Jordan, P. Thomasson, P.J. Moran, R.A. Fallows, A. Canals and P.J.S. Williams, "Simultaneous Interplanetary Scintillation and Optical Measurements of the acceleration of the Slow Solar Wind", *Annales Geophysicae*, **18**, pp.995-1002, 2000c.
- Breen, A.R., B. J. Thompson, M. Kojima, D.A. Biesecker, A. Canals, R.A. Fallows, J.A. Linker, A.J. Lazarus, Z. Mikic, P.J. Moran and P.J.S. Williams, "Measurements of the Solar Wind over a wide range of heliocentric distances a comparison of results from the first three Whole Sun Months", *Journal of Atmospheric and Solar-Terrestrial Physics*, **62**, pp.1527-1544, 2000d.
- Bromage, B.J.I., D. Alexander, A.R. Breen, J.R. Clegg, G. Del Zanna, C.F. DeForest, D. Dobrzycka, N. Gopalswamy and B.J. Thompson, "Structure of a large low-latitude coronal hole", *Solar Physics*, **193**, pp.181-193, 2000.
- Cierpka K., M.J. Kosch, M. Rietveld, K. Schlegel and T. Hagfors, "Ion-Neutral Coupling in the High-Latitude F-Layer from Incoherent Scatter and Fabry-Perot Interferometer Measurements", *Annales Geophysicae*, **18**, pp. 1145-1153, 2000a.
- Cierpka K., M.J. Kosch, M.T. Rietveld, K. Schlegel and T. Hagfors, "Direct calculation of F-region Joule heating from simultaneous ion and neutral measurements at high latitudes", *Physics and Chemistry of the Earth (B)*, **25**, pp. 439-442, 2000b.
- Cierpka K., M.J. Kosch, S. Nozawa, K. Schlegel and T. Hagfors, "Combined EISCAT and Fabry-Perot interferometer measurements of ionospheric-thermospheric coupling", *Physics and Chemistry of the Earth (C)*, **25**, pp. 563-566, 2000c.
- Davies, J.A., T.K. Yeoman, M. Lester, and S.E. Milan, "A comparison of F-region ion velocity observations from the EISCAT Svalbard and VHF radars with irregularity drift velocity measurements from the CUTLASS Finland HF radar", *Annales Geophysicae*, **18**, pp. 589-594, 2000.
- Jones G.O.L., C.J. Davis and R.E. Stockwell, "Dynasonde observations of electron concentration gradients above Tromsø" *Journal of Atmospheric and Solar-Terrestrial Physics*, **62**, pp. 1385-1391, 2000.
- Khan, H., and S.W.H. Cowley, "Effect of the IMF By component in the ionospheric flow overhead at EISCAT: observation and theory", *Annales Geophysicae*, **18**, pp. 1503-1522 2000.
- Kosch M.J., M.T. Rietveld, T. Hagfors and T.B. Leyser, "High-latitude HF-induced airglow displaced equatorwards of the pump beam", *Geophysical Research Letters*, **27(17)**, pp. 2817-2820, 2000a.
- Kosch M.J., M. Ishii, S. Nozawa, D. Rees, K. Cierpka, A. Kohsiek, K. Schlegel, R. Fujii, T. Hagfors, T.J. Fuller-Rowell and C. Lathuillere, "A Comparison of Thermospheric Winds and Temperatures from Fabry-Perot Interferometer and EISCAT Radar Measurements with Model", Advances in Space Research., 26(6), pp. 979-984, 2000b.
- Kosch M.J., M.T. Rietveld, A. Steen and T. Hagfors, "HF induced airglow: double patches", *Physics and Chemistry of the Earth* (B), **25**, pp. 475-481, 2000c.
- Lester, M., "HF coherent scatter observations of ionospheric convection during magnetospheric substorms", *Advances. in Polar Upper Atmosphere Research*, **14**, pp. 179-201, 2000.
- Lester, M., J.A. Davies, and T.K. Yeoman, "The ionospheric response during an interval of Pc5 ULF wave activity", *Annales Geophysicae*, **18**, pp. 257-261, 2000.

- Leyser T.B., B. Gustavsson, B.U.E. Brändström, Å. Steen, F. Honary, M.T. Rietveld, T. Aso, and M. Ejiri. "Simultaneous Measurements of High-frequency Pump-enhanced Airglow and Ionospheric Temperatures at Auroral Latitudes". *Advances in Polar Upper Atmosphere Research*, **14**, pp. 1-11, 2000.
- Lockwood M., I.W. McCrea, S.E. Milan, J. Moen, J-C. Cerisier and A. Thorolfsson, "Plasma structure within poleward-moving cusp/cleft auroral transients: EISCAT Svalbard Radar observations and an explanation in terms of large local time extent of events", *Annales Geophysicae*, **18**, pp. 1027-1042, 2000.
- Maynard N.C., W.J. Burke, R.F. Pfaff, E.J. Weber, D.M. Ober, D.R. Weber, J. Moen, S.E. Milan, K. Maseide, P.E. Sandholt, A. Egeland, F. Soraas, R. Lepping, S. Bounds, M. Acuna, H. Freudenreich, J.S. Machuzak, L.C. Gentile, J.H. Clemmons, M. Lester, P. Ning, D.A. Hardy, J.A. Holtet, J. Stadsnes and A.P. van Eyken, "Driving dayside convection with northward IMF: observations by a sounding rocket launched from Svalbard", *Journal of Geophysical Research*, 105, pp. 5245-5264, 2000.
- McCrea I.W., M. Lockwood, J. Moen, F. Pitout, P. Eglitis, A.D. Aylward, J-C. Cerisier, A. Thorolfsson and S.E. Milan, "ESR and EISCAT observations of the response of the cusp and polar cap to IMF orientation changes", *Annales Geophysicae*, **18**, pp. 1009-1026, 2000.
- Moran, P.J., S. Ananthakrishnan, V. Balasubramian, A.R. Breen, A. Canals, R. Fallows, P.Janardhan, M. Tokumaru, and P.J.S. Williams, "Observations of interplanetary scintillation during the 1998 whole sun month: a comparison between EISCAT, ORT and Nagoya data", *Annales Geophysicae*, **18**, 1003-1008, 2000a.
- Moran, P.J., A.R. Breen, A. Canals, J. Markkanen, P. Janardhan, M. Tokumaru and P.J.S. Williams, "Observations of interplanetary scintillation during the 1998 whole sun month: a comparison between EISCAT, ORT and Nagoya data", *Annales Geophysicae*, 18, pp. 1003-1008, 2000b.
- Pryse S.E., A.M. Smith, L. Kersley, I.K. Walker, C.N. Mitchell, J. Moen and R.W. Smith, "Multi-instrument probing of the polar ionosphere under steady northward IMF", *Annales Geophysicae*, **18**, pp. 90-98, 2000a.
- Pryse S.E., A.M. Smith, I.K. Walker and L. Kersley, "Multi-instrument study of magnetopause reconnection in the summer ionosphere", *Annales Geophysicae*, **18**, pp. 1118-1127, 2000b.
- Robinson, T.R., R. Strangeway, D.M. Wright, J.A. Davies, R.B. Horne, T.K. Yeoman, A.J. Stocker, M. Lester, M.T. Rietveld, I.R. Mann, C.W. Carlson, and J.P. McFadden, "FAST observations of ULF waves injected into the magnetosphere by means of modulated RF heating of the auroral electrojet", *Geophysical Research Letters*, **27**, pp. 3165-3168, 2000.
- Romanovsky Y., V. Alpatov, Yu. Platov, S. Chernouss, M. Kosch and A. Steen, "Optical investigations in "ERLE" project" *Physics and Chemistry of the Earth (B)*, **25**, pp. 503-506, 2000.
- Safargaleev V., W. Lyatsky, N.G.J. Gazey, P.N. Smith and V. Krivolov, "The response of the azimuthal component of the ionospheric electric field to auroral arc brightening", *Annales Geophysicae*, **18**, pp. 65-73, 2000.
- Sergienko T., B. Gustavsson, Å. Steen, U. Brändström, M. Rietveld, T.B. Leyser, and F. Honary, "Analysis of excitation of the 630.0 nm airglow during a heating experiment in Tromsø in February 16, 1999", *Journal of Physics and Chemistry of the Earth (B)*, **25(5)**, pp. 531-535, 2000.
- Smith A.M., S.E. Pryse and L. Kersley, "Polar patches observed by the ESR and their possible origin in the cusp region", *Annales Geophysicae*, **18**, pp. 1043-1053, 2000.
- Thorolfsson A., J-C. Cerisier, M. Lockwood, P.E. Sandholt, C. Senior and M. Lester, "Simultaneous optical and radar signatures of poleward-moving auroral forms", *Annales Geophysicae*, **18**, pp. 1054-1066, 2000.
- van Eyken A.P., P.J.S. Williams, S.C. Buchert and M. Kunitake, "First measurements of tidal modes in the lower thermosphere by the EISCAT Svalbard Radar", *Geophysical Research Letters*, **27**, pp. 931-934, 2000.
- Wright D.M., J.A. Davies, T.R. Robinson, P.J. Chapman, T.K. Yeoman, E.C. Thomas, M. Lester, S.W.H. Cowley, A.J. Stocker, R.B. Horne, and F. Honary, "Space Plasma Exploration by Active Radar (SPEAR): An overview of a future radar facility", *Annales Geophysicae*, 18, pp. 1248-1255, 2000.
- Yeoman, T.K., J.A. Davies, N.M. Wade, G. Provan, and S.E. Milan, "Combined CUTLASS, EISCAT and ESR observations of an isolated substorm", *Annales Geophysicae*, **18**, pp. 1073-1087, 2000a.
- Yeoman T.K., D.M. Wright, P.J. Chapman and A.B. Stockton-Chalk, "High-latitude observations of ULF waves with large azimuthal wavenumbers", *Journal of Geophysical Research*, **105**, 5453-5462, 2000b.

- Aruliah A.L. and E. Griffin, "Evidence of meso-scale structure in the high-latitude thermosphere" *Annales Geophysicae*, **19**, pp. 37-46, 2001.
- Bogdanova, Y., V.S. Semenov, R.P. Rijnbeek and P.N. Smith, "Analysis of auroral arc dynamics based on a model of magnetic reconnection in the magnetotail", *Journal of Atmospheric and Solar-Terrestrial Physics*, **63**, pp. 725-738, 2001.
- Blagoveshchenskaya N.F., V.A. Kornienko, T.D. Borisova, B. Thide, M.J. Kosch, M.T. Rietveld, R.Yu. Luk'yanov and O.A. Troshichev, "Ionospheric HF pump wave triggering of local auroral activation", *Journal of Geophysical Research*, **106**, pp. 29071, 2001.
- Breen, A.R., "Living with an active star: Solar cycle changes, eruptive events and terrestrial consequences", *Astronomy and Geophysics*, **42**, pp. 3.35-3.36, 2001.
- Fox, N.J., S.W.H. Cowley, J.A. Davies, R.A. Greenwald, M. Lester, M. Lockwood, and H. Lühr, "Ionospheric ion and electron heating at the poleward boundary of a poleward-expanding substorm-disturbed region", *Journal of Geophysical Research*, **106**, pp. 12845-12862, 2001.
- Gustavsson B., T. Sergienko, M.T. Rietveld, F. Honary, Å. Steen, B.U.E. Brändström, T.B. Leyser, A.L. Aruliah, T. Aso, M. Ejiri, and S. Marple, "First tomographic estimate of volume distribution of HF-pump enhanced airglow emission", *Journal of Geophysical Research*, 106(A12), pp. 29105, December 2001.
- Jones, T.B., M. Lester, S.E. Milan, T.R. Robinson, D.M. Wright, R.S. Dhillon, and J.A. Davies, "Radio wave propagation aspects of the CUTLASS radar", *Journal of Atmospheric and Solar-Terrestrial Physics*, **63**, pp. 99-105, 2001.
- Jussila J., A. Aikio, S. Shalimov, S. Marple, and M. Syrjäsuo. "Cosmic Radio Noise Absorption in the Vicinity of Auroral Arcs", Eos Transactions AGU, 82(47), 2001.
- Khan, H., and S.W.H. Cowley, "Effect of the IMF By component on the ionospheric flow overhead at EISCAT: observations and theory", *Annales Geophysicae*, **18**, pp. 1503-1522, 2001.
- Kosch M.J., K. Cierpka, M.T. Rietveld, T. Hagfors, K. Schlegel, "High-latitude ground-based observations of the thermospheric ion-drag time constant," *Geophysical Research Letters*, **28**, pp. 1395-1398, 2001a.
- Kosch M.J., F.Honary, C.F. del Pozo, S.R. Marple, and T. Hagfors. "High-resolution maps of the characteristic energy of precipitating auroral particles", *Journal of Geophysical Research*, **106(A12)**, pp. 28925, 2001b.
- Kotikov A.L., V.A. Kornienko, M.J. Kosch, "The peculiarities of auroral electrojet dynamics during a heating transmitter influence on the polar ionosphere", *Geomagnetism and Aeronomy*, **41(3)**, pp. 355-362, 2001.
- Lanchester B.S., M.H. Rees, D. Lummerzheim, A. Otto, M.H. Rees, K.J.F. Sedgemore-Schulthess, H. Zhu and I.W. McCrea, "Ohmic heating as evidence for strong field-aligned currents in filamentary aurora", *Journal of Geophysical Research*, 106, pp. 1785-1794, 2001.
- Lockwood M., H.J. Opgenoorth, A.P. van Eyken, A. Fazakerley, J-M. Bosqued, W. Denig, J.A. Wild, C. Cully, R. Greenwald, G. Lu, O. Amm, H. Frey, A. Strømme, P. Prikryl, M.A. Hapgood, M.N. Wild, R. Stamper, M. Taylor, I.W. McCrea, K. Kauristie, T. Pulkkinen, F. Pitout, A. Balogh, M. Dunlop, H. Rème, R. Behlke, T. Hansen, G. Provan, P. Eglitis, S.K. Morley, D. Alcaydé, P-L. Blelly, J. Moen, E. Donovan, M. Engebretson, M. Lester, J. Watermann, and M.F. Marcucci, "Coordinated Cluster, ground-based instrumentation and low-altitude satellite observations of transient poleward-moving events in the ionosphere and in the tail lobe", *Annales Geophysicae*, 19, pp. 1589-1612, 2001a.
- Lockwood M., A. Fazakerley, H. Opgenoorth, J. Moen, A.P. van Eyken, M. Dunlop, J-M. Bosqued, G. Lu, C. Cully, P. Eglitis, I.W. McCrea, M.A. Hapgood, M.N. Wild, R. Stamper, W. Denig, M. Taylor, J.A. Wild, G. Provan, O. Amm, K. Kauristie, T. Pulkkinen, A. Strømme, P. Prikryl, F. Pitout, A. Balogh, H. Rème, R. Behlke, T. Hansen, R. Greenwald, H. Frey, S.K. Morley, D. Alcaydé, P-L. Blelly, E. Donovan, M. Engebretson, M. Lester, J. Watermann, and M.F. Marcucci, "Coordinated Cluster and ground-based instrument observations of transient changes in the magnetopause boundary layer during an interval of predominantly northward IMF: relation to reconnection pulses and FTE signatures", Annales Geophysicae, 19, pp. 1613-1640, 2001b.
- Ogawa, T., S.C. Buchert, N. Nishitani, N. Sato, and M. Lester, "Plasma density suppression process around the cusp revealed by simultaneous CUTLASS and EISCAT Svalbard radar observations", *Journal of Geophysical Research*, **106**, pp. 5551-5564, 2001.
- Opgenoorth H.J., M. Lockwood, D. Alcaydé, E. Donovan, M.J. Engebretson, A.P. van Eyken, K. Kauristie, M. Lester, J. Moen, J. Waterman, H. Alleyne, M. André, M. W. Dunlop, N. Cornilleau-Wehrlin, A. Masson, A. Fazerkerley, H. Rème, R.

- André, O. Amm, A. Balogh, R. Behlke, P.L. Blelly, H. Boholm, E. Borälv, J.M. Bosqued, S. Buchert, M. Candidi, J-C. Cerisier, C. Cully, W. F. Denig, P. Eglitis, R.A. Greenwald, B. Jackal, J.D. Kelly, I. Krauklis, G. Lu, I.R. Mann, M.F. Marcucci, I.W. McCrea, M. Maksimovic, S. Massetti, P.M.E. Décréau, D.K. Milling, S. Orsini, F. Pitout, G. Provan, J.M. Ruohoniemi, J.C. Samson, J.J. Schott, F. Sedgemore-Schulthess, R. Stamper, P. Stauning, A. Strømme, M. Taylor, A. Vaivads, J.P. Villain, I. Voronkov, J.A. Wild, and M. Wild, "Coordinated ground-based, low altitude satellite and Cluster observations on global and local scales during a transient post-noon sector excursion of the magnetospheric cusp", *Journal of Geophysical Research*, 19, pp. 1367-1398, 2001.
- Rodger A.S., G.D. Wells, R.J. Moffett and G.J. Bailey, "The variability of Joule heating, and its effects on the ionosphere and thermosphere", *Annales Geophysicae*, **19**, pp. 773-781, 2001.
- Sedgemore-Schulthess K.J.F. and J-P St Maurice, "Naturally enhanced ion-acoustic spectra and their interpretation", *Surveys in Geophysics*, **22**, pp. 55-92, 2001.
- Wild, J.A., S.W.H. Cowley, J.A. Davies, H. Khan, M. Lester, S.E. Milan, G. Provan, T.K. Yeoman, A. Balogh, M.W. Dunlop, K-H. Fornacon, and E. Georgescu, "First simultaneous observations of flux transfer events at the high-latitude magnetopause by the Cluster spacecraft and pulsed radar signatures in the conjugate ionosphere by the CUTLASS and EISCAT radars", Annales Geophysicae, 19, pp. 1491-1508, 2001.
- Yeoman, T.K., and D.M. Wright, "ULF waves with drift resonance and drift-bounce resonance energy sources as observed in artificially-induced HF radar backscatter", *Annales Geophysicae*, **19**, pp. 159-170, 2001.
- Yeoman, T.K., D.M. Wright, A.J. Stocker, and T.B. Jones, "An evaluation of range accuracy in the SuperDARN over-the-horizon HF radar systems", *Radio Science*, **36**, pp. 801-813, 2001.
- Zhu H., A. Otto, M.H. Rees, B.S. Lanchester and D. Lummerzheim, "Ionosphere-Magnetosphere simulation of small scale structure and dynamics", *Journal of Geophysical Research*, **106**, pp. 1795-1806, 2001.

2002

- Baddeley, L.J., T.K. Yeoman, D.M. Wright, J.A. Davies, K.J. Trattner, and J.L. Roeder, "Morning sector drift-bounce resonance driven ULF waves observed in artificially-induced HF radar backscatter", *Annales Geophysicae*, submitted, 2002.
- Borisova T.D., N.F. Blagoveshchenskaya, I.V. Moskvin, M.T. Rietveld, M.J. Kosch and B. Thide, "Doppler shift simulation of scattered HF signals during the Tromsø HF pumping experiment on 16 February, 1996", *Annales Geophysicae*, in press, 2002.
- Breen, A.R., A. Canals, R.A. Fallows, P.J. Moran and M. Kojima, "Large-scale structure of the solar wind from interplanetary scintillation measurements during the rising phase of cycle 23", *Advances in Space Research*, **29(3)**, pp.379-388, 2002a
- Breen, A.R., P. Thomasson, C.A. Jordan, S.J. Tappin, R.A, Fallows, A. Canals and P.J. Moran "Interplanetary scintillation and optical measurements of slow and fast solar wind acceleration near solar maximum", *Advances in Space Research*, in press, 2002b.
- Breen, A.R., P. Riley, A.J. Lazarus, R.A. Fallows and A. Canals, "The solar wind at solar maximum: Comparisons of EISCAT IPS observations and in-situ measurements", *Annales Geophysicae*, in press, 2002c.
- Canals, A., A.R. Breen, P.J. Moran and L. Ofman, "Estimating random transverse velocities in the fast solar wind from EISCAT interplanetary scintillation measurements", *Annales Geophysicae*, in press, 2002.
- Cash, S.R., J.A. Davies, E. Kolesnikova, T.R. Robinson, D.M. Wright, T.K. Yeoman, and R.J. Strangeway, "Modelling electron acceleration within the IAR during a 3Hz modulated EISCAT heater experiment and comparison with FAST satellite electron flux data", *Annales Geophysicae*, submitted, 2002.
- Davies, J.A., T.K. Yeoman, I.J. Rae, S.E. Milan, M. Lester, K.A. McWilliams, and M. Lockwood, "Ground-based observations of the auroral zone and polar cap ionospheric responses to dayside transient reconnection", *Annales Geophysicae*, submitted, 2002.
- del Pozo C.F., P.J.S. Williams, N.G.J. Gazey, Sedgemore, P.N. Smith, F. Honary and M.J. Kosch, "Multi-instrument observations of the dynamics of auroral arcs: a case study", *Journal of Atmospheric and Solar-Terrestrial Physics*, in press, 2002a.
- del Pozo C.F., F. Honary, N. Stamatiou, and M.J. Kosch, "Study of auroral forms and electron precipitation with the IRIS, DASI and EISCAT Systems", *Annales Geophysicae*, submitted, 2002b.

- del Pozo C.F., M.J. Kosch, and F. Honary, "Estimation of the characteristic energy of electron precipitation", *Annales Geophysicae*, submitted, 2002c.
- Fallows, R.A., A.R. Breen, P.J. Moran, A. Canals and P.J.S. Williams, "The high-latitude solar wind in EISCAT IPS data, 1991-1999", *Advances in Space Research*, in press, 2002a.
- Fallows, R.A., P.J.S. Williams and A.R. Breen, "EISCAT measurements of solar wind velocity and the associated level of interplanetary scintillation", *Annales Geophysicae*, in press, 2002b.
- Gauld, J.K., T.K. Yeoman, J.A. Davies, S.E. Milan, and F. Honary, "SuperDARN radar HF propagation and absorption response to the substorm expansion phase", *Annales Geophysicae*, submitted, 2002.
- Kavanagh, A.J., F. Honary, I.W. McCrea, E. Donovan, E.E. Woodfield, J. Manninen, P.C. Anderson, "Substorm related changes in precipitation in the dayside auroral zone a multi instrument case study", *Annales Geophysicae*, in press, 2002.
- Khan, H., M. Lester, J.A. Davies, S.E. Milan, and P.E. Sandholt, "Multi-instrument study of the dynamic cusp during dominant IMF By conditions", *Annales Geophysicae*, submitted, 2002.
- Kolesnikova, E., T.R. Robinson, and J.A. Davies, "Predicted and observed characteristics of small-scale field-aligned irregularities generated in the F-region by low power HF heating", *Annales Geophysicae*, in press, 2002a.
- Kolesnikova, E., T.R. Robinson, J.A. Davies, M. Lester, D.M. Wright, and R.J. Strangeway, "Excitation of Alfvén waves by modulated HF heating of the ionosphere, with application to FAST observations", *Annales Geophysicae*, in press, 2002b.
- Kosch M.J., M.T. Rietveld, T.K. Yeoman, K. Cierpka and T. Hagfors, "The high-latitude artificial aurora of 21 February 1999: An analysis", *Advances in Polar Upper Atmosphere Research*, in press, 2002.
- Nielsen E., C.F. del Pozo, and P.J.S. Williams. "VHF Coherent radar signals from the E region ionosphere and the relationship to electron drift velocity and ion acoustic velocity", *Journal of Geophysical Research*, in press, 2002.
- Pancheva D., N.J. Mitchell, M.E. Hagan, A.H. Manson, . E. Meek, Yi Luo, Ch. Jacobi, D. Kurschner, R.R. Clark, W.K. Hocking, J. MacDougall, G.O.L. Jones, R.A. Vincent, I.M. Reid, W. Singer, K. Igarashi, G.I. Fraser, T. Nakamura, T. Tsuda, Yu. Portnyagin, E. Merzlyakov, A.,N. Fahrutdinova, A.M. Stepanov, L.M.G. Poole, S.B. Malinga, B.L. Kashcheyev, A.N. Oleynikov, "Global-scale tidal structure in the mesosphere and lower thermosphere during the PSMOS campaign of June-August 1999 and comparisons with the Global Scale Wave Model", Journal of Atmospheric and Solar-Terrestrial Physics, in press, 2002.
- Pryse S.E., A.M. Smith, L Kersley and I.W. McCrea, "EISCAT Svalbard Radar observations of ionospheric signatures of magnetopause reconnection during a changing IMF Bz polarity", *Annales Geophysicae*, in press, 2002.
- Rietveld M.T., B. Isham, T. Grydeland, C. la Hoz, F. Honary, T.B. Leyser, H. Ueda, M. Kosch and T. Hagfors, "HF-Pump-Induced Parametric Instabilities in the Auroral E-Region", *Advances in Space Research*, in press, 2002.
- Robinson, T.R., "Effect of multiple scatter on the propagation and and absorption of electromagnetic waves in a field-aligned-striated magnetoplasma: Implications for ionospheric modification experiments", *Annales Geophysicae*, accepted, 2002.
- Woodfield, E.E., J.A. Davies, P. Eglitis and M. Lester, "A case study of HF radar spectral width in the post midnight magnetic local time sector and its relationship to the polar cap boundary", *Annales Geophysicae*, accepted, 2002a.
- Woodfield, E.E., J.A. Davies, M. Lester, T.K. Yeoman, P. Eglitis and M. Lockwood, "Nightside studies of coherent HF radar spectral width behaviour", *Annales Geophysicae*, submitted, 2002b.
- Wright, D.M., J.A. Davies, T.R Robinson, T.K. Yeoman, M. Lester, S.R. Cash, E. Kolesnikova, R. Strangeway, R.B. Horne, M.T. Rietveld and C.W. Carlson, "The tagging of a narrow flux tube using artificial ULF waves generated by modulated high power radio waves", *Journal of Geophysical Research*, submitted, 2002a.
- Wright, D.M., T.K. Yeoman, R. Dhillon, M. Lester, J.A. Davies, S. Milan, E.E. Woodfield, and T. Bösinger, "High resolution observations of spectral width features associated with ULF wave signatures in artificial HF radar backscatter", *Journal of Geophysical Research.*, submitted, 2002b.

Ph.D THESES

2000

- Berry S.T., "Experimental studies of plasma structuring in the high-latitude ionosphere", University of Wales, 2000.
- Gauld, J.K., "Studies of the signatures of magnetospheric substorms in coherent backscatter radars", University of Leicester, 2000.
- Griffin, E., "Comparisons of high latitude thermospheric meridional neutral winds", University College London, 2000.
- Howells, V.St.C., "Radar measurements of the mesosphere and lower thermosphere", University of Wales, 2000.
- Wild, J.A., "Electrodynamics of the auroral ionosphere during magnetospheric substorms", University of Leicester, 2000.

2001

- Dhillon, R.S., "Radar studies of natural and artificial waves and instabilities in the auroral atmosphere", University of Leicester, 2001
- Fallows, R.A., "Studies of the solar wind throughout a solar cycle", University of Wales, 2001.
- Smith A.M., "Multi-instrument studies of magnetosphere/ionosphere interaction in the noon sector", University of Wales, 2001.

CONFERENCE PROCEEDINGS AND OTHER PUBLICATIONS

2000

- Breen, A.R. and G. Woan, "Radio scintillation observations of the solar wind recent results and proposals for a new-generation system", submitted to ESA Conference Proceedings of the 3rd Space Weather Workshop, February 2002d
- Cowley, S.W.H., J.A. Davies, A. Grocott, H. Khan, M. Lester, K.A. McWilliams, S.E. Milan, G. Provan, P.E. Sandholt, J.A. Wild, and T.K. Yeoman, "Solar wind-magnetosphere-ionosphere interactions in the Earth's plasma environment", Proceedings of the Royal Society, submitted, 2002.
- Davies, J.A., S.W.H. Cowley, M. Lester, and N.J. Fox, "EISCAT VHF radar observations in the region of the poleward-expanding auroral bulge", *Proceedings of the 5th International Conference on Substorms*, **ESA SP-443**, pp.283-286, 2000.
- Dhillon, R.S., D.M. Wright, R. Andre, and T.R. Robinson, "ACFs and turbulence characteristics from artificial field-aligned irregularities", *Proceedings of the SuperDARN Workshop*, Beechworth, Australia, 2000.
- Wild, J.A., T.K. Yeoman, and J.A. Davies, "High-time resolution radar observations of high-latitude flows during an isolated substorm", *Proceedings of the SuperDARN Workshop*, Beechworth, Australia, 2000.
- Woodfield, E.E., J.A. Davies, P. Eglitis, and M. Lester, "A multi-instrument study of spectral width boundary motion in data from the CUTLASS, Finland HF radar", *Proceedings of the SuperDARN Workshop*, Beechworth, Australia, 2000.
- Yeoman, T.K., and D.M. Wright, "Drift resonance and drift bounce resonance energy sources for ULF waves observed in artificially-induced back scatter", *Proceedings of the SuperDARN Workshop*, Beechworth, Australia, 2000.

2001

Lanchester B.S., M.H. Rees, S.C. Robertson, D. Lummerzheim, M. Galand, M. Mendillo, J. Baumgardner, I. Furniss and A. D. Aylward "Proton and electron precipitation over Svalbard - first results from a new Imaging Spectrograph (HiTIES)", Submitted to *Proceeds of Atmospheric Studies by Optical Methods*, Oulu, 2001.

5 APPENDIX B: UK EISCAT CAMPAIGNS IN 2000 AND 2001

CAMPAIGN 68

Experiments From: 4 to 9 February 2000

Campaign Team:

No UK personnel attended the campaign

UK Hours Used: KST 3

This campaign was a collaboration with Germany, who supplied the personnel and contributed most of the radar time.

CAMPAIGN 69

Experiments From: 22 to 28 March 2000

Campaign Team:

Farideh Honary Lancaster Tromsø Vikki Howells RAL Tromsø

UK Hours Used: KST 5

This was a multi-national campaign, also involving Germany, Japan and Sweden, which used the heater only.

CAMPAIGN 70

Experiments From: 1 to 16 April 2000

Campaign Team:

Ian McCrea RAL Svalbard

UK Hours Used: ESR 18

CAMPAIGN 71

Experiments From: 2 to 5 May 2000

Campaign Team:

Tim Stubbs ICST Svalbard

UK Hours Used: ESR 11

CAMPAIGN 72

Experiments From: 21 to 31 August 2000

Campaign Team:

Ian McCreaRALSvalbardVikki HowellsRALSvalbard

UK Hours Used: ESR 12

CAMPAIGN 73

Intended to be a major UK heating campaign, but cancelled because of the continuing unavailability of the mainland radars.

CAMPAIGN 74

Experiments From: 30 October to 4 November 2000

Campaign Team:

Ian FurnissUCLSvalbardIan McWhirterUCLSvalbard

Jonathan Ruxton UCL Svalbard

UK Hours Used: ESR 6, KST 8

The mainland part of this campaign (using heating only) was a collaboration with Germany

CAMPAIGN 75

Experiments From: 22 November to 5 December 2000

Campaign Team:

Betty Lanchester Southampton Svalbard

Stu RobertsonSouthamptonSvalbardIan FurnissUCLSvalbardMatthew HarrisUCLSvalbardSteve CrothersRALTromsø

UK Hours Used: ESR 70, KST 69

2000 Summary

In addition to the above, the UK used 22 hours of KST time during passive interplanetary scintillation experiments in May and September 2000. The usage of UK Special Programme time in 2000 was 117 hours ESR, 107 hours KST. This represented 43% of the total mainland SP time and 26% of the total ESR SP time. Because the mainland sites were unusable except for IPS and heating experiments between January and November, the UK used less than half of its mainland allocation in 2000. The ESR allocation was fully utilised.

The breakdown of UK observing time by institute in 2000 was as follows. Aberystwyth 41 hours (22 KST, 19 ESR), Imperial College 23 hours (ESR), Lancaster 23 hours (KST), RAL 64 hours (24 KST, 40 ESR), Southampton 24 hours (ESR). The remaining time was used in testing and pooled experiments.

CAMPAIGN 76

Experiments From: 21 to 30 January 2001

Campaign Team:

Stu Robertson Southampton Svalbard
Ian McWhirter UCL Svalbard

UK Hours Used: ESR 49

(This campaign was a collaboration with Norway)

CAMPAIGN 77

Experiments From: 15 to 25 February 2001

Campaign Team:

Mike Kosch Lancaster Tromsø Andrew Kavanagh Lancaster Tromsø

UK Hours Used: KST 25

(This campaign was a collaboration with Germany)

CAMPAIGN 78

Experiments From: 25 April to 9 May 2001

Campaign Team:

Nigel WadeLeicesterTromsøDarren WrightLeicesterTromsøJackie DaviesLeicesterTromsøKathryn McWilliamsLeicesterTromsø

Emma WoodfieldLeicester Tromsø

Adrian Grocott Leicester Tromsø
Ian Mann York Tromsø
Joe Matthews York Tromsø

UK Hours Used: KST 102

CAMPAIGN 79

Experiments From: 8 to 26 June 2001

Campaign Team:

Owen Jones BAS Tromsø
Vikki Howells RAL Tromsø
Chris Davis RAL Tromsø

UK Hours Used: KST 63

(This campaign was a collaboration with Norway)

CAMPAIGN 80

Experiments From: 8 to 19 November 2001

Campaign Team:

Mike Kosch Lancaster Tromsø

Andy Kavanagh Lancaster Tromsø

Stu Robertson Southampton Svalbard

UK Hours Used: ESR 12, KST 15

(This campaign was a collaboration with Germany and Finland)

CAMPAIGN 81

Experiments From: 14 to 20 December 2001

Campaign Team:

Betty Lanchester Southampton Svalbard

Ian FurnissUCLSvalbardVikki HowellsRALSvalbardRicky SimsAberystwythSvalbardPaul GallopRALTromsø

UK Hours Used: KST 21, ESR 54

(This campaign was a collaboration with Norway)

2001 Summary

In addition to the above, the UK used 24 hours of KST time during interplanetary scintillation experiments in May and September 2001. Also, 47 hours of radar time were contributed to Unusual Programmes in response to storm alerts, aimed at detecting signatures of Polar Cap Absorption. The UK usage of EISCAT Special Programme time in 2001 was 156 hours ESR and 259 hours KST. This represented 30% of the total KST Special Programme time and 41% of the total ESR Special Programme time. On both radars, the UK's nominal allocation of Special Programme time was exceeded by about 25%.

The breakdown of UK Special Programme usage by institute in 2001 was as follows. Aberystwyth 55 hours (KST 25, ESR 30), BAS 29 hours (KST), Central Lancashire 41 hours (18 hours KST, 23 hours ESR), Lancaster 37 hours (KST), Leicester 84 hours (KST), RAL 33 hours (KST), Southampton 41 hours (ESR) and York 24 hours (KST). The remainder was accounted for in testing time and pooled experiments.

6 APPENDIX C: THE UK EISCAT USER COMMUNITY

UNIVERSITY OF BATH

Telephone User ID

Dr CN Mitchell 01225 826610 C.N.Mitchell

E-mail User ID @bath.ac.uk

<u>Fax</u> 01225 826305

Address

Department of Electronic and Electrical Engineering University of Bath Claverton Down Bath BA2 7AY

BRITISH ANTARCTIC SURVEY

	Telephone	User ID
Dr I.J. Coleman	01223 221586	I.J.Coleman
Dr.M.P. Freeman	01223 221543	M.P.Freeman
Dr R.M. Horne	01223 221542	R.Horne
Dr G.O.L. Jones	01223 221546	O.Jones
Dr M. Pinnock	01223 221534	M.Pinnock
Dr A.S. Rodger	01223 221535	A.Rodger

E-mail User ID @bas.ac.uk

<u>Fax</u> 01223 221226

Address

British Antarctic Survey High Cross Madingley Road Cambridge CB3 0ET

CENTRAL LANCASHIRE UNIVERSITY

Telephone User ID

Mr. M.J. Birch 01772 893736 mjbirch

Dr. B.J.I. Bromage 01772 893584 bjibromage

E-mail User ID @uclan.ac.uk

<u>Fax</u> 01772 892996

Address

Department of Physics, Astronomy and Mathematics University of Central Lancashire Preston PR1 2HE

IMPERIAL COLLEGE

Telephone User ID

 Prof P. Cargill
 0207 594 7773
 p.cargill

 Mr T.J. Stubbs
 0207 594 7759
 tj.stubbs

E-mail User ID @ic.ac.uk

<u>Fax</u> 0207 594 7772

Address

Space & Atmospheric Physics Group The Blackett Laboratory, Imperial College, Prince Consort Road, London SW7 2BW

LANCASTER UNIVERSITY

	Telephone	User ID
Dr. C.F. del Pozo	01524 594674	C.del.Pozo
Dr. J.K. Hargreaves	01524 593969	J.Hargreaves
Dr. F. Honary	01524 593055	F.Honary
Mr. A.J. Kavanagh	01524 594674	A.J.Kavanagh
Dr M. Kosch	01524 593016	M.Kosch
Mr. S. Marple	01524 592699	S.Marple
Mr. A. Senior	01524 594674	A.Senior
Dr. R. Seviour	01524 592699	R.Seviour

E-mail User ID @lancaster.ac.uk

<u>Fax</u> 01524-592713

Address

Ionosphere and Radio Propagation Group Department of Communication Systems Faculty of Applied Sciences Lancaster University LA1 4YR

LEICESTER UNIVERSITY

	Telephone	User ID
Dr. N.F. Arnold	0116 252 2079	nfa1
Miss L.J. Baddeley	0116 223 1302	ljb14
Miss S.R. Cash	0116 252 2083	sreash
Prof. S.W.H. Cowley	0116 223 1331	swhc1
Dr. J.A. Davies	0116 252 3548	jaq
Mr. R.S. Dhillon	0116 252 3565	rsd6
Mr A. Grocott	0116 223 1302	ag27
Prof. T.B. Jones	0116 252 3561	tbj
Dr. H. Khan (currently on sabbatical)	0116 252 3548	hk13
Prof. M. Lester	0116 252 3580	mle
Dr. S.E. Milan	0116 223 1896	ets
Dr .G. Proven	0116 252 2083	gp3
Prof. T.R. Robinson	0116 252 3562	txr
Mr. N.M. Wade	0116 252 3568	nmw
Dr. J.A. Wild	0116 252 2083	jaw11
Miss E.E. Woodfield	0116 252 2083	eew4
Dr. D.M. Wright	0116 252 3568	dmw7
Dr. T.K. Yeoman	0116 252 3564	yxo

E-mail User ID@ion.le.ac.uk

<u>Fax:</u> 0116 252 3555

Address

Radio & Space Plasma Physics Group Department of Physics and Astronomy University of Leicester Leicester LE1 7RH

RUTHERFORD APPLETON LABORATORY

	Telephone	User ID
Mr. S.R. Crothers	01235 446564	s.r.crothers
Dr. C.J. Davis	01235 446710	c.j.davis
Mr. I. Finch	01235 446535	i.finch
Dr. K.S.C. Freeman	01235 446519	k.s.c.freeman
Mr. P. Gallop	01235 445160	p.gallop
Dr. V. StC. Howells	01235 445044	v.howells
Prof. M. Lockwood	01235 446496	m.lockwood
Dr. I.W. McCrea	01235 446513	i.w.mccrea
Ms. L. Williams	01235 445759	liz.williams

E-mail User ID@ rl.ac.uk

<u>Fax</u> 01235 445848

Address

Space Science and Technology Department Rutherford Appleton Laboratory Chilton Didcot Oxon OX11 0QX

UNIVERSITY OF SHEFFIELD

	Telephone	User ID
Prof. G.J. Bailey	0114 2223744	G.Bailey
Prof. R.J. Moffett	0114 2223780	R.Moffett
Dr. JM Rees	0114 2223782	J.Rees
Dr. Y.Z. Su	0114 2223793	Y.Su

E-mail User ID@sheffield.ac.uk

<u>Fax</u> 0114 2223739

Address

Upper Atmosphere Modelling Group Applied Mathematics Department Hicks Building University of Sheffield Sheffield S3 7RH

SHEFFIELD HALLAM UNIVERSITY

	Telephone	User ID
Mrs. J. Porteous	0114 2253268	j.porteous
Dr. A.M. Samson	0114 2253305	a.m.samson
Ms. S.L. Woodall	0114 2254776	s.l.woodall

E-mail User ID@shu.ac.uk

<u>Fax</u> 0114 2253066

Address:

School of Science and Mathematics Sheffield Hallam University City Campus, Pond Street Sheffield S1 1WB

SOUTHAMPTON UNIVERSITY

	Telephone	User ID
Mr N Ivchenko	02380592048	nvi
Dr. B.S. Lanchester	02380592049	bsl
Mr S K Morley	02380592048	skm
Prof. M.H. Rees	02380592048	mhr
Prof. H. Rishbeth	023 8059 2048	hr
Mr. S.C. Robertson	023 8059 2048	scr
Miss A Stockton-Chalk	02380592048	asc
Miss K Throp	02380592048	kt

E-mail User ID@phys.soton.ac.uk

<u>Fax</u> 02380592048

Address

Solar Terrestrial Physics Department of Physics and Astronomy University of Southampton Southampton SO17 1BJ

UNIVERSITY OF SUSSEX

	Telephone	User ID
Mr. G.R. Lewis	01273 678662	G.R.Lewis
Dr. R.P. Rijnbeek	01273 678699	R.P.Rijnbeek
Dr. P.N. Smith	01273 678662	P.N.Smith

E-mail UserID@sussex.ac.uk

<u>Fax</u> 01273 678097

Address

Space Science Centre
Physics and Astronomy Subject Group
School of CPES
University of Sussex
Falmer
Brighton
BN1 9QH

UNIVERSITY COLLEGE, LONDON

	Telephone	User ID
Dr. A.L. Aruliah	020 7679 9017	anasuya
Dr. A.D. Aylward	020 7679 9021	alan
Dr. I. Furniss	020 7679 9026	ianf
Mr. E. Griffin	020 7679 9020	eoghan
Dr. G. Millward	020 7679 9019	george
Dr. I. Muller-Wodarg	020 7679 9019	ingo

Email User ID@apl.ucl.ac.uk

<u>Fax</u> 020 7679 9024

Address

Atmospheric Physics Laboratory Department of Physics and Astronomy University College London 67-73 Riding House Street London W1W 7ER

UNIVERSITY OF WALES, ABERYSTWYTH

	Telephone	UserID
Dr N. Balan	01970 622821	nab
Dr. A.R. Breen	01970 622814	azb
Miss A Canals	01970 621907	aac99
Dr M. Denton	01970 622821	mick.denton
Dr. R. Fallows	01970 621907	raf
Prof. L. Kersley	01970 622813	lek
Mr N. Malan	01970 622821	niel.malan
Mr J. Matthews	01970 622821	jdm99
Mr A. Parry	01970 622821	arp01
Dr. S.E. Pryse	01970 622801	sep
Mr R. Sims	01970 622821	rws97
Prof. P.J.S.Williams	01970 622817	pjw

E-mail User ID@aber.ac.uk

<u>Fax</u> 01970 622826

Address

Department of Physics University of Wales Penglais Aberystwyth Dyfed SY23 3BZ

UNIVERSITY OF WARWICK

Telephone User ID

Dr SC Chapman 01203 524916 S.C.Chapman

E-mail User ID@warwick.ac.uk.

<u>Fax</u> 01203 692016

Address

Space & Astrophysics Group Physics Dept. University of Warwick Coventry CV4 7AL

YORK UNIVERSITY

Telephone UserID

Dr. I.R. Mann 01904 432240 ian

Dr. R.A. Mathie 01904 432279 rod

E-mail User ID@aurora.york.ac.uk

<u>Fax</u> 01904 432214

Address

Magnetospheric Physics Group University of York Heslington York YO10 5DD